Aus der Abteilung für Klinische Chemie und Klinische Biochemie
in der Chirurgischen Klinik-Innenstadt
der Ludwig-Maximilians-Universität München

Leiterin der Abteilung: Prof. Dr. rer. nat. Dr. med. habil. Marianne Jochum

Role of the intracellular domains in the regulation and the signaling of the human bradykinin B_2 receptor

Dissertation
zum Erwerb des Doktorgrades der Humanbiologie
an der
Medizinischen Fakultät der Ludwig-Maximilians-Universität zu München

Vorgelegt von

Göran Wennerberg

aus Stockholm

2010

Mit Genehmigung der Medizinischen Fakultät
der Ludwig-Maximilians-Universität München

Berichterstatter:	PD Dr. rer. nat. Alexander Faussner
Mitberichterstatter:	Prof. Dr. Nikolaus Plesnila Prof. Dr. Franz-Xaver Beck
Mitbetreuung durch den promovierten Mitarbeiter:	
Dekan:	Prof. Dr. med. Dr. h.c. M. Reiser, FACR,FRCR
Tag der mündlichen Prüfung:	27.01.2010

D.2 Methods

ABBREVIATIONS

ACE	angiotensin-converting enzyme
ATP	adenosine-5´-triphosphate
BK	bradykinin
[^{3}H]BK	tritium-labeled bradykinin
B9430	D-Arg[Hyp^3, Igl^5, D-Igl^7, Oic^8]BK
BSA	bovine serum albumin
CHAPS	3-[(3-cholamidopropyl)dimethylammonio]-1-propanesulfonic acid
Ci	Curie, 1 Ci = 2.22 × 10^{12} disintegrations/min
CMV	cytomegalovirus
DAG	diacylglycerol
DMEM	Dulbecco´s modified Eagle´s medium
DTT	1,4-dithiothretiol
EDTA	ethylendiamintetraacetic acid
eGFP	enhanced green fluorescent protein
eYFP	enhanced yellow fluorescent protein
ERK1/2	extracellular signal-regulated kinase 1/2
FCS	fetal calf serum
FRT	Flp recombinase target
GPCR	G protein-coupled receptor
GRK	G protein-coupled receptor kinase
GTP	guanosine-5´-triphosphate
h	hour
HA	hemagglutinin
HEPES	2-[4-(2-hydroxyethyl)-1-piperazinyl]ethanesulfonic acid
HEK cell	human embryonic kidney cell
HRP	horseradish peroxidase
Icatibant	D-Arg[Hyp^3, Thi^5, D-Tic^7, Oic^8]BK
ICL-1	first intracellular loop
ICL-2	second intracellular loop

ICL-3	third intracellular loop
Ins 1,4,5-P_3	*myo*-inositol 1,4,5-triphosphate
IP	inositol phosphate
KD	kallidin
KLK	kallikrein
min	minute
NPC17731	D-Arg0[Hyp3, D-HypE(trans-propyl)7, Oic8]BK
PAGE	polyacrylamide gel electrophoresis
PBS	phosphate buffered saline
PCR	polymerase chain reaction
PKA	protein kinase A
PKC	protein kinase C
PLC-β	phospholipase C-β
RIPA	radio-immunoprecipitation assay
RT	room temperature
s	second
SDS	sodium dodecyl sulfate
TBS	Tris-buffered saline buffer
TBST	Tris-buffered saline buffer with 0.1% Tween 20
TMD	transmembrane domain
Tris	tris(hydroxymethyl)-aminomethane
wt	wild type

A ZUSAMMENFASSUNG

Ziel der Doktorarbeit war die Analyse der Beteiligung der intrazellulären Domänen an der Regulation des humanen B_2 Bradykinin Rezeptors im Hinblick auf Signaltransduktion, Rezeptor-Desensibilisierung, und Rezeptor-Internalisierung.

Im ersten Teil wurde der Einfluss von Rezeptordichte und Zelltyp sowohl auf Internalisierung wie auch Signaltransduktion des B_2 Rezeptors untersucht. Es wurden die Eigenschaften des B_2 Rezeptors, stabil mit unterschiedlichem Expressionslevel exprimiert unter der Kontrolle zweier verschieden starker Promotoren in HEK 293 Zellen und endogenem B_2 Rezeptor in humanen Fibroblasten analysiert. Wir konnten zeigen, dass zwei B_2 Rezeptor-Antagonisten, Icatibant und B9430, die sich von Bradkyinin (BK) durch die Insertion von artifiziellen Aminosäuren unterscheiden, unter bestimmten Bedingungen zu partiellen Agonisten werden; zu diesem partiellen Agonismus kam es nur in HEK 293 Zellen, die eine hohe B_2 Rezeptor-Expression zeigten, wohingegen dies in niedriger (HEK 293) oder endogen (Fibroblasten) exprimierenden Zellen nicht zu beobachten war. Allerdings resultierte langzeitige B9430-Stimulation in niedrig exprimierenden HEK293, wie auch in Fibroblasten, in einer starken Reduktion der Oberflächenbindung des Rezeptors, vergleichbar mit dem Effekt des endogenen Agonisten BK. Weitere Studien zeigten, dass im Gegensatz zu BK, welches die Oberflächenbindung durch Einleitung von Rezeptor-Internalisierung reduzierte, B9430 die Bindung an der Zelloberfläche durch eine Erniedrigung der B_2 Rezeptor-Affinität herabsetzte, ohne dessen Internalisierung zu bewirken, ein Mechanismus, der so bisher noch nicht beschrieben wurde.

Im zweiten Teil wurde die Rolle der intrazellulären Schleifen des B_2 Rezeptors genauer erforscht. G-Proteine, Rezeptor-Kinasen und Adapter-Proteine des Internalisierungs-Komplexes interagieren sehr wahrscheinlich mit cytosolischen Domänen des Rezeptors. Um die Rezeptorsequenzen, die an diesen Interaktionen beteiligt sind, genauer zu definieren, wurden systematisch alle drei intrazellulären Schleifen entweder als Punktmutationen oder in Gruppen von 3-5 Aminosäuren zu Alanin mutiert (insgesamt 14 Mutanten), wobei alle Konstrukte stabil und isogen in HEK 293 Zellen exprimiert wurden. Unsere Ergebnisse zeigen, dass Veränderungen in der intrazellulären Schleife 1 (ICL-1) die Oberflächenexpression des Rezeptors

stark beeinflussen, wohingegen Rezeptor-Signalvermittlung und Internalisierung unverändert bleiben. Für die Aufrechterhaltung der Rezeptorlevel ist die DRY-Sequenz am N-Terminus der intrazellulären Schleife 2 (ICL-2) und die TERR-Sequenz am C-Terminus der intrazellulären Schleife 3 (ICL-3) von noch größerer Bedeutung, denn Gruppen-Mutationen verhindern entweder komplett die Oberflächenexpression des Rezeptors (erstere) oder reduzieren diese sehr stark (letztere). Sowohl ICL-2 als auch ICL-3 sind an der Interaktion mit dem G-Protein $G_{q/11}$ beteiligt, jedoch auf unterschiedliche Art und Weise. Sequenzen in ICL-2 beeinflussen eher die Kopplung, wohingegen Regionen in ICL-3 bevorzugt bei der Aktivierung von $G_{q/11}$ eine Rolle spielen.

Aufgrund der bisher erhaltenen Ergebnisse wurde die Rolle der Aminosäuren der DRY- und TERR-Sequenz näher untersucht. Für bovines Rhodopsin wurde gezeigt, dass das Arginin im DRY motif (R3.50 Nummerierung entsprechend Ballesteros und Weinstein) (Ballesteros et al., 1998) und ein Glutamat am cytosolischen Ende der Transmembran 6 (Ballesteros/Weinstein Position 6.30), entsprechend dem Glutamat in der TERR-Sequenz des B_2 Rezeptors, interhelikal interagieren, wobei sie Rhodopsin in seiner inaktiven Konformation halten. Diese Interaktion in bovinem Rhodopsin ist auch bekannt als “ionic lock” (“ionische Sperre”) und wird vermutlich als Folge von Rezeptor-Aktivierung unterbrochen. Da der B_2 Rezeptor einer der ganz wenigen Peptidrezeptoren der G-Protein-gekoppelten Rezptoren ist, bei dem neben Arginin 3.50 auch Glutamat 6.30 konserviert ist, wurde im dritten Teil der Doktorarbeit die strukturelle und funktionelle Rolle dieser beiden Aminosäuren im B_2 Rezeptor analysiert. Zusätzlich wurde die Hypothese überprüft, ob diese beiden Aminosäuren auch im B_2 Rezeptor eine ionische Bindung bilden, die daran beteiligt ist, seinen inaktiven Zustand aufrecht zu erhalten. Dieses Ziel wurde durch die Generierung von zwei Punktmutationen des Rezeptors, R3.50A und E6.30A, und deren ausführliche biochemische und funktionelle Charakterisierung, verfolgt.
Unsere Studie zeigt, dass R3.50 eine duale Rolle spielt: es ist (i) entscheidend für die produktive Interaktion mit G-Proteinen und (ii) ist wahrscheinlich Teil einer Interaktion, in der es die Transmembrandomänen TM3 und TM6 durch eine Ionenbindung mit Glutamat 6.30 und über einer Wasserstoffbrücke mit Threonin 6.26 verknüpft, wodurch die inaktive Konformation des Rezeptors in Abwesenheit von Agonisten stabilisiert wird. Auf den zweiten Punkt deutet die Tatsache, dass – mit Ausnahme der G-Protein Aktivierung – beide Mutanten, R3.50A und E6.30A, ein beinahe identisches Muster konstitutiver und semi-aktiver Aktivität zeigen, wie man es erwarten würde, wenn beide Aminosäuren miteinander interagieren.

Glutamat 6.30 dürfte einen zusätzlichen Interaktionspartner haben, da seine Mutation quantitativ immer stärkere Effekte zeigte als die Mutation von Arginin 3.50. Da eine saure Aminosäure an Position 6.30 unter den Peptiderezeptoren der G-Protein-gekoppelten Rezptoren nicht konserviert ist und häufig durch ein positiv geladenes Arginin oder Lysin ersetzt ist, müssen in dieser Unterfamilie unterschiedliche Mechanismen zur Stabilisierung des inaktiven Zustands existieren.

Die G-Protein-gekoppelten Rezptoren sind ideale therapeutische Angriffspunkte, da sie einerseits auf der Zelloberfläche lokalisiert relativ gut zugänglich sind, andererseits durch ihre selektive Bindung endogener Liganden und ihre zellspezifische Expression hochspezifisch wirken. Genauere Kenntnisse über Strukturen, Unterschiede und Gemeinsamkeiten in ihrer Regulation, zu denen auch die vorliegende Arbeit ihren Beitrag leistet, sollten es ermöglichen ihr therapeutisches Potential durch rationale, struktur-basierte Medikamentenentwicklung noch besser auszuschöpfen.

B INTRODUCTION

B.1 The kallikrein-kinin system (KKS)

B.1.1 Historic background

In 1925 the German surgeon Emil-Karl Frey observed a strong reduction in blood pressure when he injected the urine of humans into dogs. Together with the biochemist Heinrich Kraut, he attributed this effect to a substance with potential biological effects (Frey & Kraut 1926; Frey, 1926). This substance was later termed kallikrein (KLK) (Kraut et al., 1930). In 1937, the biochemist Eugen Werle found that KLK is a proteolytic enzyme, which liberates the biologically active polypeptide kallidin (KD) from a plasma protein termed kininogen (Werle et al., 1937). Werle also observed the degradation/inactivation of kinins, identified these inactivators as peptidases, and termed them "kininases" (Werle & Grund, 1939).

In 1949, it was discovered that trypsin, when incubated with blood, releases an agent that contracts the guinea-pig ileum (Andrade & Rocha e Silva et al, 1949). Since the response of this tissue developed slowly, the authors called the agent "bradykinin" (brady = slow). Later, bradykinin (BK) was purified and identified as a nonapeptide (Andrade & Rocha e Silva et al, 1956). The exact sequence of BK was published by Swiss chemists and the nonapeptide could thereafter be chemically synthesized (Boissonnas et al., 1960).

B.1.2 Kinins

Nowadays, the peptides that are referred to as kinins comprise BK and Kallidin (Lys-BK) and their carboxypeptidase cleavage products, des-Arg^{9}-BK and des-Arg^{10}-Kallidin. BK is a positively charged nonapeptide (Arg-Pro-Pro-Gly-Phe-Ser-Pro-Phe-Arg) that can be found in almost all secretions of the body, i.e. urine, saliva, and sweat, but also in feces and several tissues, such as the heart, vasculature, blood, kidneys, liver, skin, small intestine, colon, pancreas, salivary glands, reproductive organs, lungs, and adrenal glands (Campbell et al., 1993); (Hibino et al., 1994); (Madeddu et al., 2001); (Meneton et al., 2001); (Patel et al., 1999); (Schremmer-Danninger et al., 1999). KD has been found in the heart, urine, and blood circulation (Campbell et al., 1999); (Duncan et al., 2000).

BK is released from its precursor, the high molecular weight kininogen (HMWK), through the action of plasma kallikrein. Kallidin is released from high and low molecular weight kininogen

through tissue kallikrein. BK can also be derived from KD by several amino peptidases through cleavage of the amino-terminal lysine. Cleavage of the carboxy-terminal arginine of BK and KD by carboxypeptidases yields the truncated derivatives des-Arg^{9}-BK and des-Arg^{10}-Kallidin.
BK is produced in the body in response to many kinds of injuries and under inflammatory conditions. It is one of the most potent elicitors of pain and participates in normal physiological regulation (Stewart, 2004).

B.1.3 Kinin receptors

The effects of the kinins are mediated by their binding to the bradykinin receptors, subtypes B_1 and B_2. These receptors belong to family A of the superfamily of G protein-coupled receptors (GPCRs) and share 36% sequence identity. In Figure B-1 a schematic view of the human B_2 receptor (B_2R) is shown with comparison to the B_1 receptor (B_1R). The region of the potential Helix VIII in the C-terminus before the palmitotylation site is highly conserved. On the other hand, the sequence after Helix VIII shows no conservation (Menke et al., 1994) and is much shorter for the B_2 receptor (Hess et al., 1992).
BK and KD are selective high affinity ligands of the B_2 receptor, whereas des-Arg^{9}-BK and des-Arg^{10}-Kallidin are selective ligands of the B_1 receptor. The B_2 receptor is generally present in a wide variety of tissues, in contrast to the B_1 receptor, which is expressed *de novo* under certain pathological conditions like inflammation and sepsis.
Genomic sequencing of the human chromosomal regions encoding the B_1 and B_2 receptors revealed that the genes are located in a tandem orientation with the B_2 receptor gene being proximal to the B_1 receptor gene, separated by an intergenic region of only 12 kb (Cayla et al., 2002). The close proximity of the two genes strongly suggests that they evolved from a common ancestor by a gene duplication event.
B_1R is one of few receptors belonging to GPCR family A which does not get internalized (Austin et al., 1997). Upon ligand stimulation, it responds with translocation to caveolae but these remain essentially on the cell surface (Sabourin et al., 2002); (Lamb et al., 2002). No phosphorylation of B_1R either under basal conditions or after stimulation has been detected (Blaukat and Muller-Esterl, 1997); (Pizard et al., 1999).
The full-length human B_2R is composed of 391 amino acids with a calculated molecular weight of 41 kDA (AbdAlla et al., 1996). In most primary and cultured cells, B_2R is modified by

complex glycosylation resulting in a broad 60-80 kDa band after electrophoretic separation (Blaukat et al., 1996).

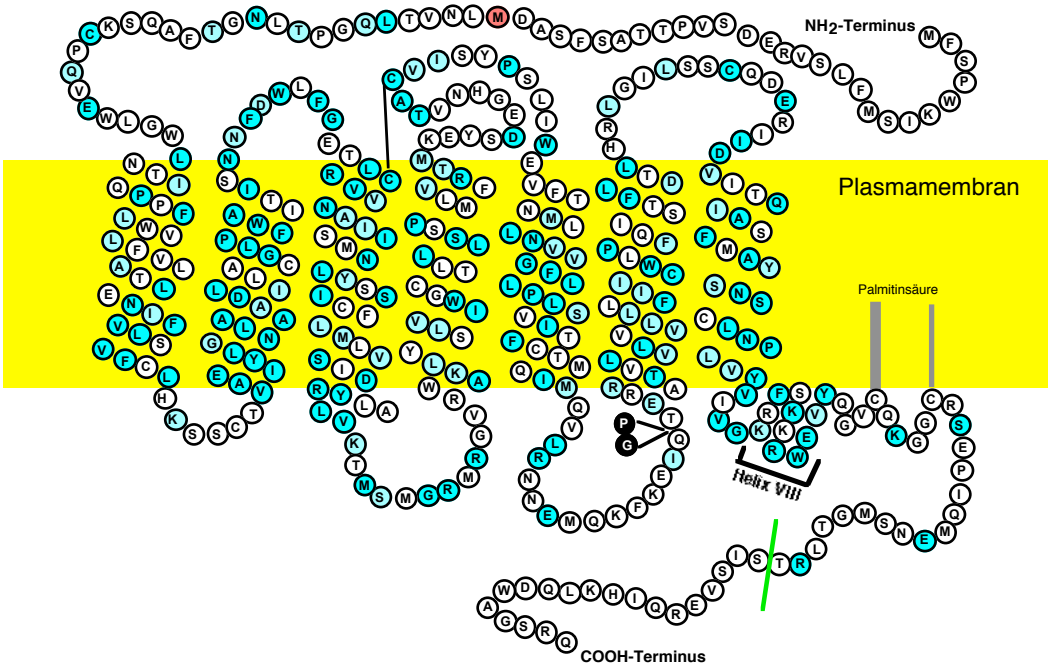

Fig. B-1: Schematic view of the sequence of the human B_2 receptor compared to the B_1 receptor.

Depicted are the seven transmembrane domains, the three extracellular and intracellular loops and the position of the potential Helix VIII in the cytosol. Dark blue or light blue highlighted circles indicate that the corresponding amino acid is identical or similar, respectively. The third methionine, which is the starting point of all expression constructs used in this work, is marked red. The primary palmitoylation point at Cys^{324} is shown with a wide grey bar, the alternative position Cys^{329} with a thinner grey bar. The green line marks the shorter B_1 C-terminus. The black symbols (P, G) indicate additional residues present in the B_1 receptor.

B.1.4 The signaling pathways of the kinin receptors

The kinin receptors couple after ligand stimulation to $G\alpha_{q/11}$ proteins leading to activation of phospholipase C-β (PLC-β) and subsequent generation of second messengers: inositol-1,4,5-triphosphate (Ins 1,4,5-P_3), diacylglycerol (DAG) and release of intracellular calcium. In the blood vessels this increase in intracellular calcium can activate the NO/cGMP pathway that primarily mediates the strong hypotensive effect. NO diffuses from the endothelium to the smooth muscle where it activates guanylate cyclase. Prostaglandin I_2 (prostacyclin) is another secondary mediator frequently released by kinins from the endothelium. Prostacyclin stimulates

cyclic AMP production in the smooth muscle cells. DAG and calcium activate several isoforms of protein kinase C (PKC) that participate in a number of cellular signaling pathways, including those that control cell proliferation (Tippmer et al., 1994); (Nishizuka, 1992).

Kinin receptors can also activate phospholipase A_2 and D as well as sphingosine kinase resulting in increased cellular concentrations of lipidic second messengers: arachidonic acid (subsequently converted to prostaglandins), phosphatidic acid, and sphingosine 1-phosphatase (Burch and Axelrod, 1987); (Blaukat et al., 2000); (Blaukat et al., 2001).

Bradykinin induced $G\alpha_i$ stimulation has also been observed in several cell types. This involves the activation of the ERK/MAPK cascade and mitogenic signaling in certain tumour cell lines (Liebmann, 2001). The B_2 receptor gene knockout mouse exhibits elevated blood pressure, increased heart/body weight ratio and an exaggerated pressure response to angiotensin II infusion and chronic dietary salt loading (Madeddu et al., 1997).

B.1.5 Regulation of kinin receptors

The kinins have a very short half-life, <15 s in the plasma (Roberts and Gullick, 1990). The physiologically active concentrations are presumably only locally generated. Kininases can cleave the kinins into shorter peptides with other biological specificities or into inactive peptides. Kininase I is also known as ACE (angiotensin I converting enzyme). It is localized primarily to the pulmonary vasculature. It destroys almost all circulating BK on a single passage through the pulmonary circulation. ACE is a carboxypeptidase, which cleaves BK successively at the 7-8 and 5-6 bonds. ACE not only degrades the kinins but also transforms inactive Angiotensin I into active Angiotensin II. This provides a connection between the KKS and the RAS (Renin Angiotensin System). Any circulating BK that escapes cleavage by ACE can be cleaved by circulating carboxypeptidase N (CPN), which removes the C-terminal Arg residue. The resulting [des-Arg^9]-BK is inactive at B_2 receptors but is the preferred agonist for B_1 receptors. BK is also cleaved by neutral endopeptidases (NEP; neprilysin), which are membrane-bound in much of the vasculature. They cleave BK at the Phe^5 residue. Finally, BK is also cleaved by aminopeptidases, which remove the N-terminal arginine residue. Any single cleavage of the peptide chain totally inactivates BK for action at the B_2 receptors. Thus, the development of peptide antagonists based on BK would likely necessitate blockage of the activities of all these enzymes. This holds true for peptidic antagonists but it is not decisive in development of small compounds.

B.2 G proteins and G protein-coupled receptors (GPCRs)

B.2.1 G proteins

The binding of extracellular ligands to GPCRs modulates their ability to catalyze guanine nucleotide exchange on intracellular heterotrimeric G proteins. The G proteins were discovered through intensive research on adenylylcyclase, an enzyme that converts ATP (Adenosin-5´-triphosphate) to cAMP (cyclic Adenosin-3´, 5´-monophosphate). That gave rise to the question how the signal is mediated from the receptor to the adenylylcyclase and through which mechanisms. Rodbell et al. showed that a hormone could activate the adenylylcyclase only when GTP is present (Rodbell et al., 1971). Because this protein could bind GTP, it was called GTP-binding protein or short form: G protein. Sternweis et al. and Northup et al. could purify, isolate and characterize this stimulating G protein, termed Gs (Sternweis et al., 1981); (Northup et al., 1980). The finding that treatment of the cells with pertussis toxin blocked the inhibition of the adenylylcyclase (Katada and Ui, 1979) gave rise to the characterization of the inhibitory G_i proteins (Bokoch et al., 1984); (Katada et al., 1984).

In the meantime more G proteins have been discovered and it is now clear which important impact they have by transmitting the signals between the receptors on the cell surface and the intracellular effector proteins. For their experiments, which lead to the discovery of the G proteins, A.G. Gilman and M. Rodbell were awarded the Nobel price in Medicine 1994.

B.2.2 Functionality

G proteins are heterotrimeric, composed of α-, β- and γ-subunits. In the inactive state the α-subunit is GDP-bound and displays a high affinity for the βγ-subunit. Through agonistic binding to the receptor, GDP is exchanged to GTP. That gives rise to a conformational change which provides the dissociation of the active α-subunit from the βγ-subunit. The GTP bound Gα and the βγ-complex are then able to interact with different effector enzymes and ion-channels leading to the observed physiological response. Because of its intrinsic GTPase activity, the Gα-subunit hydrolyzes bound GTP to GDP; the GDP-bound α-subunit then re-associates with the βγ-subunit returning all subunits to the inactive state.

The α-subunit has a molecular weight of 39-52 kDa, the β-subunit 35-36 kDa and the γ-subunit ~7-10 kDa. The α-subunit is divided into four groups according their DNA-sequence homology:

G_s, G_i, G_q and G_{12}. G_q stimulates the β-isoform the Phospholipase C (Taylor et al., 1991); (Lee et al., 1992).

B.2.3 Superfamily of GPCRs

GPCRs, or seven transmembrane receptors, constitute of one of the largest superfamilies in the human genome (Lagerstrom and Schioth, 2008). All GPCRs display a similar structure. They are composed of a single polypeptide chain of variable length that spans the lipid bilayer seven times, forming transmembrane helices and alternating extracellular and intracellular loops.

Based on sequence similarity, the GPCRs are divided into three subfamilies: Family A: rhodopsin/β-adrenergic-receptor-like, family B: glucagon-receptor-like and family C: metabotropic glutamate neurotransmitter receptor-like.

Family A is by far the largest family with more than 300 identified receptors (Fig. B-2). The members of this family do not share a high overall sequence identity but they do have a few highly conserved residues and motifs (ca. 20 amino acids in all) in analogous positions, mostly located in the transmembrane regions. The E/DRY sequence at the cytosolic end of transmembrane domain III (TMD III) is one of the most conserved motifs. Another highly conserved sequence is the NPxxY sequence (where x usually represents a hydrophobic residue and N is occasionally substituted for D) located at the C-terminus of TMD VII. High conservation of protein sequences often indicates important functional and structural roles.

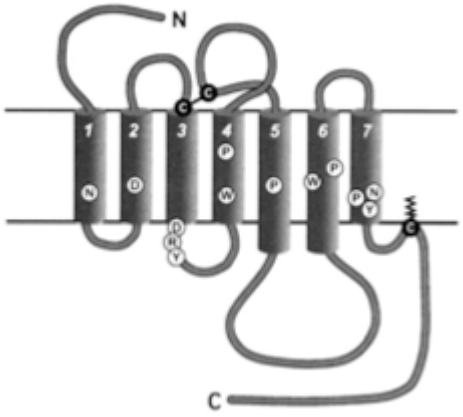

Fig. B-2: Family A: rhodopsin/β-adrenergic-receptor-like. Family A receptors are characterized by a series of highly conserved residues (*black letter in white circles*). A majority of the receptors have a palmitoylated cysteine in the carboxy-terminal tail causing formation of a putative fourth intracellular loop (Figure taken from U. Gether, Endocrine Reviews, Vol: 21: 90-113, 2000).

Family B (glucagon-receptor-like GPCRs) includes approximately 20 different receptors of a variety of peptide hormones and neuropeptides, such as vasoactive intestinal peptide (VIP), calcitonin and glucagon. Characteristic of family B receptors is a large extracellular amino terminus containing several cysteines, forming a network of disulfide bridges. (Fig. B-3, left). Family C receptors include among others the metabotropic glutamate and γ-aminobutytic acid (GABA) receptors, calcium receptors and putative taste receptors (Fig. B-3, right).

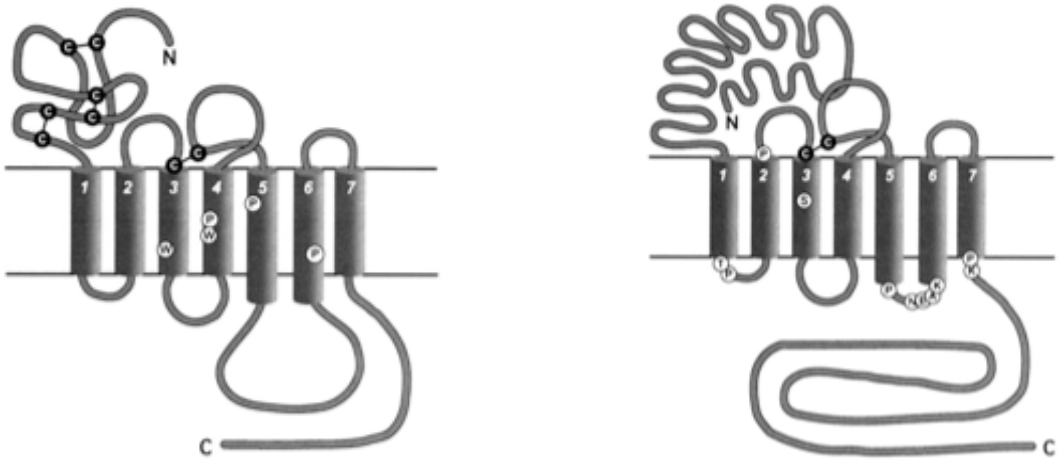

Fig. B-3: Family B: glucagon-receptor-like and family C: metabotropic glutamate neurotransmitter receptor-like GPCRs. Family B receptors (left) are characterized by a long amino terminus containing several cysteines presumably forming a network of disulfide bridges. Family C receptors (right) are characterized by a very long amino terminus (~600 amino acids). Another characteristic of the C receptors is a very short and highly conserved third intracellular loop (Figure taken from U. Gether, Endocrine Reviews, Vol: 21: 90-113, 2000).

B.2.4 The highly conserved DRY motif

The E/DRY or DRY motif is located at the boundary between TMD III and intracellular loop 2 of class A GPCRs (rhodopsin family). It is one of the most intensively researched conserved motifs and is named for the single letter designation of its constituent amino acids, Asp-Arg-Tyr. Intensive work has been focused on understanding the mechanisms of receptor activation and interaction with G proteins, and both the acidic (Asp) and basic (Arg) residues are known to be important for isomerization of receptors between inactive and activated conformations (Flanagan, 2005).

One part of this thesis focused on the role of the highly conserved arginine positioned at R3.50 (numbering according to the numbering scheme of Ballesteros and Weinstein) (Ballesteros et al., 1998) in the DRY motif. The numbering scheme from Ballesteros and Weinstein is used here and

later in this study. According to the numbering scheme, the most conserved residue in a transmembrane segment is named by the number of the helix followed by the number 50. Upstream residues are then named by counting down, downstream residues by counting up from 50. From the structure of some prototypical receptors belonging to family A GPCRs it is known that this basic arginine R3.50 forms stabilizing interactions with the neighboring aspartic acid or glutamic acid (E3.49) and/or with another charged residue (E6.30) on helix 6 (Ballesteros et al., 2001); (Angelova et al., 2002); (Greasley et al., 2002); (Shapiro et al., 2002); (Zhang et al., 2005), thereby constraining GPCRs in the inactive conformation. The crystal structure of the ground state of rhodopsin indicates that the highly conserved arginine is engaged in a double salt bridge with the adjacent glutamic acid (E3.49) and with the glutamic acid (E6.30) on helix 6 (Palczewski et al., 2000); (Teller et al., 2001), suggesting that disruption of these salt bridges may be a key step in receptor activation (Cohen et al., 1993); (Greasley et al., 2001); (Angelova et al., 2002). These stabilizing interactions in bovine rhodopsin keeping the receptor in its inactivated state are also known as the "ionic lock". Mutation of the glutamic acid/aspartic acid of the E/DRY motif has been proposed to induce a conformational change that repositions the arginine from its polar pocket, resulting in the ability of some GPCRs to adopt an active conformation (Scheer et al., 1996); (Scheer et al., 1997); (Cotecchia et al., 2002). For the human bradykinin B_2 receptor it is, to our knowledge, not known if the highly conserved arginine R3.50 forms stabilizing interactions with the neighboring aspartic acid (D3.49) and/or with another charged residue (E6.30) on helix 6 or other additional residues. Therefore we set out to investigate this question with a focus on residues R3.50 and E6.30 (Results section E.3).

B.2.5 Crystal structures of GPCRs

The first crystal structure of a GPCR was that of inactive bovine rhodopsin (Palczewski et al., 2000). In 2007 the structure of the human β_2-adrenergic receptor (β_2AR) was solved (Rasmussen et al., 2007). It was crystallized in a complex with an antibody fragment (β_2AR-Fab). This was followed by the higher resolution structure of an engineered β_2AR with T4 lysozyme replacing the third cytoplasmic loop (β_2AR-T4) (Cherezov et al., 2007). These structures contain the inverse antagonist carazolol. They define the overall architecture of β_2AR and the structure of the ligand-binding pocket. In 2008 the crystal structure of the turkey β_1-adrenergic receptor was reported (Warne et al., 2008). This 2.7 Å resolution crystal structure is in complex with the

inverse antagonist cyanopindolol. The modified receptor was thermostably improved by earlier extensive mutagenesis. The ligand-binding pocket contains 15 side chains from amino acids residues in four transmembrane α-helices and extracellular loop 2. In the crystal structure of the β_2AR (Rasmussen et al., 2007) it is argued that the "ionic lock" (described in B.2.4) is not present in the inactive conformation because the distance (6.2 Å) between R131 (R3.50) and E268 (E6.30) is too long for formation of a hydrogen bond. This suggests that at least for this receptor, the ionic look is not an essential feature of the inactive state. In Fig. B-4 a comparison of the β_2AR and rhodopsin structures is shown (Rasmussen et al., 2007).

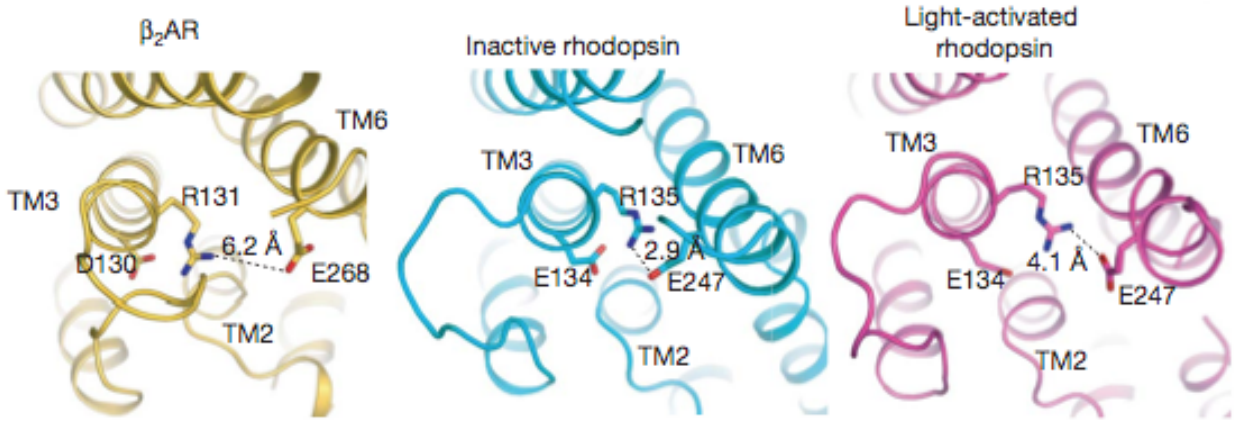

Fig. B-4: Comparison of β_2AR and rhodopsin structures (Rasmussen 2007): β_2AR is compared with structures of inactive and light-activated rhodopsin around the conserved E/DRY sequence in TM3. The dashed line shows the distance between the arginine in TM3 and glutamate in TM6.

The crystal structure of the ligand-free GPCR opsin was recently reported (Park et al., 2008). In 2008 the first crystal structure of a GPCR in its activated state was reported (Scheerer et al., 2008). In this structure, a synthetic peptide derived from the main receptor binding site of the heterotrimeric G protein, the carboxy terminus of the α-subunit (GαCT)-stabilizes Opsin. Compared with the inactive receptor structures, the hallmarks of the activated Ops*-GαCT complex structure are an outward tilt of transmembrane helix 6 and a smaller motion of transmembrane helix 7 at the inner surface of the cell membrane. These movements open a cleft that presents the ligand-binding site to the G protein. Further, the "ionic lock" is broken and arginine R3.50 is released from E3.49 and E6.30. In Scheerer and colleagues' opsin complex the activating ligand, all-*trans* retinal, is not present. It is well known that active conformations of unliganded receptors, including opsin, exist in equilibrium with the inactive state (Scheerer et al., 2008).

B.3 Receptor antagonists

A receptor antagonist is a type of receptor ligand or drug that does not provoke a biological response by itself upon binding to a receptor, but blocks or dampens agonist-mediated responses. In pharmacology, antagonists have affinity but no efficacy for their cognate receptors, and their binding will disrupt the interaction and inhibit the function of an agonist or inverse agonist at the receptor. The effects of antagonists are mediated by binding either to the active site or allosteric sites on receptors. They may also interact at unique binding sites that are not normally involved in the biological regulation of the receptor's activity. The longevity of the antagonist-receptor complex determines whether the antagonistic activity is reversible or irreversible. The majority of antagonists achieve their potency by competing with endogenous ligands or substrates at structurally defined binding sites on receptors (Hopkins and Groom, 2002). Antagonists of GPCRs are widely used drugs. Two classical examples are angiotensin receptor blockers (ARBs) and β-adrenergic blockers (β blockers), which block the angiotensin II type 1 receptors and β-ARs, respectively.

A milestone in BK antagonist research was the discovery of icatibant, also known as HOE-140 or Je049. This was achieved in Germany in 1991 by investigators at Hoechst. They introduced a tetrahydroisoquinoline-3-carboxylic acid (Tic) and an octahydroindole-2-carboxylic acid (Oic); the latter change blocked the action of carboxypeptidase N (CPN). HOE-140 was the first BK antagonist with high potency and duration of action in vivo (Lembeck et al., 1991). The drug Firazyr (icatibant) was launched in 2008 in all EU countries for the treatment of hereditary angioedema (HAE) through inhibition of the B_2R. There are, however, also some reports that icatibant might not always act entirely as an antagonist. (Houle et al., 2000) found that a GFP (green fluorescent protein)-fusion protein of the rabbit B_2R (80% sequence identity with human B_2R) responded to prolonged incubation with icatibant with slow translocation into the cells. Liebmann showed that in some tumor cell lines icatibant acted as a mitogenic agonist, stimulating cell growth and ERK1/2 phosphorylation (Liebmann, 2001). The latter was also reported for HEK 293 cells expressing recombinant B_2R (Morissette et al., 2007).

The next major improvement in the development of BK antagonists came from the Stewart laboratory with the introduction of α-(2-indanyl)-glycine (Igl) (Gera and Stewart, 1996); (Stewart et al., 1996). This introduction was done in for example B9430 with a D-Igl at position 7 and L-Igl at position 5. This gave an extremely potent and long-acting antagonist highly resistant to kininases. B9430 exhibits high potency at B_2 receptors but it is also a quite potent antagonist for

B_1 receptors (Stewart et al., 1996). This property suggests that it may also have promise as an agent for treatment of chronic, as well as acute, inflammation.

Non-peptide bradykinin B_2 antagonists that are potent, specific and orally available have been reported by investigators at Fujisawa (Griesbacher and Legat, 1997), Sanofi (Pruneau et al., 1999) and Novartis (Dziadulewicz et al., 2000). Until now there are no reports of clinical trials of non-peptide BK antagonists. The Stewart laboratory reports that non-peptide BK antagonists have been developed as anti-cancer agents (Stewart, 2004). Potent antagonists such as B9430 did not inhibit cancer cell growth in vitro or in vivo. But when B9430 was cross-linked at the amino end with a suberimidyl linker, the dimeric product, B-9870, was a potent anti-cancer compound, both in vitro and in vivo in nude mouse xenografts (Chan et al., 1996). B-9870 (also known as CU-201) is active against a wide range of cancers, and is under development at the US National Cancer Institute as a possible treatment for lung cancer (Chan et al., 2002).

B.4 Functional selectivity

In the past the definition of whether a ligand of a G protein-coupled receptor (GPCR) was considered an agonist, partial agonist or antagonist depended only on the resulting activation of the cognate G protein α-subunit(s) through the receptor after binding. An activated GPCR was generally assumed to be turned off by phosphorylation via GRKs (G protein-coupled receptor kinases), followed by recruitment of arrestins to the phosphorylated residues, which consequently resulted in sequestration of the receptor to intracellular compartments via clathrin-coated pits or caveolae. In recent years, however, it has become clear that stimulation of a GPCR may also result in G protein-independent activation of other signaling pathways. It is now widely accepted that different ligands can induce different receptor conformations which may result in differential activation of the various pathways (Perez and Karnik, 2005); (Vauquelin and Van Liefde, 2005); (Urban et al., 2007). Some terms for this phenomenon include functional selectivity, agonist-directed trafficking, and biased agonism. Recently, it has been suggested that the number of different terms should be limited by using the term “functional selectivity” or as a viable alternative, “ligand-induced differential signaling” (Urban et al., 2007). In the extreme case a functional selective ligand can act as both an agonist and an antagonist at one receptor. Better knowledge of the potential functionally selective conformations of receptors could be of great help when dealing with drug discovery. Drugs could then be developed that affect specific

conformations of a given GPCR that could then couple to specific signaling pathways that may, ultimately, lead to reduced side effects.

In the present study much work was done with icatibant and B9430 mostly known as antagonists for the B_2R. As seen later, both peptides seem to have the properties of being functional selective ligands upon coupling and activation of the wild type B_2 receptor.

C AIMS OF THE THESIS

A future rational, structure-based and therefore less expensive development of agonists and antagonists would greatly benefit from a better understanding of the regulation and signal transduction mechanisms of the G-protein-coupled receptors (GPCRs). Deeper insights into the similarities and, in particular, the differences in this regard between GPCR subfamilies and receptor subtypes should result in more specific drugs with fewer side effects.

The principal goal of this thesis was to investigate the role of the intracellular domains in the signal transduction and regulation of the human bradykinin B_2 receptor. B_2R belongs to the subfamily of the peptide receptors in the family of the rhodopsin/β-adrenergic-like GPCRs.

For the this purpose we applied the following working program:

- Pharmacological and biochemical characterization of the endogenously and recombinantly expressed wild type human bradykinin B_2 receptor, including receptor binding properties, internalization, and functional selectivity of various B_2 agonists and antagonists.
- Mutagenesis studies (either as point mutants or in groups of 3-5 amino acids to alanines) on the intracellular receptor domains to identify sequences participating in interactions with G proteins, receptor kinases and arrestins.
- Determination of the presence of the "ionic lock" and the role of the participating amino acids in the inactive human bradykinin B_2 receptor.

D MATERIAL AND METHODS

D.1 Material

D.1.1 Equipment

Balances:	
Analytic Balance, A 120 S (0-12 g range)	Sartorius, Göttingen
Analytic Balance, 3716MP (0-250 g range)	Sartorius, Göttingen
β-Counter:	
Liquid Scintillation Analyzer, Mod. 2300TR	Packard, Meriden, CT
β-γ-Counter, LB122	Berthold Technology, Canada
Cell Incubators:	
Type B5060 EC-CO_2	Heraeus Sepatech, München
Centrifuges:	
Kontron, Centrikon H-401 with rotor A8.24	Kontron Instruments, Eching
Heraeus, Varifuge 3.2 RS	Heraeus Sepatech, München
Heraeus, Sepatech Biofuge A (rotor 1230)	Heraeus Sepatech, München
Heraeus, Sepatech Biofuge A (rotor 3042)	Heraeus Sepatech, München
Clean Bench:	
BDK 7419, Mod. UVF 6.18S	BDK, Sonnenbühl-Genkingen
Herasafe type HS18/2	Heraeus Instruments, München
ELISA-Reader:	
DigiScan 400	ASYS Hitech GmbH, Austria
PCR Thermal Cycler:	
Primus type 25	MWG-Biotech, Ebersberg
Power supply:	
Type EPS 301	Amersham-Pharmacia-Biotech
Mod. 2103	LKB, Biochrom
Protein Transfer Appartus:	
XCell *SureLock*^{TM} Mini-cell	Invitrogen, Karlsruhe
Snap i.d. protein detection system	Millipore, Schwalbach, Germany
Sonifier:	

Type B12	Branson Sonic Power Company, Danburg
Spectral Confocal Microscope:	
Zeiss LSM 410	Carl Zeiss, Thornwood, NY, USA
Fluorescence Microscope:	
Olympus IX-70	Olympus Optical Co., LTD, Tokyo, Japan
Other Equipments:	
2D-Electrophoresis apparatus, HTLE-7000-02	CBS, Del Mare, USA
Dounce homogenizer, type 853202	B.Braun, Melsungen, Germany

D.1.2 Chemicals and materials

Chemicals for the molecular biology techniques

Gel extraction Kit	Qiagen (Hilden, Germany)
QIAprep Spin Miniprep (and Maxiprep) Kit	Qiagen (Hilden, Germany)
PCR primers	Invitrogen (Groningen, Netherlands)

Enzymes

Restrictase *Bam HI*	New England BioLabs (England)
Restrictase *Hind III*	Hybaid (Heidelberg, Germany)
Restrictase *Xho I*	New England BioLabs (England)
T_4-DNA ligase	Roche (Mannheim, Germany)
Taq DNA polymerase	Qiagen (Hilden, Germany)
Pfu DNA polymerase	Strategene (La Jolla, CA, USA)

Cell culture

DMEM –medium	PAA (Cölbe, Germany)
DMEM phosphate-free-medium	PAA (Cölbe, Germany)
Dulbecco´s PBS (1×)	PAA (Cölbe, Germany)
Trypsine/EDTA (1×)	PAA (Cölbe, Germany)
Poly-D-lysine hydrobromide	Sigma (Taufkirchen, Germany)
FuGENE 6	Roche (Mannheim, Germany)
FCS	PAA (Cölbe, Germany)

Hygromycin B	PAA (Cölbe, Germany)

Enzyme inhibitors

Aprotinin	Sigma (Taufkirchen, Germany)
Bacitracin	Sigma (Taufkirchen, Germany)
Captopril	Sigma (Taufkirchen, Germany)
Leupeptin	Sigma (Taufkirchen, Germany)
1.10-Phenantroline	MERCK (Darmstadt, Germany)
Pefabloc SC	MERCK (Darmstadt, Germany)
Pepstatin A	Sigma (Taufkirchen, Germany)
Sodium orthovanadate	Sigma (Taufkirchen, Germany)

Detergents

CHAPS	Sigma (Taufkirchen, Germany)
Nonident P-40	Sigma (Taufkirchen, Germany)
SDS	Serva (Heidelberg, Germany)
Triton X-100	Sigma (Taufkirchen, Germany)
Tween 20	Sigma (Taufkirchen, Germany)

Antibodies

Anti-HA-antibody, rat monoclonal clone 3F10	Roche (Mannheim, Germany)
Anti-HA matrix, immobilized, rat monoclonal	Roche (Mannheim, Germany)
Anti-HA Affinity Gel beads	Sigma (Taufkirchen, Germany)
Red Anti-HA Affinity Gel beads	Sigma (Taufkirchen, *Germany)*
Phospho-p44/42 MAPK mouse monoclonal	Cell Signaling (Beverley, MA)
P42 MAP Kinase mouse monoclonal	Cell Signaling (Beverley, MA)
Anti-β-arrestin mouse monoclonal	BD Transduction labs (Franklin Lakes, NJ)
HRP-labeled-anti-HA antibody, rat monocl.	Roche (Mannheim, Germany)
HRP-labeled goat anti-rabbit antibody	DAKO (Glostrup, Denmark)
HRP-labeled rabbit anti-rat antibody	DAKO (Glostrup, Denmark)
HRP-labeled horse anti-mouse antibody	New England BioLabs, England

Radioactive chemicals

Myo-[2-^{3}H]-inositol (21Ci/mmol)	Perkin-Elmer Life Sciences (Boston, MA)
[2,3-Prolyl-3,4-^{3}H]bradykinin (108 Ci/mmol)	Perkin-Elmer Life Sciences (Boston, MA)
[^{3}H]NPC17731	Perkin-Elmer Life Sciences (Boston, MA)

Protein biochemistry

NuPAGE Novex 4-12 % Bis Tris Gel	Invitrogen (Karlsruhe, Germany)
NuPAGE LDS sample buffer	Invitrogen (Karlsruhe, Germany)
Nitrocellulose membrane 0.45 μm	BioRad (Munich, Germany)
Whatman Filterpaper Nr.1	Whatman, Ammerbuch, Germany
HyperFilm ECL	Amersham (Buckinghamshire, UK)
Chemiluminescence's reagents plus	Perkin-Elmer Life Sciences (Boston, MA)

Miscellaneous

AG 1-X8 anion exchange columns	BioRad (Munich, Germany)
Sulfo-NHS-SS-Biotin	Pierce (Rockford, IL)
Bradykinin	Bachem (Heidelberg, Germany)
Icatibant	Jerini AG (Berlin, Germany)
Liquid scintillation mixture	ZINSSER ANALYTIC (Frankfurt, Germany)
Micro BSA protein assay reagent	Pierce (Rockford, IL)

• B9430 was a generous gift from Dr. John M. Stewart (University of Colorado Health Sciences Center, Denver, CO)

• All other reagents were of analytical grade and are commercially available from MERCK, SIGMA and ROTH.

D.1.3 Strains and cell lines

***E. coli* Top 10 (Invitrogen)**

Lab. Strain # 1557

Genotype: F^- mcrA Δ(*mrr-hsd*RMS-*mcr*BC) ϕ80*lac*ZΔM15 Δ*lac* X74 *deoR* A1 *ara*D139 Δ(*ara-leu*)7697 *gal*U *gal*K *rps*L (Str^R) *end*A1 *nup*G

***Flp-In™T-Rex™-293* (Invitrogen)**

Cell type: Human Embryonic Kidney (HEK) cells

Cytogenetics: 2n=46

This cell line contains a single stably integrated FRT site at a transcriptionally active genomic locus.

Human foreskin fibroblasts (HF-15)

Provided generously from Prof. Roscher (Forschungszentrum der Univ. Kinderklinik der LMU, Munich, Germany)

D.1.4 Expression vectors

pcDNA5/FRT vector

Comments for pcDNA/FRT

CMV promoter: bases 232-819

forward priming site: bases 769-78
T7 promoter/priming site: bases 863-882
Multiple cloning site: bases 895-1010
BGH reverse priming site: bases 1022-1039
BGH polyadenylation signal: bases 1028-1252
FRT site: bases 1536-1583
Hygromycin resistance gene (no ATG): bases 1591-2611
SV40 early polyadenylation signal: bases 2743-2873
pUC origin: bases 3256-3929 (complementary strand)
bla promoter: bases 4935-5033 (complementary strand)
Ampicilin (*bla*) resistance gene: bases 4074-4934 (complementary strand)

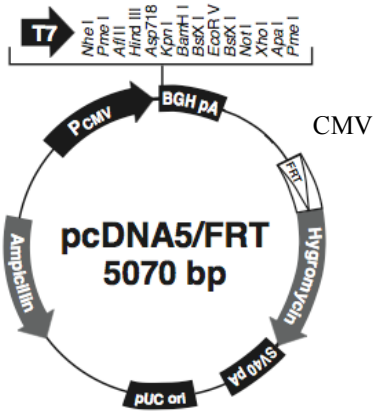

Fig. D-1: Schematic representation of the pcDNA5/FRT (Invitrogen).

The vector was designed for stable expression of the gene of interest in mammalian hosts. It has a multiple cloning site that contains cleavage sites for several common restriction endonucleases.

pOG44 vector

Comments for pOG44 vector:
CMV promoter: bases 234-821
Synthetic intron: bases 871-1175
FLP gene: bases 1202-2473
SV40 early polyadenylation signal: bases 2597-2732
pUC origin: bases 3327-3993
Ampicilin resistance gene: bases 4138-4998

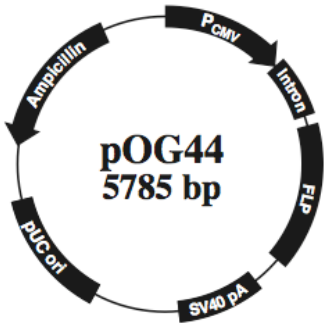

Fig. D-2: Schematic representation of the vector pOG44 (Invitrogen).

This vector expresses the Flp recombinase under the control of the CMV promoter. Flp recombinase is a member of the integrase family of recombinases, which mediates a site-specific recombination reaction between interacting DNA molecules via pairing of interacting FRT (*FLP* Recombinase Target) sites.

D.1.5 Oligonucleotides used as primers for PCR amplification

General primers:

CMV SE	5'-GTA CAT GAC CTT ATG GGA CTT TCC-3'
BGH AS	5'-GGC AAC TAG AAG GCA CAG TCG AGG-3'
Bam HI - B_2R SE	5'-GGATCC*ATGCTCAATGTCACCTTGC-3'
Xho I - B_2R AS	5'-CTCGAG*TTTGCTCACTGTCTGC-3'
Bam HI - GFP SE	5'-GCTGGATCC*ATGGTGAGCAAGGGCGAGGAG-3'
Xho I - GFP AS	5'-ACATCTCGA*GTTACTTGTACAGCTCGTCCATGCC-3'

Chimera primers:

B_2**eYFP** SE	5'-GGACTGGGCAGGGAGCAGACAG**ATGGTGAGCAAGGGCGAGGAG**-3'

* underlined sequence represents the restriction site for the indicated restrictase.

All other primers were designed following these standard rules:

- the length of primer complementary to the template should be 18-25 nucleotides
- the G+C content should be between 40 and 60%
- „GC clamp" at the 3' end
- the melting temperature was calculated by the formula:

$$T_m \text{ (in C°)} = 2(A+T) + 4(G+C)$$

where (A + T) is the sum of the A and T residues and (G + C) is the sum of the G and C residues in the oligonucleotide, which should not be less than 50°C.

D.1.6 Computer programs and Data analysis

- Adobe Acrobat 7.0 Professional
- EndNote 8.0
- Internet (Firefox, Safari)
- MacVector 7.2.3
- Microsoft Office 2004 (Word, Excel, Powerpoint)
- All data analysis was performed using GRAPHPAD PRISM for Macintosh, Version 4.0c (GraphPad Software, Inc., San Diego, CA, USA). Data were assessed by appropriate analysis of variance (ANOVA), with subsequent *post hoc* analysis using the Student-Newman-Keuls test. Alternatively, paired *t*-tests were used as indicated.

D.1.7 Solutions

Solutions used in molecular and cell biological methods

TAE buffer	40 mM Tris, 20 mM acetate, 2 mM EDTA pH 8.3
Loading buffer	30% (w/v) glycerol, 0.25% (w/v) bromophenol blue, 0.25% (w/v) xylencyanol FF, 0.25% (w/v) orange G
SOC medium	20g/l Bacto-tryptone, 5 g/l Bacto-yeast extract, 10 mM $MgCl_2$, 20 mM glucose, 10 mM NaCl, 10 mM KCl pH 7.0
LB growth medium	10 g/l Bacto-tryptone, 5 g/l Bacto yeast extract, 10 g/l NaCl

Solutions used in protein chemical methods

RIPA buffer	50 mM Tris-HCl, 150 mM NaCl, 1% Nonident P-40, 0.5% sodium deoxycholate, 0.1% SDS, 2 mM EDTA, pH 7.5
Lysis buffer	0.1% Triton X-100, 10mM Tris-HCl, 150 mM NaCl, 25 mM KCl, pH 7.4
Stripping buffer (BPA assay)	50 mM glutathione, 0.3 M NaCl, 75 mM NaOH, 1% FCS
Tris-buffered saline (TBS) buffer	50 mM Tris-base, 150 mM NaCl pH 7.5
TBST buffer	TBS buffer with 0.1% Tween 20
Blocking buffer	5% milk powder in TBS buffer containing 0.1% Tween 20
MOPS SDS Running buffer	From Invitrogen
Transfer buffer	From Invitrogen
LDS Sample buffer	From Invitrogen

Solutions used in pharmacological methods

Incubation buffer	40 mM PIPES, 109 mM NaCl, 5 mM KCl, 0.1% glucose, 0.05% BSA, 2 mM $CaCl_2$, 1 mM $MgCl_2$, 2mM bacitracin, 0.8 mM 1.10-phenantroline, 100 μM captopril, pH 7.0
Dissociation solution	0.2 M acetic acid, 0.5 M NaCl, pH 2.7

D.2 Methods

D.2.1 Molecular biological methods

D.2.1.1 Polymerase chain reaction (PCR)

DNA Fragments were amplified and mutagenized by PCR.

Primers were designed following these standard rules. Firstly, the length of primer complementary to the template should be 18-25 nucleotides to minimize problems of nonspecific annealing. Secondly, the G+C content should be between 40 and 60%. Thirdly, the melting temperature was calculated by the formula:

$$T_m \text{ (in C°)} = 2(A+T) + 4(G+C),$$

where (A + T) is the sum of the A and T residues and (G + C) is the sum of the G and C residues in the oligonucleotide, which should not be less than 50°C. The designed primers were synthesized by Invitrogen and are listed in section D.1.5.

Two important properties are required of a thermostable DNA polymerase used for mutagenesis of a plasmid template: an efficient proofreading activity and a lack of terminal transferase activity. Therefore, in all following reactions *Pfu* or *Taq* polymerase was used.

The PCR was used for the following purposes:

D.2.1.2 Attachment of the restriction sites

To clone a DNA insert into a vector, both were treated with two restriction enzymes that created compatible ends. Whereas cloning vector pcDNA5/FRT has sites for *Bam*HI and *Xho*I restriction endonucleases in its multiple cloning site (Fig. D-1), cleavage sites for above cited restrictases by DNA insert were introduced using PCR. For that pairs of primers with restriction sites for *Bam*HI in the 5' region of the sense primer and for *Xho*I in the 5' region of the anti-sense primer (section D.1.5). To improve restrictive reaction 3-4 additional base pairs (bp) were introduced at the 5' end of each primer (Fig. D-3). After PCR, the amplified DNA fragment was digested with the appropriate restriction enzymes and ligated into the multiple cloning site of the linearized vector.

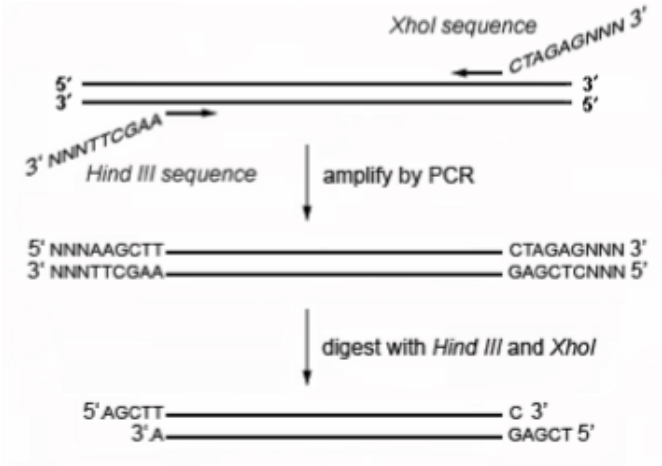

Fig. D-3: Cloning of PCR product by addition of restriction sites (Figure from Dr. Irina Kalatskaya).

Specific PCR primers were designed to amplify a region of interest with the *Hind* III (at the beginning) and the Xho I (at the end) recognition sequences for the restriction endonuclease included at the 5' end of the primer. To achieve high efficiency digestion, additional nucleotides were included on both sides of the restriction endonuclease sequence.

D.2.1.3 Site-directed mutagenesis

We used site-directed mutagenesis to design the constructs that were used in section E.2 and E.3. For the site-directed mutagenesis of the B_2R the so called "megaprimer method" was applied. This method uses three oligonucleotide primers and two rounds of PCR. One of the oligonucleotides is mutagenic, containing the desired base substitution(s), and the other two are forward and reverse primers that lie upstream and downstream from the binding site for the mutagenic oligonucleotide. The flanking primers were complementary to sequences in the cloned gene or to adjacent vector sequences. The mutagenic primer was oriented towards the nearer of the flanking primers so that the length of the megaprimer was kept to a minimum (Fig. D-4, A).
The mutagenic oligonucleotide was designed to a length of 20-35 bases, depending on how many bases had to be changed for the desired mutations. The mutation, and therefore the mismatched region of the primer, was located in the middle of the primer with at least 10-15 correctly matched bp on each side of the mismatched region (for less than 3 miss-matching bp).

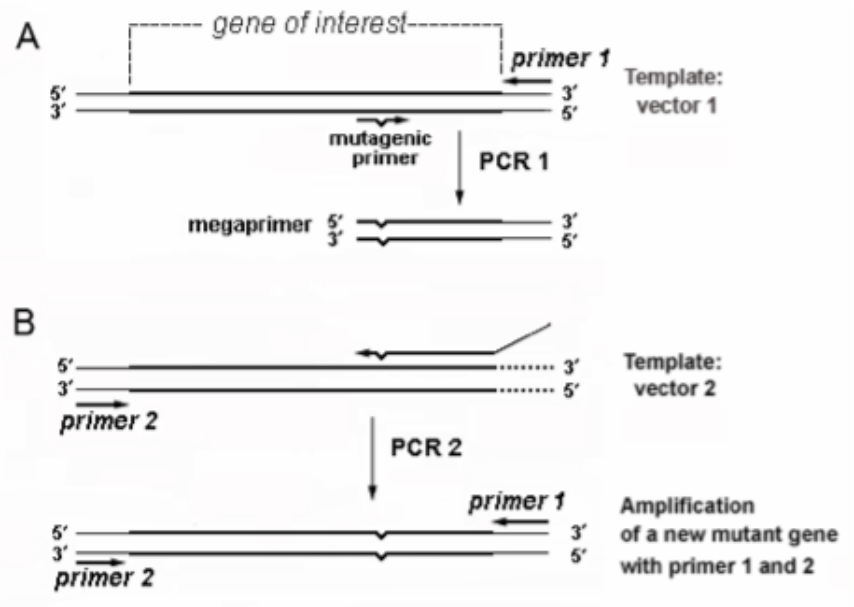

Fig. D-4: The principle of the "megaprimer method" (Figure from Dr. Irina Kalatskaya).

A) PCR1 was performed with a mutagenic primer and an outside primer (primer 1) to generate and amplify a double-stranded megaprimer.

B) The "megaprimer" was purified and used with an additional outside primer (primer 2) in PCR2 to obtain the desired full-length mutant. To increase the efficacy of PCR2, the primer 1 was added to the reaction mixture and as template was wild type DNA embedded into another vector not containing a site for primer 1.

The first PCR was performed according to Table 1 using the mutagenic internal primer designed as it was described before and the first flanking primer (Figure D-4, A).

Tab. 1. Composition of the first PCR used in the megaprimer method.

Components	Working concentration	Stock	Volume
Template 1	0.1 µg	-	-
PCR buffer	1×	10×	3 µl
Pfu polymerase	0.05 U/µl	2.5 U/µl	0.6 µl
Primer 1	0.2 µM	10 µM	0.6 µl
Mutagenic primer	0.2 µM	10 µM	0.6 µl
DMSO	1×	5×	3 µl
dNTP	0.8 mM	10 mM	2.4 µl
H_2O	-	-	to 30 µl

The first PCR was carried out according to the following **cycle program 1**:

Denaturation	*92°C*	*3 min*
Cycle (25 ×)		
Denaturation	*92°C*	*30 sec*
Annealing	*50°C*	*30 sec*
Elongation	*72°C*	*60 sec/1000 bp*
Elongation	*72°C*	*10 min*
Storage	*4°C*	*∞*

The product of this first PCR – the "megaprimer" – was purified as described in section D.2.1.7. In the first and second PCR the used wild type templates were embedded into two different vectors. In this case the usage of primer 1 in the PCR 2 led to preferable amplification of the newly synthesized mutated DNA as to amplification of the wild type template (Fig. D-4, B). The reaction mixture of the PCR 2 was prepared using Template 2 (0.1 μg), Primer 1/Primer 2 (0.2 μM) and Megaprimer (50 ng/μl). The same amounts of *Pfu* polymerase, DMSO, dNTP and H_2O were used as in Table 1. A longer region of the template DNA was amplified using 35× cycles, annealing at 53°C and the first elongation for 90 sec. The final PCR product containing the desired mutation was separated by gel electrophoresis (section D.2.1.3) and purified from the agarose gel (section D.2.1.7).

D.2.1.4 Generation of the B_2eYFP chimera

The coding region of the B_2R and the enhanced yellow fluorescent protein (eYFP) were fused using the megaprimer method in a two-step reaction. The stop codon of the B_2R was omitted, whereas the first methionine of the eYFP-construct was included. A 43-bp chimera-primer containing the 22 bp encoding the C-terminal amino acids of B_2R followed by 21 bp encoding the proximal end of the eYFP gene (Fig. D-5, A). As described before, a megaprimer was prepared in the PCR 1 according to Table 1 using the pEYFPC-3 (CLONTECH) gene as template and chimera primer (Fig. D-5, B).

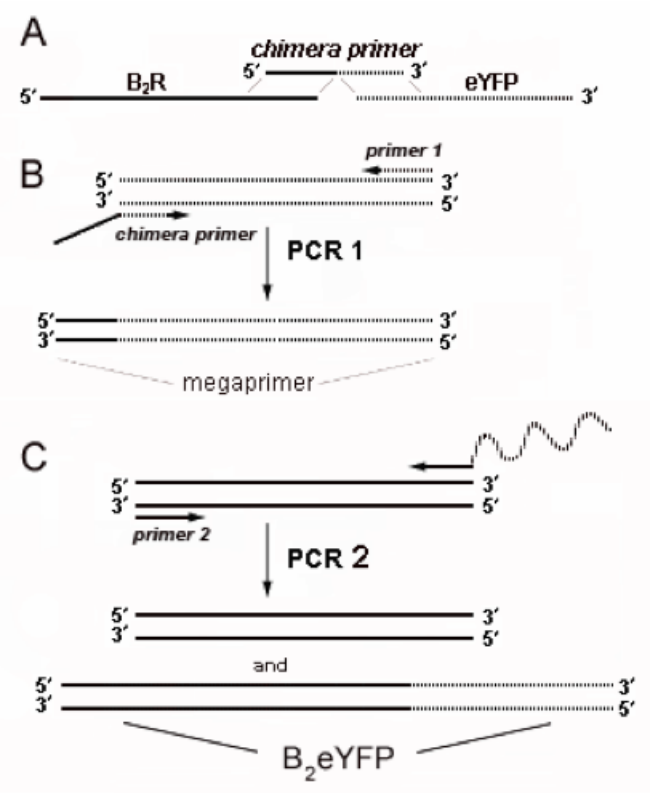

Fig. D-5: Generation of the eYFP chimera (Figure from Dr. Irina Kalatskaya).

A) PCR 1 was performed with a mutagenic chimera primer and the reverse primer for eYFP (primer 1) to generate and amplify a double-stranded megaprimer.

B) The megaprimer was purified and used with the forward primer for B_2R (primer 2) in PCR 2 to obtain the desired full-length chimera mutant.

The first PCR reaction was carried out using cycle program 1 (D.2.1.3) besides 10 min for the first denaturation instead of 3 min. The megaprimer was purified by agarose gel electrophoresis and extracted using a gel extraction kit.

A second PCR mixture (Figure D-5, C) contained B_2R gene (0.3-0.4 µg) as the template, the megaprimer (5 µl) described above and the reverse primer for eYFP (0.6 µl). The amounts of PCR buffer, *Pfu* polymerase, DMSO, dNTP and H_2O were the same as in Table 1. The second PCR reaction was carried out using the following cycle program 1 (D.2.1.3) besides 10 min for the first denaturation instead of 3 min, annealing performed at 45°C (instead of 50°C) and the first elongation for 2 min (instead of 60 sec). The final PCR product was a 1.8-kb fragment containing the B_2R coding sequence fused to the eYFP gene. This B_2eYFP fragment was extracted from the agarose gel (section D.2.1.7).

D.2.1.5 DNA cleavage with restriction endonucelases

Optimal buffer conditions were chosen for each restriction enzyme digest according to supplier's information. The reaction mixture was prepared on ice according to the protocol for DNA restriction mentioned below. DNA was usually digested at 37°C for about 1 h.

Protocol for DNA restriction

DNA	2 µg
Restrictase	2 µl (2 unit)
Buffer	2 µl
H_20	to 20 µl

D.2.1.6 Agarose gel electrophoresis

For preparation of the gels, agarose was dissolved in TAE buffer (D.1.7 Solutions) in a microwave oven. The final concentration of agarose was 0.5-2 % depending on the size of the separated DNA fragments. Ethidium bromide was added to a final concentration of 1 µg/ml for later visualization of the DNA under UV light. Loading buffer (D.1.7 Solutions) was added to the samples (ratio 1:5) before loading the gel in order to control the separation during the run. The running buffer was also TAE. Electrophoretic separation was achieved by constant currents at 5-7 V/cm for about 30 min. The gels were observed under UV light (312 nm) and the size of the fragments were determined by comparing their mobility with that of DNA standards. To avoid DNA damage by UV radiation exposure to UV was kept as short as possible.

D.2.1.7 Extraction of DNA fragments from agarose gels

After separation of the DNA fragments by agarose gel electrophoresis, the band corresponding to the fragment of interest was isolated using the QIAquick gel extraction kit (Qiagen) following the protocol of the supplier.

» The band of interest was cut out with a scalpel.

» The agarose gel slice containing the DNA fragment was solubilized by addition of the buffer QX1 and by incubation for 10 min at 50°C. The high concentration of a chaotropic salt in buffer QX1 disrupts hydrogen bonding between sugars in a agarose polymer and promotes the dissociation of DNA binding proteins from the DNA fragments.

» The DNA fragment was selectively bound to a silica-gel resin in the presence of a high concentration of a chaotropic salts (QX1).
» Salts were washed out by the PE buffer containing ethanol.
» Residual PE buffer was removed by an additional centrifugation step.
» DNA was typically eluted with 10 µl of 10 mM Tris-HCl, pH 8.5 or water, as elution is most efficient under low salt concentrations and basic conditions. As the pH is critical for binding and therefore the DNA recovery, the pH was controlled even when water was used.

D.2.1.8 Ligation of DNA fragments

The insert obtained after adding restriction sites by PCR (section D.2.1.1) and pcDNA5/FRT vector were cleaved with *Hind*III and *Xho*I (section D.2.1.2). A 3-5 molar excess of DNA fragment (estimated by intensity of the bands on the agarose gel) was added to a linearized vector (0.1-1.0 µM) in a final volume of 10 µl at RT. 1 µl (1 U/µl) of T_4 ligase as well as 1 µl of T_4 ligase buffer were then added on ice. The ligation mixture was incubated 1 h in a water bath at 16°C.

D.2.1.9 LB growth medium and plates for culture of *E. coli* strains

LB (Luria Bertani) growth medium (see Solutions D.1.7) was sterilized by autoclaving for 20 min at a pressure of 1.2×10^5 Pa and a temperature of 121°C. Ampicillin was added to the media at a concentration of 50 mg/ml when the temperature was below 50°C. 15 g/l agar was added for the preparation of LB plates before autoclaving. For short term storage the *E. coli* strains were spread onto agar plates containing the appropriate antibiotics and then stored at 4°C.

D.2.1.10 Transformation of *E.coli*

Transformation of *E.coli* strains was performed by heat shock with slight modification of the supplier's protocol. 2 µl of the ligation reaction (section D.2.1.8) or plasmid (< 0.1 µg) was added to 15-25 µl of competent cells (*E.coli* TOP 10) and mixed gently in a 1.5 ml reaction cup. After incubation on ice for 30 min, the cells were heat shocked for 30 sec in a water bath at 42°C without shaking. The tubes were immediately transferred onto ice and incubated there for another 2 min. After addition of 100 µl of SOC medium (D.1.7 Solutions) the tube was shaken at 37°C for 1 h and then again placed on ice. The whole volume of the transformation mixture was spread on a LB plate containing 50 mg/ml ampicillin and incubated overnight at 37°C.

D.2.1.11 Colony-PCR

To screen and select cell colonies that had the correct plasmid insert colony-PCR was used. This method is appropriate for determining whether or not a specific colony on a plate has the desired sequence. The reaction mixture was prepared in an application tube on ice using Primer 1 and Primer 2 (0.5 µM), *Taq* polymerase (0.05 U/µl) and H_2O to 7.55 /µl. The same amount of PCR buffer, DMSO and dNTP as in Table 1 were used and the PCR was carried out using cycle program 1 (section D.2.1.3). A small part of a colony was picked from the agarose plate with a plastic tip and resuspended in 15 µl of reaction mixture. Usually 3-4 colonies were checked. Analysis of the PCR products was performed by agarose gel electrophoresis (section D.2.1.6).

D.2.1.12 Plasmid preparation from *E.coli*

For most purposes like testing of recombinant DNA by restriction endonuclease digestion, for DNA sequencing or transfection with the *Flp-In* system plasmid DNA was prepared from 6 ml overnight cultures of recombinant *E.coli* using the QIAprep Spin Miniprep Kit. This kit is based on a modified alkaline lysis procedure protocol (Birnboim and Doly, 1979) of the cell pellet.

Bacteria were lysed under alkaline conditions in the presence of RNase A, and the lysate was subsequently neutralized. Afterwards, the remainder of the bacteria containing the chromosomal DNA was discarded by centrifugation, and the soluble plasmid DNA was selectively bound to a silica-gel membrane of QIAprep column which was washed twice in order to eliminate all the other contaminants (proteins, RNA, and low molecular weight impurities). Elution from the column was achieved by addition of water or 10 mM Tris-HCl, pH 8.5.

D.2.1.13 Confirmation of correctness of DNA sequence

If a new plasmid was made only by cleavage and restriction, correctness of DNA ligation was checked by cleavage using the same restriction nucleases.

As the DNA-polymerases sometimes induce mistakes, after site-directed mutagenesis or generation of chimera, DNA sequencing was performed by a commercial service (MediGenomix, Martinsried, Germany).

D.2.1.14 Determination of DNA concentration

The concentration of DNA was determined spectroscopically by measuring the absorbance at 260 nm. For a 50 µg/ml solution of dsDNA the absorption coefficient was set to be 1 (1 cm

pathlength) (Sambrook and Gething, 1989). 5 µl of DNA sample was dissolved in 495 µl of water or TAE buffer. The final concentration of DNA was calculated by the following formula:

$$C_{DNA}\ (\mu g/ml) = 50\ \mu g/ml \times \text{dilution factor } (\times 50) \times OD_{260}.$$

The purity of the preparation was estimated by measuring the UV absorption spectrum at 260 and 280 nm. The absorbance ratio A_{260nm}/A_{280nm} (between 1.8 and 2.0) provided the purity of the protein.

D.2.2 Cell culture methods

D.2.2.1 Culture of mammalian cells

HEK 293 cells were grown as adherent monolayers in DMEM supplemented with 10% fetal calf serum (FCS) and 100 Unit·ml^{-1}/100 µg·ml^{-1} penicillin-streptomycin at 37°C, 5% CO_2/air. HEK 293 cells double every 18-24 h, under optimal conditions. They were normally subcultured twice a week according to the following procedure: The old medium was removed and the cells were washed twice with PBS. Thereafter, the appropriate volume of EDTA-trypsin solution was added to the culture flasks and the cells were incubated for 5 min at 37°C. Trypsinization was stopped by resuspending the cells in complete growth medium. The cells could now be plated on cell culture plates for experiments. For experiments that required a lot of rinsing were the plates shortly pretreated with 0.01% poly-D-lysine hydrobromide in PBS to improve cell adherence to the flask surface.

D.2.2.2 Cell freezing and thawing

To freeze the cells, they were spun down under sterile conditions for 5 min at 900 rpm. The cell pellet was then resuspended in cold freezing medium (DMEM with 10% FCS, penicillin-streptomycin supplemented with 7.5% DMSO. Aliquots of 1.8 ml were quickly dispensed into freezing vials (4°C). The cells were stored at -80°C overnight. The next day, they were transferred to liquid nitrogen.

For cell thawing a freezing vial was removed from the liquid nitrogen and put in a water bath at 37°C. The cells were then dispensed in 5 ml of complete growth medium that was pre-incubated at 37°C. After approximately 1 h the medium was changed to new complete growth medium.

D.2.2.3 *Flp-In* expression system

We used the *Flp-In*™ system from Invitrogen as our expression system. It allows integration and expression of our gene of interest in mammalian cells at a specific genomic location.

The *Flp-In*™ system contains three main components (Fig. D-6):

» The first major component is the *Flp-In*™ cell line containing a single integrated FRT site (*FLP* Recombinase Target). Flp-In™ T-Rex™-293 cell line was bought from Invitrogen.

» The second major component is the pcDNA5/FRT (Fig. D-1) expression vector into which the gene of interest was cloned. Expression of the gene of interest is controlled by the CMV

promoter. The vector also contains a hygromycin resistance gene with FRT site, which, is part of the 5' coding region and lacks a promoter and the ATG initiation codon.

» The third major component of the of the *Flp-In*™ system is the pOG44 (Fig. D-2) plasmid, which, transiently expresses the Flp recombinase under control of the CMV promoter. Flp recombinase is a member of the integrase family of recombinases that mediates a site-specific recombination between interacting DNA molecules via pairing the interacting FRT sites.

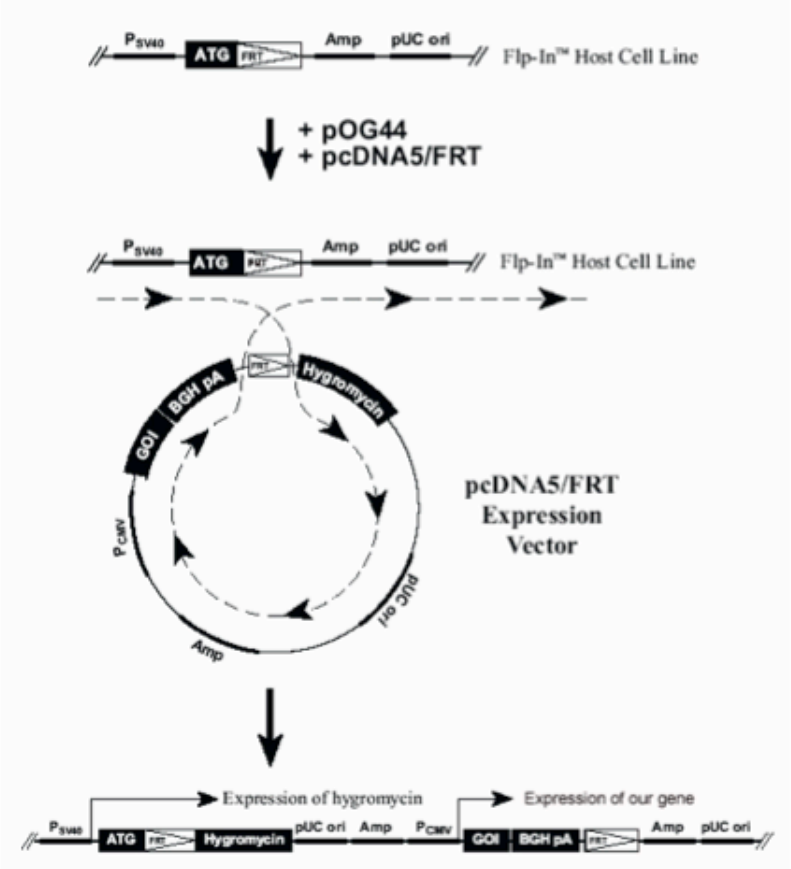

Fig. D-6. Diagram of the *Flp-In*™ system (Figure taken from Invitrogen).

pUC ori: replication origin, Amp: ampicillin resistance gene, BGH pA: bovine growth hormone polyadenylation sites, SV40 pA: simian virus polyadenylation sites, P_{CMV}: cytomegalovirus promoter.

The pOG44 plasmid and the pcDNA5/FRT vector with the gene of interest were co-transfected into the *Flp-In*™ *T-Rex*™*-293* cell line (Fig. D-3). Upon co-transfection, the Flp recombinase expressed from pOG44 mediated a homologous recombination between the FRT sites (integrated into the genome and on pcDNA5/FRT) such that the pcDNA5/FRT construct was inserted into the genome at the integrated FRT site. This insertion brought the SV40 promoter and the ATG initiation codon (integrated in the *Flp-In*™ cell line) into functional proximity with the

hygromycin resistance gene. Thus, stable *Flp-In*™ expression cell lines can be selected for hygromycin resistance.

The wild type B2R gene and all other constructs started with the third encoded methionine (Hess et al., 1992), which initially was assumed to be the start codon. All receptor coding sequences were preceded at the N-terminus by a single hemagglutinin (HA)-tag (MGYPYDVPDYAGS), with the last two amino acids (Gly-Ser) of the tag being generated by the insertion of the *Bam*HI site and were cloned into the *Hind*III and the *Xho*I sites of the pcDNA5/FRT vector (Fig. D-1). The nature of the tag did not influence the pharmacological properties of the constructs.

D.2.2.4 Transfection of HEK 293 cells

This protocol was found to be best suited for our cells: 100 µl of serum-free medium, 1.6 µg of pOG44, 0.4 µg of plasmid of interest and 5 µl of FuGENE HD Transfection Reagent were mixed in a well of 96-well plate. The mixture was incubated at 37°C for 15 min. The mixture was added drop wise directly to the cells (with <60% confluence) growing on 6- or 12-well plates in the complete DMEM medium supplemented with FCS.

For transient transfections 2.0 µg plasmid of interest was used. This was mixed together with 100 µl of serum-free medium and 5 µl FuGENE HD Reagent in a well of 96-well plate.

The following day the cells were trypsinized and transferred to a 100-mm dish. After 2 days, hygromycin B was added to the medium at a final concentration of 250 µg/ml and selection was started. After another 3-5 days the medium was changed and the cells were incubated without hygromycin.

Within approximately 12 days after transfection 6-20 clones were usually observed. Single clones were then transferred to a 12-well plate by picking with a plastic tip. When enough cells were available the ligand binding was estimated in a binding assay at 4°C using radiolabeled bradykinin ([^{3}H]BK). Clones exhibiting similar high binding activity were considered to represent a single insertion of the pcDNA5/FRT vector, containing the receptor gene, at the recombinase target site. Cells with twice as much binding activity were presumed to have an additional insertion of the vector (rare), clones with less binding activity were assumed to be inhomogeneous and were not further propagated or reselected with hygromycin B.

D.2.3 [^{3}H]Bradykinin binding studies

D.2.3.1 Expression levels of constructs.

Maximal binding of [^{3}H]BK to confluent monolayers of HEK 293 cells, stably and isogenically expressing the indicated constructs, was estimated with at least 3 different clones in 24-wells after incubation with 200 µl of approximately 30 nM [^{3}H]BK for 90 minutes on ice.

D.2.3.2 Equilibrium binding experiments at 37°C and 4°C.

For the determination of the equilibrium binding affinity constant K_d at 4°C and in particular at 37°C, receptor sequestration was inhibited by pretreatment of the cell monolayers on 24-well/48-wells with 100 µM phenyl arsine oxide (PAO) in incubation buffer for 5 min at 37°C. Thereafter, the cells were washed three times with ice-cold PBS, 0.3/0.2 ml of incubation buffer with degradation inhibitors (2 mM bacitracin, 0.8 mM 1.10-phenanthroline, and 100 µM captopril) containing increasing concentrations of [^{3}H]BK (10 concentrations ranging from approximately 0.01 nM to 50 nM) were added quickly on ice, and the cells immediately warmed up to 37°C in a water bath. For the determination of the affinities at 37°C the incubation was stopped after 30 min by placing the trays on ice and rinsing the cells four times with ice-cold PBS. Surface bound [^{3}H]BK (>95% of totally bound radioactivity in cells pretreated with PAO) was than dissociated by a 10 min incubation with 0.2 ml of an ice-cold dissociation solution, transferred to a scintillation vial and counted in a β-counter after addition of scintillation fluid. For determination of the affinities at 4°C the incubation at 37°C was followed by an additional incubation on ice. After 90 min these cells were also washed with ice-cold PBS and [^{3}H]BK binding measured as described above. Nonspecific binding was determined in the presence of 5 µM of unlabeled BK and subtracted from total binding being determined with [^{3}H]BK alone to calculate specific binding.

To determine the B_{max} and K_d, our data were fitted to the "One Site Binding Equation", using nonlinear regression. It describes the binding of a ligand to a receptor that follows the law of mass action:

$$Y = B_{max} \times X / (K_d + X)$$

where B_{max} is the maximal binding and K_d is the concentration of ligand required to reach half-maximal binding. All data analysis was performed using GraphPad Prism version 4.0c. This equation describes a rectangular hyperbola or a binding isotherm (Fig. D-7).

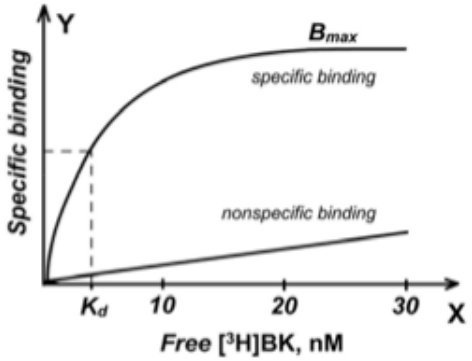

Fig. D-7: Ligand concentration-receptor bound curve.

A schematic representation of total and nonspecific radioactive ligand binding is shown. The concentration of free radioligand was plotted on the X-axis. Y-values reflect the total number of receptors expressed in cpm, sites/cell or fmol/mg protein. Nonspecific binding is usually linear with the concentration of radioligand.

Maximal binding capacities of the stable clones (B_{max}) were either calculated from the equilibrium binding curves or estimated by incubation of the cells on ice with a saturating concentration of [^{3}H]BK (30 nM).

D.2.3.3 Competitive inhibition [^{3}H]BK binding to cold drugs.

Confluent monolayer in 96-well plates were washed with ice-cold PBS and incubated on ice with 100 µl incubation buffer (D.1.7 Solutions) containing 2 nM [^{3}H]BK and increasing concentrations (10^{-11} – 10^{-5} M) of unlabeled BK, icatibant, or B9430. After 90 min the cells were rinsed with ice-cold PBS and treated for 10 min on ice with 200 µl dissociation solution. The supernatants containing the dissociated, formerly surface bound [^{3}H]BK was thereafter transferred to scintillation vials and counted after addition of scintillation fluid in a β-counter. Non-specific binding was measured in the presence of 5 µM unlabeled BK.

D.2.4 Determination of second messengers after $G_{q/11}$ activation

D.2.4.1 Measurement of total inositol phosphate (IP) release

80% confluent cell-monolayers of stably transfected HEK 293 cells on 12-well dishes were labeled overnight with 1 µCi [^{3}H]-inositol/ml in 0.5 ml DMEM containing fresh FCS and penicillin/streptomycin. The next day, the monolayers were placed on ice, rinsed three times with ice-cold PBS and pre-incubated on ice in incubation buffer supplemented with 50 mM LiCl with

or without addition of increasing concentrations (10^{-11} – 10^{-5} M) of BK, icatibant and B9430. After 90 min the accumulation was started by placing the cells in a water bath at 37°C. The stimulation was terminated after 30 min by exchanging the buffer for 0.75 ml of ice-cold 20 mM formic acid solution and putting the tray on ice for additional 30 min. Subsequently, the supernatant was combined with another 0.75 ml of formic acid solution followed by 0.2 ml of a 3% ammonium hydroxide solution. The mixtures were applied directly off the trays to AG 1-X8 anion exchange columns (2-ml volume). The columns were washed with 1 ml of 1.8% ammonium hydroxide and 9 ml of 60 mM sodium formate/5 mM tetraborate buffer followed by 0.5 ml 4 M ammonium formate/0.2 M formic acid. Total inositol phosphates were finally eluted in 3 ml of the latter buffer and counted in β-counter after addition of scintillation liquid. The [^{3}H]BK binding was measured in parallel by incubation of the cells on ice with a saturating concentration of [^{3}H]BK (10nM).

D.2.4.2 Basal and stimulated IP accumulation in fibroblasts HF-15 after pro-longed stimulation

Fibroblasts HF-15 were incubated with 1 μCi [^{3}H]-inositol/ml in 500 μl of medium containing 10% fetal calf serum that was pretreated for 2 h at 54°C (heat inactivated serum). At the same time were the cells stimulated with 10 μM BK, 5 μM B9430 or 5 μM icatibant, respectively overnight. The next day stimulation was performed with or without addition of increasing concentrations (10^{-11} – 10^{-6} M) of BK in the presence of 50 mM LiCl for 30 min at 37°C (as described in section D.2.4.1).

D.2.4.3 Time and Concentration-dependent release of intracellular [Ca^{2+}].

Nearly confluent monolayers on 96-well plates were washed twice with PBS and incubated 1 h in cell culture medium containing dye loading buffer (containing HBSS, Probenicid, CaDye) at 37°C in the incubator to allow uptake. Thereafter, plates were placed in a Cellux reader and stimulated after recording the baseline for ten seconds by addition of increasing concentrations of BK, B9430 or icatibant (seven concentrations starting from 0.01 nM to 10 μM). The absorption was recorded every 1.5 sec for 5 min. For the calculation of E_{max} the baseline was subtracted.

D.2.5 Receptor sequestration and ligand internalization assays

D.2.5.1 Down-regulation assay

The HEK 293 cells were plated on 48-well dishes with DMEM containing fresh FCS and penicillin/streptomycin. Confluent cell monolayers in 48-well plates were incubated with 10 μM BK, 5 μM icatibant or 5 μM B9430 in 500 μl of medium containing 10% fetal calf serum that was pretreated for 2 h at 60°C to reduce its proteolytic activity (inactivated serum, 60°C). At the indicated times, both bound and free unlabeled ligand was removed by treating the cell monolayers immediately with ice-cold dissociation solution for 10 min and rinsing them with PBS. Alternatively, for recovery experiments the cells were first washed with 1 ml of cell culture medium at 37°C containing fresh (to promote degradation of residual BK) fetal calf serum, incubated in another 1 ml of medium for 1 h at 37°C and then treated with the dissociation solution. To measure the remaining surface binding all cells were incubated with 2 nM [^{3}H]BK in incubation buffer on ice. After 90 min, free [^{3}H]BK was removed by rinsing the cells with PBS and surface-bound [^{3}H]BK was determined after dissociation with ice-cold dissociation solution as described above. Non-specific binding was measured in the presence of 5 μM unlabeled BK.

D.2.5.2 Internalization of [^{3}H]BK or [^{3}H]NPC17331.

Cells on 24-well plates were rinsed three times with PBS and incubated with 0.2 ml of 2 nM [^{3}H]BK or 2 nM [^{3}H]NPC17331 respectively in incubation buffer for 90 min on ice in order to obtain equilibrium binding. [^{3}H]ligand internalization was started by placing the plates in a water bath at 37°C. The internalization process was stopped at the indicated times by putting the plates back on ice and washing the cells four times with ice-cold PBS. Subsequently, surface bound [^{3}H]ligand was dissociated by incubating the cell monolayers for 10 min with 0.2 ml of ice-cold dissociation solution. The remaining monolayer with internalized [^{3}H]ligand was lysed in 0.2 ml 0.3 M NaOH and transferred with another 0.2 ml water to a scintillation vial. The radioactivity of both samples was determined in a β-counter after addition of scintillation fluid. Non-receptor-mediated [^{3}H]ligand surface binding and internalization were determined in the presence of 5 μM unlabeled BK and subtracted from total binding to calculate the specific values. Internalization was expressed as amount of internalized [^{3}H]ligand as a percentage of the combined amounts of internalized and surface bound [^{3}H]ligand.

D.2.6 Protein biochemical methods

D.2.6.1 SDS-polyacrylamid-gelelectrophoresis

The separation of proteins from lysates of eukaryotic cells was performed with discontinuous electrophoresis (Laemmli, 1970). The presence of SDS in the gels and buffer results in denaturation of the proteins. The separation in according to their molecular weight is due to the attachment of detergents, which provide a negative charge on the proteins. SDS-PAGE gel electrophoresis was performed under reducing conditions in precast 4-12 % minigels applying the NuPAGE Bis-Tris-buffer system using XCell *SureLock* Mini-cell (invitrogen). For detection of the protein of interest, they were transferred after electrophoresis on nitrocellulose membranes, once again using the XCell *SureLock*^{TM} Mini-cell. The membranes were then incubated in blocking buffer (D.1.7 Solutions) at RT for 1 h or overnight at 4°C to block nonspecific binding sites on the membrane. The appropriate primary antibody was added at RT for 2 h or overnight at 4°C in fresh blocking buffer. The unbound antibodies were removed by rinsing with TBST buffer (D.1.7 Solutions) before adding the corresponding secondary horseradish peroxidase-labeled (HRP) antibody at RT for 1 h. For detection of the proteins the Western Blot Chemiluminescence Reagent Plus (Perkin-Elmer) was used and then exposed to the film.

D.2.6.2 Immunoblotting after solubilization with RIPA

Monolayers in six-well trays were washed three times with PBS and solubilized in RIPA buffer (D.1.7 Solutions) including 0.5 mM Pefabloc SC and 10 μM each 1.10-phenathroline, aprotinin, leupeptin and pepstatin A for 30 min at 4°C with gentle agitation. The lysate was centrifuged at 6.240 x *g* for 15 min at 4°C. The supernatant (protein concentration ~1 mg/ml) was mixed with LDS sample buffer and incubated 10 min at 70°C. The proteins (~15 μg total protein/lane) were run on 4 - 12% SDS-polyacrylamide gels. The following protein transfer and antibody detection was performed as described in section D.2.6.1.

D.2.6.3 Protein levels of B_2 receptor during prolonged agonist/antagonist treatment

Cells were plated on 6-well plates. When the cells were approximately 80% confluent the medium was changed to a medium supplemented with 10% fetal calf serum that was pretreated for 2 h at 60°C to reduce its proteolytic activity (inactivated serum). The cells were treated for 1 or 16 hours with 10 μM BK, 5 μM B9430 and 5 μM icatibant. After incubation the plates were washed three times with PBS. The cells were solubilized in Lysis buffer (D.1.7 Solutions)

including 0.5 mM Pefabloc SC and 10 μM each of 1.10-phenanthroline, aprotinin, leupeptin and pepstatin A. The lysates were centrifuged for 20 min at 13.000 rpm at 4°C. The EZview Red Anti-HA Affinity Gel beads (SIGMA) were equilibrated twice with Lysis buffer without inhibitors. 200 μl of supernatant was incubated with the equilibrated EZview Red Anti-HA Affinity Gel beads for 1 hour at 4°C. The mixture was then washed three times with Lysis buffer without inhibitors, resuspended in 40 μl 1X sample buffer with 0.1 M DTT, and incubated for 6 min at 95°C. Following electrophoresis and antibody detection was performed as described in section D.2.6.1.

D.2.6.4 MAPK kinases ERK1/2

For the detection of phospho-ERK1/2 and total-ERK confluent cells on 6-well plates were incubated for 24 hours in DMEM medium supplemented with reduced serum (0.5 % FCS). The next day the cells were washed three times with PBS and incubated on ice with 1 ml of incubation buffer containing 2 mM bacitracin, 0.8 mM 1.10-phenanthroline and 100 μM captopril pH 7.4 ± 1 μM of BK, icatibant and B9430. After 30 minutes stimulation was started by placing the trays in a water bath at 37°C for 10 min. The monolayers were then washed with ice-cold PBS and scraped off in 0.3 ml Complete Lysis-M EDTA-Free Lysis Buffer (Roche, Mannheim, Germany) containing a protease inhibitor cocktail (complete Mini, EDTA-free; Roche). The phosphatase inhibitors, 25 mM NaF, 1 mM sodium orthovanadate were also added. The lysates were centrifuged at 14000 rpm in a microfuge for 10 min. 30 μl of supernatant was taken and transferred to a new microtube. 10 μl of 4X NuPAGE LDS Sample Buffer was added containing 0.1 M DTT. Probes were briely vortexed and then heated at 99°C for 6 min. The probe samples were centrifuged for 2 min and 20 μl was loaded on a 4-12% SDS-PAGE gel. The separated proteins were transferred to a 0.45-μm nitrocellulose membrane. The following procedure was according to the Snap i.d. protein detection system (Millipore). The unspecific sites were blocked for 10 min in blocking buffer. The primary antibodies total-ERK (monoclonal, Cell Signaling, dilution 1/2000) and phospho-ERK1/2 (monoclonal, Cell Signaling, dilution 1/2000) were added for 10 min in 0.1% milk powder in TBST. The membranes were washed three times for with TBST before adding the corresponding secondary peroxidase-labeled horse anti-mouse Ig (1:2000) for 10 min in 0.1% milk powder in TBST. The antibodies were then revealed by Western Blot Chemiluminescence Reagent Plus.

D.2.6.5 Biotinylation Protection Assay

Confluent cells were washed twice with ice cold PBS and subsequently incubated with 0.3 mg/ml disulfide-cleavable sulfo-NHS-SS-Biotin (Pierce) in PBS for 30 min at 4°C. After rinsing twice with ice cold Tris-buffered saline (TBS) to quench the biotinylation reaction, cells were equilibrated in OPTI MEM I (Invitrogen) for 30 min at 37°C and further incubated in the absence (NS = non-stimulated) or presence of 10 μM bradykinin, 5 μM B9430 and 5 μM icatibant. After rinsing with ice cold TBS all cells except those labeled "Total" were stripped with Stripping buffer (D.1.7 Solutions) for 30 min at 4°C. Glutathione was quenched with 50 mM iodoacetamide and 1% BSA for 20 min. at 4°C. All cells were washed twice with ice cold PBS and lysed with Lysis buffer containing protease inhibitors (0.5 mM Pefabloc SC and 10 μM each 1.10-phenanthroline, aprotinin, leupeptin and pepstatin A). Lysates were centrifuged for 15 min. with 14.000 rpm at 4°C in a microfuge, the supernatant was added to anti-HA high affinity matrix (SIGMA) pre-equilibrated with extraction buffer, and incubated with gentle mixing for 1 hour at 4°C. Subsequently, the matrix was washed extensively with extraction buffer and denaturated with NuPAGE LDS sample buffer (Invitrogen) for 5 min. at 95°C without reducing agent. Proteins were fractionated by SDS polyacrylamide gel electrophoresis, transferred to nitrocellulose membrane and blocked for 1 hour in blocking buffer. Biotinylated proteins were detected by the Vectastain avidin-biotinylated enzyme complex immuno-peroxidase reagent (Vector Laboratories) and developed with Western Blot Chemiluminescence Reagent Plus.

D.2.7 Receptor phosphorylation

Confluent cells on 6-well plates were washed twice with phosphate-free DMEM, incubated for 3 h at 37 °C in the same medium, and labeled with 0.2 mCi/ml [^{32}P]orthophosphate for 10-12 h. After a 5-min exposure to 1 μM BK at 37 °C, cells were solubilized in 0.5 ml RIPA buffer supplemented with 0.5 mM Pefabloc SC and 10 μM each 1,10 phenanthroline, aprotinin, leupeptin, and pepstatin A and phosphatase inhibitors (25 mM NaF, 1 mM sodium orthovanadate, 0.3 μM okadaic acid) for 1 h at 4°C with gentle rocking. The lysate was centrifuged at 6.240 × *g* for 20 min at 4 °C. The supernatant (0.5 ml with ~ 1.5 mg of total protein) was incubated with 35 μl of protein G-agarose and 2.5 μl of antiserum AS346 for 3 h at 4 °C. The mixture was then washed twice with RIPA buffer and once with distilled water, resuspended in 30 μl of LDS sample buffer, and incubated 6 min at 95 °C. Following electrophoresis on 10% SDS-

polyacrylamide gels, the fractionated proteins were electroblotted onto 0.45-µm nitrocellulose. The proteins of interest were identified by autoradiography.

D.2.8 Epifluorescence microscopy

HEK 293 cells with stable tetracycline-inducible expression of the indicated receptor-eYFP (enhanced yellow fluorescent protein) fusion constructs were seeded on poly-Lysine-treated chamber-slides (Nunc, Langerselbold, Germany). After 24 - 48 h the culture medium was exchange for OPTI-MEM (Invitrogen) and receptor expression induced by addition of tetracycline. After 16 h induction cells were treated either with vehicle or 1 µM of the indicated compounds for 30 min at 37°C. Images were taken halfway through the cells with an epifluorescence microscope (Olympus X70) with z-stack mechanisms using a 60x/1.4 oil immersion objective with no zoom.

D.2.9 Determination of the protein concentration

Total protein was quantified with the Micro BSA Protein Assay reagent kit from Pierce using BSA as standard.

E RESULTS

E.1 Functional selectivity of B9430 and icatibant concerning PLC activation receptor down-regulation, and ERK1/2 activation depends on human bradykinin B_2 receptor density and cell type

E.1.1 Expression and equilibrium dissociation constants K_d of recombinantly and endogenously expressed human B_2R

In order to determine the influence of the receptor density on the effects of bradykinin or the two pseudopeptides B9430 and icatbant (sequences shown in Tab. 2) we used two cell lines stably expressing the recombinant bradykinin B_2 receptor (B_2R). In the cell line B_2wt_{HIGH} the expression was under the control of the strong CMV (cytomegalovirus) promoter, resulting in the expression of almost 11 pmol receptor/mg proteins. In the cell line B_2wt_{LOW} with the expression under the control of the P_{min} promoter (consisting of only the last 51 nucleotides of the CMV promoter) the expression was, at 2.4 pmol/mg protein, considerably lower. Through the employment of the Flp-In system (Invitrogen) both receptor constructs were isogenically expressed, i.e. the receptor genes were inserted at an identical unique locus in the genome of the host HEK 293 cells. To compare our results with a cell line that endogenously expresses the B_2R we also used the well established human foreskin fibroblast cell line HF-15 (Roscher et al., 1983) that in our experiments had a B_{max} of estimated 300 fmol/mg protein (Fig. E-1). The expression level had no significant influence on the receptor affinity (see Table 3, page 68) as for the recombinant and the endogenously expressed B_2R similar affinities were determined at 4°C (B_2wt_{HIGH} K_d: 2.8 ± 0.7 nM; B_2wt_{LOW} K_d: 2.0 ± 0.2 nM) or have been published (fibroblast K_d: 4.6 nM ± 0.5 nM) (Roscher et al., 1983).

Tab. 2: Sequences of BK and pseudopeptides

BK:	Arg-Pro-Pro-Gly-Phe-Ser-Pro-Phe-Arg
Icatibant:	DArg-Arg-Pro-Hyp-Gly-Thi-Ser-DTic-Oic-Arg
B9430:	DArg-Arg-Pro-Hyp-Gly-Igl-Ser-DIgl-Oic-Arg

Hyp, trans-4-hydroxyproline; Oic, octahydroindole-2-carboxylic acid; Igl, α-(2-indanyl)glycine; Thi, β-(2-thienyl)-alanine; Tic, 1,2,3,4-tetrahydroisoquinoline-3-carboxylic acid

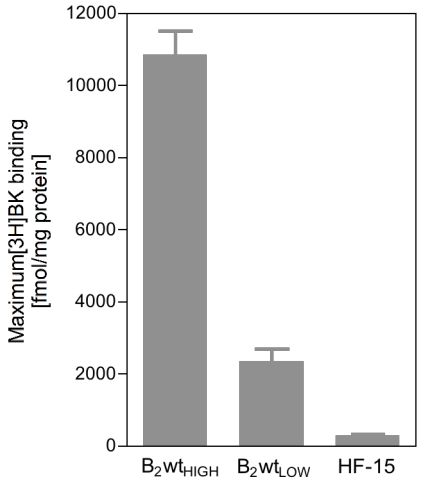

Fig. E-1: Bradykinin B_2 receptor expression levels in B_2wt_{HIGH} and B_2wt_{LOW} and B_2R in foreskin fibroblasts.

Maximal [^{3}H]BK binding B_{max} of HEK 293 cells isogenically and stably expressing high (B_2wt_{HIGH}) or low (B_2wt_{LOW}) amounts of recombinant receptor and of endogenously expressing foreskin fibroblasts HF-15 was determined with approximately 30 nM [^{3}H]BK on ice as described in „Materials and Methods“. The columns represent the mean ± SEM of at least four binding experiments. The receptor expression in B_2wt_{HIGH} was under control of the CMV-promoter, whereas in B_2wt_{LOW} the weaker Pmin promoter was used.

E.1.2 Binding affinities and potencies of (pseudo)peptides

The binding affinities of the two pseudopeptides icatibant and B9430 that differ from BK through the insertion of several non naturally occurring amino acids (see Tab. 2) were determined in comparison with BK in a competition experiment with [^{3}H]BK (Fig. E-2-A). Both compounds displaced the specific binding of 2 nM [^{3}H]BK with low IC_{50}-values (B9430, 15.94 ± 0.03 nM; icatibant, 13.86 ± 0.03 nM; n = 4). The IC_{50}-value obtained for BK was 8.32 ± 0.03 nM (n = 4).

Stimulation of the B_2R leads to the activation of phospholipase C via G protein $G_{q/11}$ resulting in the release of inositoltrisphosphate. Stimulation of B_2wt_{HIGH} with increasing concentrations of BK resulted in a sigmoid stimulation curve of inositolphosphate (IP) accumulation with a maximum 12-fold increase over basal IP activity, determined as amount of IP in cells kept on ice (Fig. E-2-B). The compounds icatibant and B9430, formally known as antagonists, acted when added to the B_2wt_{HIGH} as partial agonists with an E_{max} of 4-fold (icatibant) and 7-fold (B9430) stimulation over basal thus displaying 60% and 30% of the efficacy, respectively, of BK. The potencies for B9430 15.50 ± 0.11 nM and icatibant 17.68 ± 0.12 nM) (n = 4) reflected well their affinities as determined from the competition binding assay despite the different temperature conditions of both assays. The potency for BK (0.79 ± 0.34 nM) differed from its affinity (8.32 ± 0.03 nM).

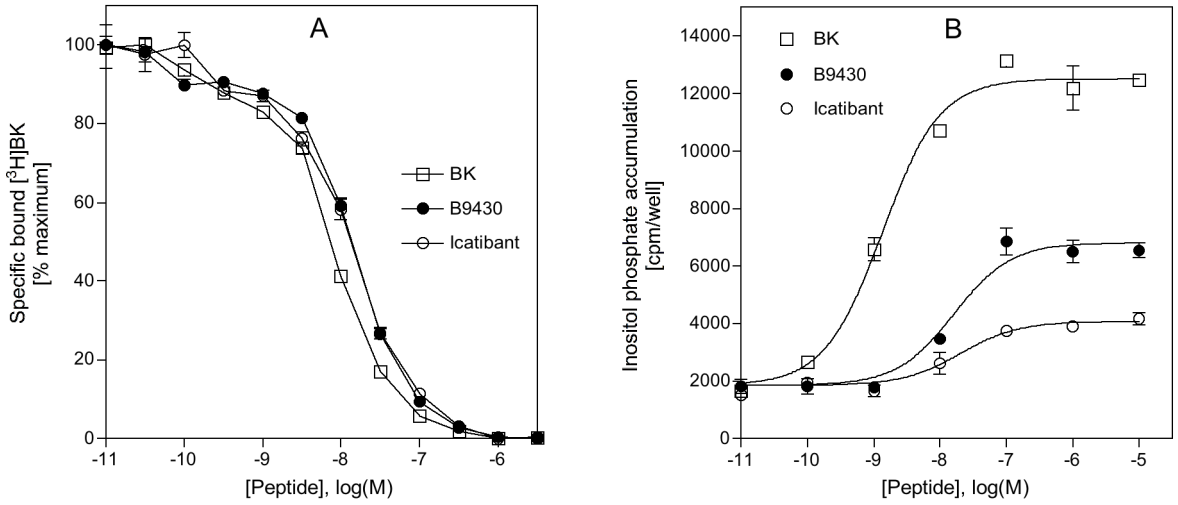

Fig. E-2: Competition inhibition of (pseudo)peptides and concentration-response IP assay in B_2wt_{HIGH}.

(A) Competitive inhibition of 2 nM [^{3}H]BK binding by unlabeled (pseudo)peptides. The IC_{50} values (BK 8.32 ± 0.03 nM, B9430 15.94 ± 0.03 nM or icatibant 13.86 ± 0.03nM) are the means ± SEM of 4 experiments done in duplicates. (B) Potencies for B_2wt_{HIGH}. 12-well plates were incubated overnight with 0.5 µCi [^{3}H]inositol in 0.5 ml in medium. Stimulation was performed with or without addition of increasing concentrations (10^{-11} – 10^{-5} M) of BK, icatibant or B9430 in the presence of 50 mM LiCl for 30 min at 37°C as described in „Materials and Methods“. One representative experiment out of three done in duplicates is shown. The EC_{50} values obtained from three independent experiments: BK 0.79 ± 0.34 nM, B9430 15.50 ± 0.11 nM, icatibant 17.68 ± 0.12 nM .

E.1.3 Lower receptor expression levels turn partial agonists in antagonists

As the partial agonism (seen in Fig. E-2, B) might have been due to the high receptor overexpression we took a closer look at the influence of receptor density on this property. In fact, in the lower expressing B_2wt_{LOW} and in the endogenously expressing fibroblasts HF-15, icatibant and B9430 no longer acted as partial agonists even at a concentration of 1 µM (Fig. E-3). They were not able to significantly stimulate IP accumulation in these cells, demonstrating that their partial agonism can only be observed with high receptor overexpression.

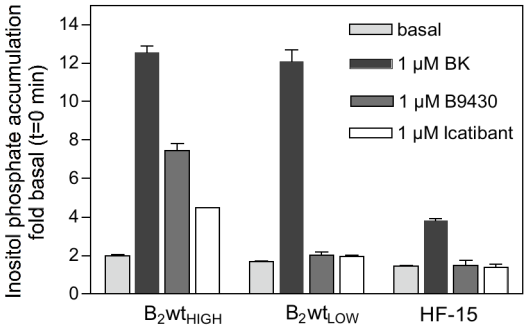

Fig. E-3: Basal and stimulated accumulation of total inositol phosphates.

HEK 293 cell lines B_2wt_{HIGH} and B_2R_{LOW} and foreskin fibroblasts HF-15 in 12-well plates were incubated overnight with 0.5 µCi [^{3}H]inositol in 0.5 ml medium. Stimulation was performed in the presence of 50 mM LiCl and 1 µM BK, B9430 and icatibant for 30 min at 37°C as described in „Materials and Methods". Each value represents the mean ± SEM of at least three independent experiments done in triplicates, given as fold over the IP content of non-stimulated but otherwise identically treated control cells that had remained on ice.

E.1.4 Real-time determination of intracellular Ca^{2+} mobilization.

The determination of IP accumulation requires stimulation of the cells in the presence of 50 mM LiCl as a phosphatase inhibitor for 30 min to obtain a clear specific signal. In interpreting how a receptor interacts with its cognate G protein, a process that is supposed to happen within seconds, this method may not be optimal, as the long stimulation time might diffuse the real kind of interaction between receptor and G protein. We therefore decided to use real-time recording of the Ca^{2+} mobilization to determine the effects of stimulation with BK and the pseudo-peptides on the different cell lines.

In B_2wt_{HIGH} addition of 1 µM BK resulted rapidly in a strong transient signal that decreased within one minute but stayed clearly above the basal level during the recording time of 5 min (Fig. E-4, left). Both pseudopeptides also generated a distinct signal that was transient and returned to the basal level within 1 min. Interestingly, the relative heights of the peaks reflected the efficiencies determined in the IP assay despite the quite different biological assays. In the lower expressing HEK 293 cells B_2wt_{LOW}, BK generated a strong signal that again did not return to the basal level (Fig. E-4, middle). The pseudopeptides, however produced only very poor signals that hardly were above the basal level. In the HF-15 cells stimulation with 1 µM BK produced a strong transient signal that within 1 min returned almost completely to the basal level, whereas the two pseudopeptides did not have any stimulating effect in these cells (Fig. E-4, right).

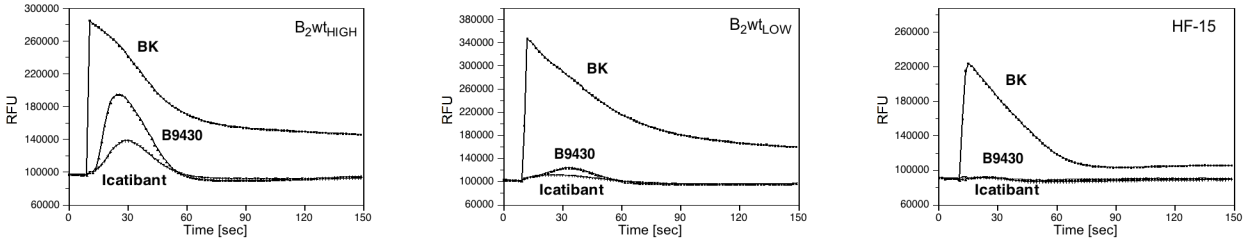

Fig. E-4: Time-dependent pseudo peptide stimulated rise in intracellular [Ca^{2+}] in different cell lines.

Cells in 96-well plates were incubated with dye loading buffer (containing HBSS, Probenicid, CaDye) for 1 h at 37°C. After recording the baseline for 10 seconds the (pseudo)peptides were added (1 µM BK, 0.6 µM B9430, or 1 µM icatibant) and Ca^{2+} mobilization was recorded every 1.5 sec for 5 min in a Cellux reader (Perkin-Elmer). (RFU, relative fluorescence units)

E.1.5 Concentration-dependent rise in intracellular [Ca^{2+}].

The potencies of the (pseudo)peptides concerning the release of Ca^{2+} were determined (Fig. E-5). The EC_{50}-values of calcium release determined with different BK concentrations were: B_2wt_{HIGH}: 0.12±0.11 nM, B_2wt_{LOW}: 0.34±0.09 nM; HF-15: 3.27±0.23 nM (n = 4). The results for the high and low expressed wild type are more or less in agreement with the EC_{50}-values obtained from the accumulation of inositolphosphates B_2wt_{HIGH}: 0.79±0.34 nM, B_2wt_{LOW}: 0.67±0.22 nM (Tab.3). The EC-value (1.29±0.21 nM) obtained from the accumulation of IP for HF-15 has been determined once (concentration-response curve is not shown). But as seen in Fig. E-5 the EC-values for B9430 and icatibant on Ca^{2+} were shifted a lot in this assay compared to the EC-values obtained from the IP accumulation.

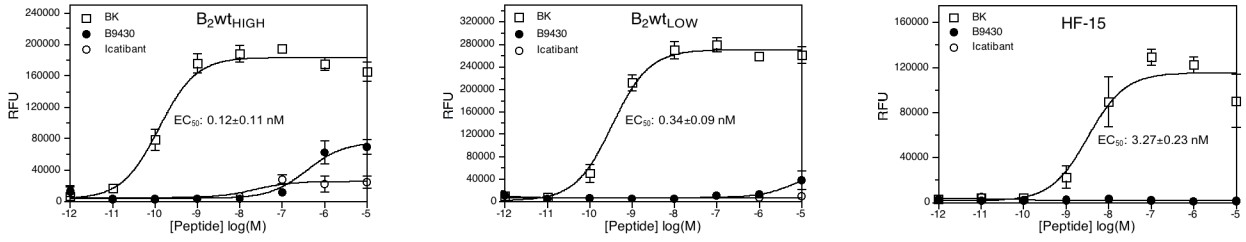

Fig. E-5: Concentration-dependent rise in intracellular [Ca^{2+}].

Cells in 96-well plates were incubated with dye loading buffer (containing HBSS, Probenicid, CaDye) for 1 h at 37°C. After recording the baseline for 10 seconds increasing concentrations (10^{-12} – 10^{-5} M) were added of BK (□), B9430 (●), and icatibant (○) and Ca^{2+} mobilization was recorded every 1.5 sec in a Cellux reader (PerkinElmer) for 5 min. The peaks of the curves obtained for each concentration were used to calculate EC_{50}-values. Each point represents the mean ± SEM from four experiments done in duplicates. (RFU, relative fluorescence units).

E.1.6 Effect of long-term stimulation on recombinantly expressed B_2R depends on receptor density

As was seen for B_2wt_{HIGH}, icatibant and B9430 were able to induce an increase in IP (and hence increase of intracellular Ca^{2+}) under certain circumstances. To investigate whether their agonistic activity was limited only to G protein activation, we next compared the effect of a long-term incubation with BK, icatibant or B9430 on the number of surface B_2R, to determine whether the pseudopeptides are able to induce down-regulation of the B_2R.

Upon BK stimulation a strong reduction in [^{3}H]BK surface binding was detected, approx. 60 % after 16 hours (Fig. E-6, left). On the other hand, B9340 showed only poorly, and icatibant showed no significant effect at all on the amount of cell surface binding. In contrast, there was a strong effect of BK but also of B9430 stimulation on surface binding in B_2wt_{LOW}. Within two hours binding was reduced to 20% for BK and to 35% by incubation with B9340 (Fig. E-6, right). Icatibant again had no significant effect.

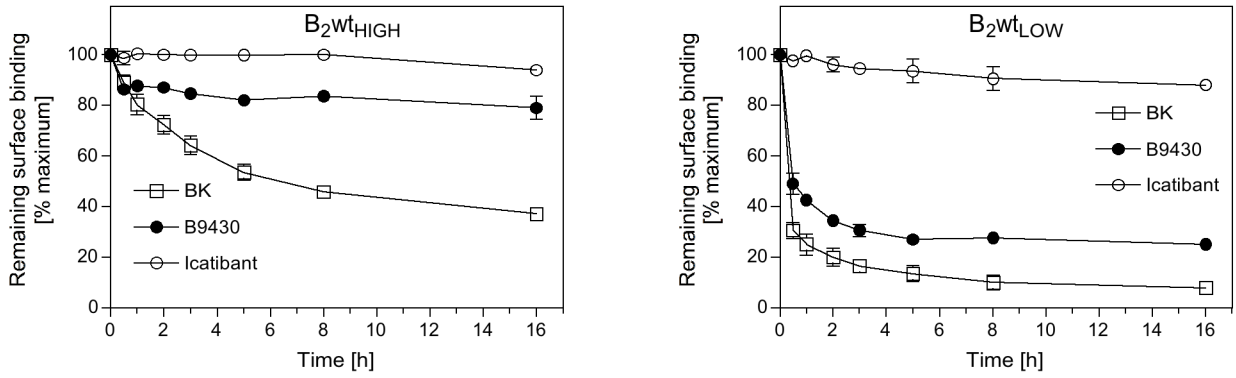

Fig. E-6: Effect of prolonged stimulation with BK, B9430 and icatibant on surface binding.

B_2wt_{HIGH} (left) and B_2wt_{LOW} (right) were incubated with 10 μM BK or 5 μM B9430 and icatibant in medium at 37°C. At the times indicated, all free and bound pseudopeptides were removed with an acetic acid/NaCl solution. Thereafter, the remaining specific surface binding was determined with 2 nM [^{3}H]BK at 4°C as described in "Materials and methods". Symbols represent the mean ± SEM for at least three experiments performed in duplicates.

E.1.7 Effect of long-term stimulation on the sequestration and the recycling of endogenously expressed B_2R (down-regulation assay)

In the fibroblasts we also determined besides the effect of the pseudopeptides on the surface binding of B_2R and whether there were differences in the recovery of binding. In order to measure recovery we stimulated the cells for the indicated times, the monolayers were then washed and further incubated for 1 hour at 37°C in medium containing fresh FCS to promote degradation of residual BK and to allow recovery of binding at the cell surface.

The B_2R in fibroblasts responded to stimulation with a rapid reduction in binding of [^{3}H]BK. Stimulation with 10 µM BK resulted in a reduction by 70% within 30 min that was slightly further decreased by a prolonged stimulation for up to 8 h (Fig. E-7, left). Prolonged stimulation also greatly reduced the recovery at the cell surface when the ligand was removed, suggesting that under these conditions most loss of binding is irreversible.

As shown for cell line B_2wt_{LOW}, compound B9430 was able to induce a fast and strong binding reduction of the B_2R. This effect of B9430 was also detected in the fibroblasts (reducing binding even stronger than BK) (Fig. E-7, middle). The recovery of binding was similar to that seen after BK stimulation. In contrast to its effect on the recombinant cell lines, icatibant was able to induce significant binding reduction in the fibroblasts, more than 40% reduction after 30 min and almost 60% after 8 h (Fig. E-7, right). The reduction of binding after stimulation with icatibant displayed a fairly strong potential to be recovered.

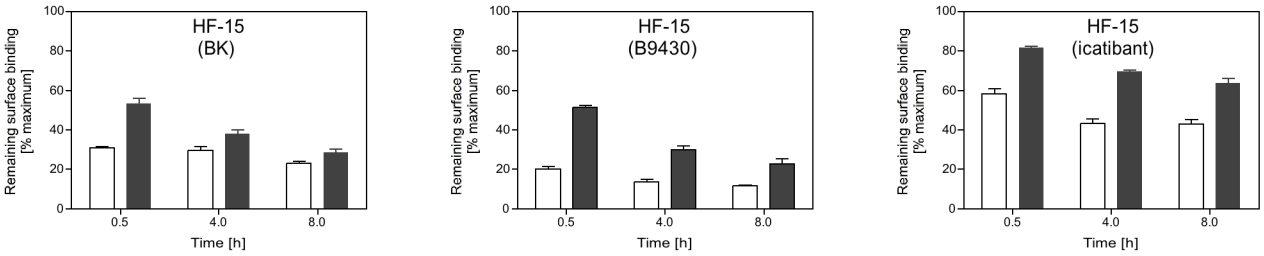

Fig. E-7: Surface binding and recovery upon BK, B9430 and icatibant stimulation in foreskin fibroblasts.

Foreskin fibroblasts HF-15 were incubated with 10 µM BK (left), 5 µM B9430 (middle) or icatibant (right) in medium at 37°C as described in "Materials and methods". At the times indicated, the cells were either immediately treated with acetic acid/NaCl solution to remove bound and free peptide (open columns) or first washed with 1 ml of cell culture medium at 37°C containing fetal calf serum and incubated in another 1 ml of medium for 1 h at 37°C (to promote dissociation and degradation of bound peptides) and then treated with the acetic acid/NaCl solution (dark columns). The remaining specific surface binding was determined with 2 nM [^{3}H]BK at 4°C as described in the "Materials and methods". Symbols represent the mean ± SEM of three experiments performed in duplicates.

E.1.8 Protein levels of B_2 receptor during prolonged agonist/antagonist treatment

A quick reduction of surface binding was seen in B_2wt_{LOW} upon BK and B9430 stimulation, and in the fibroblasts B9430 induced an even stronger reduction than BK. Given this significant loss of surface binding upon exposure to these peptides, we investigated whether total levels of B_2R protein are also influenced under these conditions. For this experiment we took advantage of the hemagglutinin tag fused to the N-terminus of the receptor. The tagged receptor was selectively bound upon lysis of the cells to a high-affinity hemagglutinin matrix. Thus, in an immunoblot (with a primary high-affinity hemagglutinin antibody) it was possible to detect all tagged receptors, both extracelluarly and intracellularly localized receptors, hence total B_2R protein. Degradation of total B_2wt_{LOW} was only detected upon prolonged (16 hours) stimulation with BK (Fig. E-8). This decrease after 16 h of BK exposure was in agreement with the decrease of surface binding seen after 16 hours in the down-regulation assay. But in the down-regulation assay a significant loss of binding was seen already after 1 hour exposure to BK that was not the case on the protein level. Even though B9430 showed a 70% decrease of surface binding after 16 hours in the down-regulation assay, no receptor degradation was detected in the immunoblot. Should be mentioned that this Western Blot is kind of overexposured so a comparision should be taken with care.

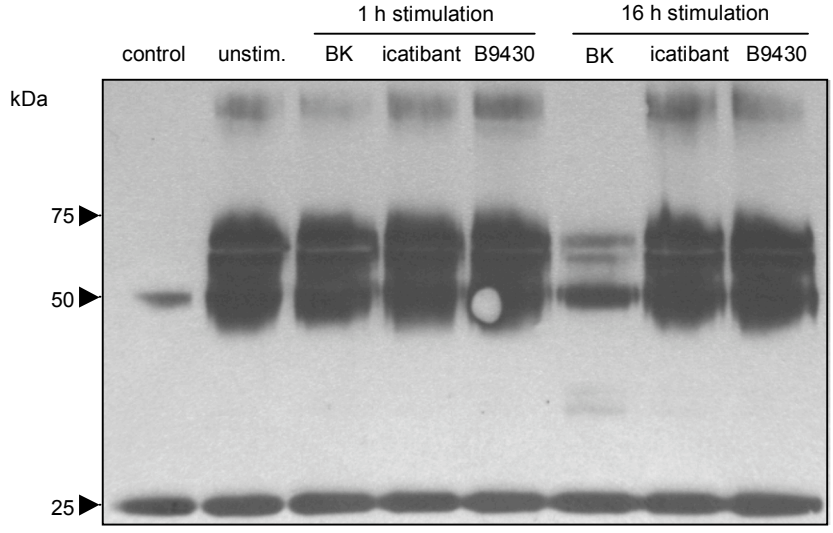

Fig. E-8: Analysis of degradation of B_2wt_{LOW} upon ligand binding: immunoblotted with anti-HA antibody.

HEK 293 cells expressing B_2wt_{LOW} having a hemagglutinin (HA) tag on the N-terminus were treated for 1 or 16 hours with 10 µM BK, 5 µM B9430 and 5 µM icatibant. As a control, HEK 293 cells expressing B_2wt_{LOW} with a Strep-tag on the N-terminus were used. After incubation, 200 µl of each lysate were incubated with equilibrated EZview™ Red Anti-HA Affinity Gel beads (SIGMA) for 1 hour at 4ºC. The immunoprecipitates were subjected to SDS-PAGE and Western blotting using anti-HA antibody as described in "Materials and Methods". One representative experiment out of three is shown.

E.1.9 Receptor localization studies using eYFP-constructs

Our next approach to determine the localization of B_2wt_{LOW} upon ligand stimulation was to use epifluorescence microscopy. We visualized the localization of the receptor constructs by eYFP (enhanced yellow fluorescent protein) genetically fused to their C-termini. HEK 293 cells stably expressing the construct of YFP fused to the C-terminus of B_2wt (B_2wt_{LOW}-eYFP) under the control of the P_{min} promoter were used for this purpose. B_2wt_{LOW}-eYFP was located almost exclusively at the membrane without stimulation (Fig. E-9). Upon BK stimulation the receptors were found in intracellular vesicles of various sizes. On the other hand, after challenge with icatibant and B9430, no intracellular localization of receptors could be detected. Even though a strong reduction in binding was seen after B9430 stimulation of B_2wt_{LOW} in the down-regulation assay (E-6), the two latter assays performed (degradation of total B_2wt_{LOW} and here epifluorescence microscopy) did not display any degradation or intracellular localization of B_2wt_{LOW} upon B9430 stimulation. Therefore we set out to perform one more assay where intracellular receptors can be detected, namely the biotinylation protection assay (BPA).

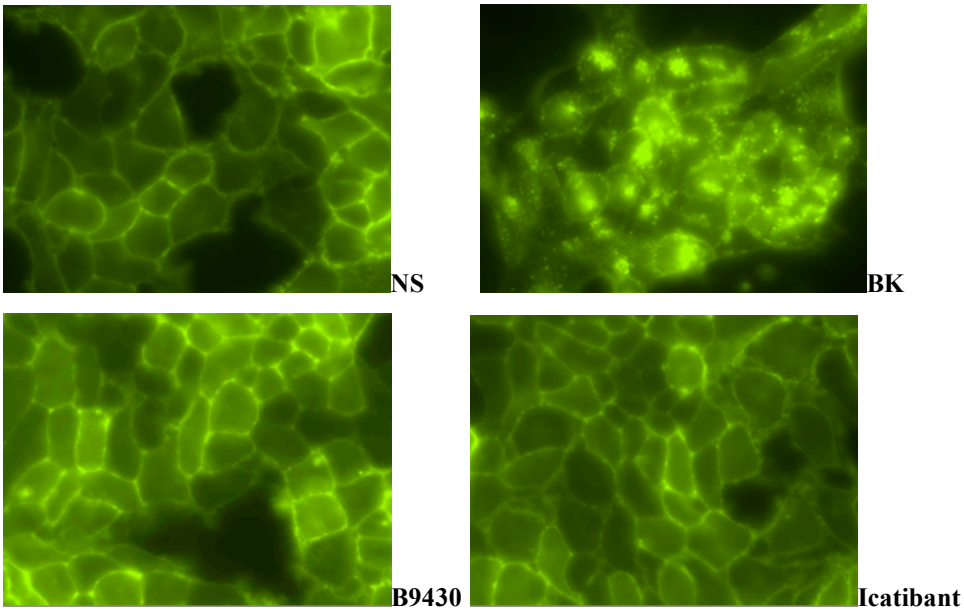

Fig. E-9: Localization of wild type-eYFP fusion protein by epifluorescence microscopy.

HEK 293 cells stably expressing the B_2wt_{LOW}-eYFP construct were incubated in the absence (NS = nonstimulated) or in the presence of 5 μM BK, B9430 and icatibant respectively for 1 h at 37°C and examined by epifluorescence microscopy.

E.1.10 Biotinylation Protection Assay

With the biotinylation protection assay (BPA) surface receptors (total) and intracellular receptors could be localized. The cell surface receptors were labeled with a membrane-impermeable biotin derivate. Internalized receptors were then selectively monitored by their protection from extracellular stripping with a reducing agent. Once again, B_2wt_{LOW} could be intracellularly detected, but only upon BK stimulation (Fig. E-10). Upon icatibant and B9430 stimulation no intracellularly localized receptors were observed.

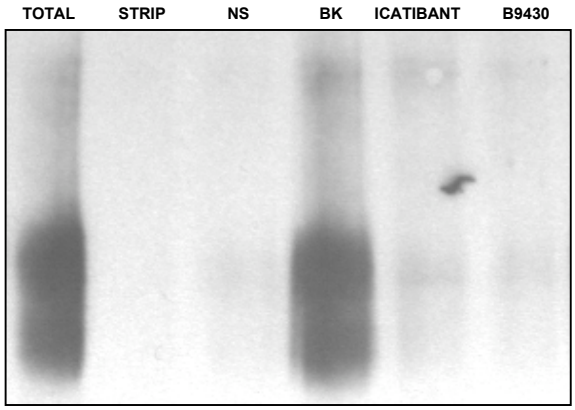

Fig. E-10: Ligand-dependent receptor endocytosis as determined by BPA.

HEK 293 cells stably expressing B_2R (B_2wt_{LOW}) having a hemagglutinin tag at the N-terminus were labeled at 4ºC with a biotin reagent containing a reducible linker (total). The two first lanes serving as controls were then incubated with phenyl arsine oxide for 5 min at 37 ºC (to block receptor sequestration) and then incubated with BK for 1 h at 37ºC. The cells for the other lanes were incubated in the absence (NS) or presence of 10 μM BK, 5 μM B9430 or 5 μM icatibant for 1 hour at 37 ºC. All the cells besides total were subsequently stripped with glutathione (strip). The receptors were immunoprecipitated with Anti-HA agarose beads and visualized by Vectastin followed by development with ECL reagents as described for biotinylation protection assay under "Materials and Methods". One representative experiment out of three is shown.

B9430 induced a loss of surface binding as seen in the down-regulation assay. But the binding assay in the down-regulation assay was performed only with one non-saturating concentration of [^{3}H]BK (2nM), as this ligand is quite expensive. As three additional assays could not display receptor localization in intracellular compartments upon B9430 stimulation, ligand-induced receptor sequestration as the cause for this reduction in binding could be excluded. However, a decrease in B_2R receptor affinity induced by pre-stimulation with B9430 could be a possible explanation for these discrepancies. To test this hypothesis, we performed equilibrium binding curves and scatchard plot analyses to determine receptor affinities.

E.1.11 Binding of [^{3}H]BK to B_2wt_{LOW} after long-term treatment with BK, icatibant and B9430.

Cells were pre-incubated with the indicated ligands overnight followed by determination of equilibrium binding receptor affinity and B_{max} at 4°C. Determination of specific binding is shown in Fig. E-11, A. Scatchard plots of the data are shown in Fig. E-11, B. The scatchard plot showed a shift in receptor affinity upon prolonged stimulation with B9430, indicated by the slope of the line. The K_d values shifted from 7.6±2.1 nM (basal, control cells not pre-incubated with ligand) to 31.2±20.0 nM (cells pre-incubated with B9430). The surface binding (B_{max}) remained almost the same 9.6±2.4 pmol/mg protein (basal) and 9.4±2.3 pmol/mg protein (B9430). The K_d and B_{max} value for BK-treated cells was 7.7±3.5 nM and 0.86±0.25 pmol/mg protein, respective values for icatibant were 8.7±4.5 nM and 8.6±2.9 pmol/mg protein. Data represent the mean ± SEM of four experiments performed in duplicates.

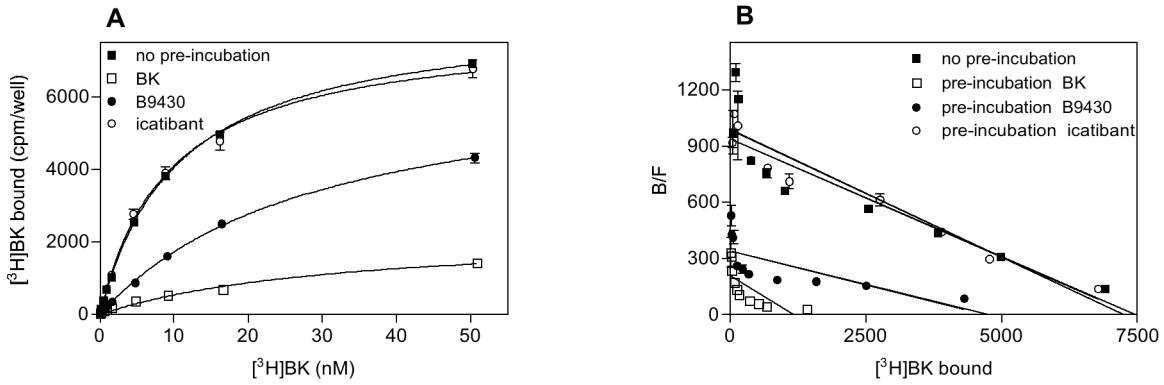

Fig. E-11. Binding of [^{3}H]BK to B_2wt_{LOW} after long-term incubation with BK, icatibant and B9430.

(A) HEK 293 cell expressing B_2wt_{LOW} were treated for 16 hours with 10 µM BK (□), 5 µM B9430 (●) and 5 µM icatibant (o) respectively. Thereafter, free and bound (pseudo)peptides were removed with acetic acid/NaCl solution, and the cells incubated with the increasing concentrations of [^{3}H]BK. Nonspecific binding was determined in the presence of 5 µM of unlabeled BK and subtracted from total binding being determined with [^{3}H]BK alone to calculate specific binding. One representative experiment out of four is shown. (B) Scatchard plot of the data. Lines were computed by linear regression. The K_d´s and B_{max} values calculated from data of four experiments: in control cells (basal), the K_d was 7.6 nM and B_{max} 9.6 pmol/mg protein, respective value for the BK-treated cells were 7.7 nM and 0.86 pmol/mg protein, for B9430 treated cells 31.2 nM 9.4 pmol/mg protein; and for icatibant-treated cells, 8.7 nM and 8.6 pmol/mg protein.

E.1.12 MAPK kinases ERK1/2

Many GPCRs can activate the Ras/mitogen-activated protein (MAP) kinase pathway, which is sufficient and necessary for the control of proliferation in different cell systems (van Biesen et al., 1996). Sequestration of GPCRs is assumed to be performed through recruitment of arrestins that guide them to internalization via clathrin-coated pits. Arrestins have recently been more and more appreciated as scaffold proteins that not only play a major role in receptor sequestration but also in the activation of G protein independent signaling pathways such as mitogen-activated protein kinase (MAPK) cascades (DeWire et al., 2007). Since in the fibroblasts all peptides were able to induce a reduction in surface binding, we also looked into potential MAPK activation by these compounds.

The fibroblasts were stimulated with bradykinin, icatibant or B9430 at a saturating concentration of 1 μM for 10 min. The reference agonist, BK, induced ERK1/2 activation (Fig. E-12). On the other hand icatibant and B9430 were not capable of significantly inducing any ERK1/2 activation.

The determination of phospho-ERK was also performed with the recombinant cell lines. As shown by the lack of an effect of BK in untransfected HEK 293 cells, B_2R agonist induced ERK1/2 phosphorylation is receptor dependent (Fig. E-13). The reference agonist, BK, induced phosphor-ERK activation in B_2wt_{HIGH} and B_2wt_{LOW}. B9430 showed some inducible phospho-ERK activation in B_2wt_{HIGH}.

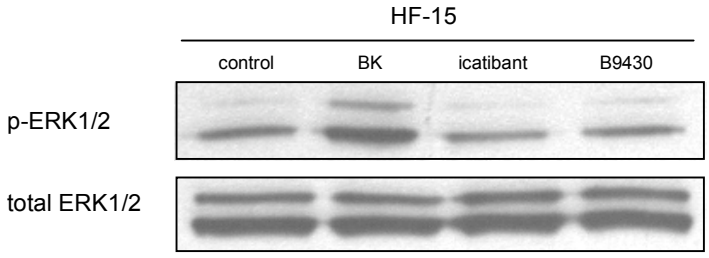

Fig. E-12: Immunoblots for phospho-ERK1/2 and total ERK1/2.

Foreskin fibroblasts HF-15 were maintained overnight in medium with reduced serum (0.5%). Stimulation was performed with 1 μM BK, B9430, or icatibant for 10 min at 37°C. Extraction and detection of total ERK1/2 (as loading control) and phospho-ERK1/2 was carried out as described in "Materials and Methods". One representative immunoblot out of two is shown.

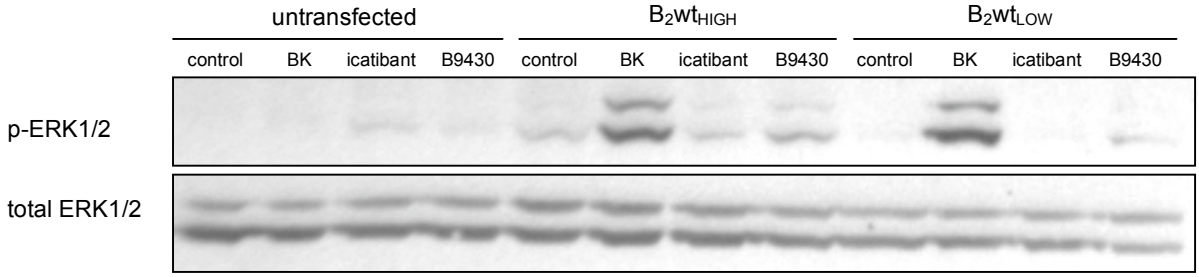

Fig. E-13: Immunoblots for phospho-ERK1/2 and total ERK1/2.

HEK 293 cell lines B_2wt_{HIGH} and B_2wt_{LOW} were maintained overnight in medium with reduced serum (0.5%). Stimulation was performed with 1 µM BK, B9430, or icatibant for 10 min at 37°C. Extraction and detection of total ERK1/2 (as loading control) and phospho-ERK1/2 was carried out as described in "Materials and Methods". Untransfected HEK 293 cells were also stimulated with 1 µM BK, B9430, or icatibant. One representative immunoblot out of at least three is shown.

E.1.13 B9430 acts as a surmountable antagonist

There have been several reports on the angiotensin AT_1-receptor concerning surmountable and insurmountable antagonism (Panek et al., 1995); (Gradman, 2002); (Fierens et al., 1999) which are often identified by concentration-response curves. Taking the angiotensin AT_1-receptor as an example, agents such as losartan only produce a parallel shift of the dose-response curve to the right without reducing the maximal response to angiotensin II. This inhibition can therefore be overcome by increasing concentrations of angiotensin II, and hence these agents are described as surmountable antagonists. By contrast, other agents such as valsartan or candersartan also depress the maximal response to angiotensin II. This inhibition cannot be overcome by increasing concentrations of angiotensin II and hence is described as insurmountable antagonism (Vanderheyden et al., 2000).

We performed a concentration-response IP assay on the HF-15 cell line. The fibroblasts were incubated for 16 hours with BK, icatibant and B9430. The next day stimulation was performed with addition of increasing concentrations (10^{-11} – 10^{-6} M) of BK and the EC_{50} values were determined. In this assay B9430 acted as a surmountable antagonist (Fig. E-14). The curve upon B9430 incubation is shifted to the right without any depression of the maximal response. BK, on the other hand, also depressed the maximal response indicating an insurmountable behavior. The

depression of the maximal response was probably due to the sequestration of the receptors that was seen in the down-regulation assay of the fibroblasts (Fig. E-7).

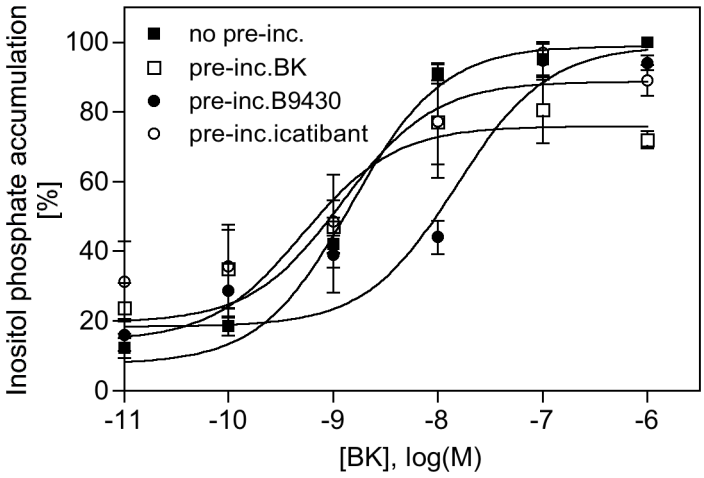

Fig. E-14: Basal and stimulated IP accumulation in fibroblasts HF-15 upon prolonged stimulation.

Fibroblasts HF-15 were incubated with 0.5 µCi [^{3}H]inositol in 0.5 ml medium overnight. 10 µM BK (□) , 5 µM B9430 (●) and 5 µM icatibant (○) respectively was added to the medium overnight. No pre-incubation (■) The next day stimulation was performed with addition of increasing concentrations (10^{-11} – 10^{-6} M) of BK in the presence of 50 mM LiCl for 30 min at 37°C as described in „Materials and Methods“. Symbols represent the mean ± SEM of three experiments performed in duplicates. The EC_{50} values for the three experiments were: non-stimulated (basal) 1.49 ± 0.08 BK; 0.52 ± 0.30 nM; B9430, 14.92 ± 0.22 nM; icatibant 1.22 ± 0.34 nM.

E.2 Alanine-screening of the intracellular loops of the B2 receptor

We set out to elucidate the participation of the intracellular receptor domains of the B_2R in its interaction with G proteins, receptor kinases and arrestins through a mutagenesis approach in intact cells. These proteins most likely interact with the cytosolic parts of the receptor, i.e. the three intracellular loops and the C-terminus. In order to more closely define the receptor sequences that are involved in these interactions and the roles they play, we systematically mutated all three intracellular loops either as point mutants or in groups of 3-5 amino acids to alanines, obtaining 14 mutants (Fig. E-15). Using the *Flp-In*^{TM} system (Invitrogen) we obtained clones of the *Flp-In*^{TM} *T-Rex*^{TM} cell line that stably expressed the human wild-type B_2R and the mutants. Expression levels of the wild type receptor in HEK 293 cells were varied as described in E.1.1 by using a vector with either the original CMV promoter for higher (B_2wt_{HIGH}) expression, or the weaker promoter (P_{min}) for lower (B_2wt_{LOW}) expression. Here it is important to mention that even cells with a low expression profile produced copy numbers of B_2R that were consistently higher than those observed in native cells. All the receptor coding sequences were preceded at the N-terminus by a single hemagglutinin (HA)-tag (MGYPYDVPDYAGS). The mutants showing strong effects compared to the lower expressed wild type were also generated in the low-expression format.

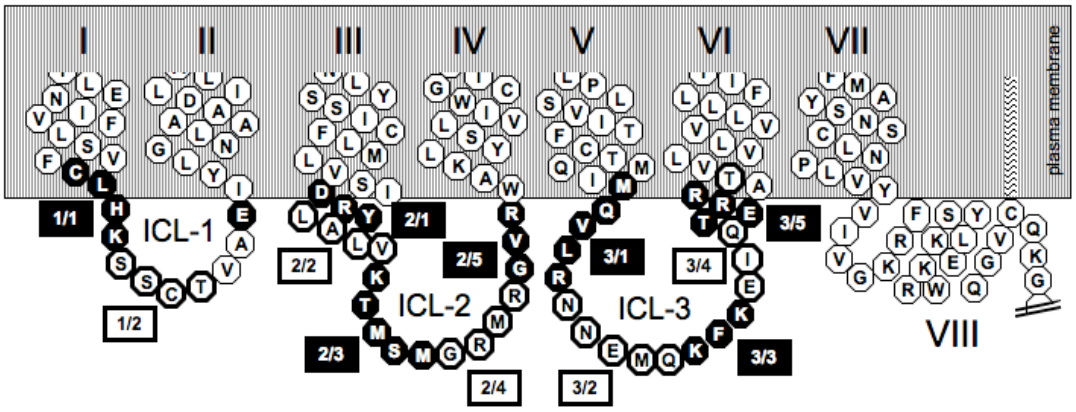

Fig. E-15: Mutated sequences in the human bradykinin B_2 receptor (Faussner, Wennerberg et al).

The sequences of the intracellular loops, parts of the transmembrane segments (I –VII) and of the proximal C-terminus containing the putative helix VIII and the palmitoylated cysteine are depicted. The clusters of amino acid residues that have been mutated to alanines are alternating depicted as black circles or white circles with a black edge with the respective construct name next to them. The point mutations E66A in the first loop and T242A at the end of the third loop are also indicated. The two-dimensional structure of the bradykinin B_2 receptor with the membrane border, the cytosolic extensions of the helical transmembrane domains III and VI and the additional cytosolic helix VIII was drawn after the structure published for inactive bovine rhodopsin (Palczewski et al., 2000

E.2.1 ICL-1 and sequences at the N-terminus of ICL-2 and at the C-terminus of ICL-3 are crucial for receptor surface expression.

Despite the isogenic expression, the maximal receptor numbers (B_{max}) of the various constructs were quite diverse and several receptor mutants – all ICL-1 mutants and construct 3/5, in particular - were significantly lower expressed than the B_2wt [11.0 ± 0.7 pmol/mg protein, B_2wt_{HIGH}] though all were under the control of the same cytomegalovirus (CMV) promoter. We already observed that icatibant and B9430 show partial agonism with high B_2wt expression. Besides the wild type receptor, we generated lower - under the control of the P_{min} promoter - expressing cell lines for some of the constructs in ICL-3 (Fig. E-16). There were two reasons for this. Firstly these constructs 3/2, 3/4 and T242A displayed very high expression levels. Secondly the constructs, as will be shown later (Fig. E-19), showed induced IP accumulation also with the poor partial agonists (B9430 and icatibant) indicating a semi-active conformation. To test if the semi-activity also held true with lower expression, the P_{min} constructs were generated.

Of the constructs with alanine substitutions in the sequence of ICL-1, mutant 1/2 displayed particularly low surface receptor binding activity with only 6% of that obtained for B_2wt_{HIGH}. Exchange of the highly conserved DRY-sequence located at the transition of the cytosolic extension of helix 3 and the N-terminus of ICL-2 for three alanines resulted in a binding deficient construct (<20 fmol/mg protein). All other constructs with mutations made in ICL-2 were well expressed. The mutants made in ICL-3 all revealed high expression levels with the exception of mutant 3/5 - positioned at the C-terminus of ICL-3- that displayed only 6% of that obtained for B_2Rwt.

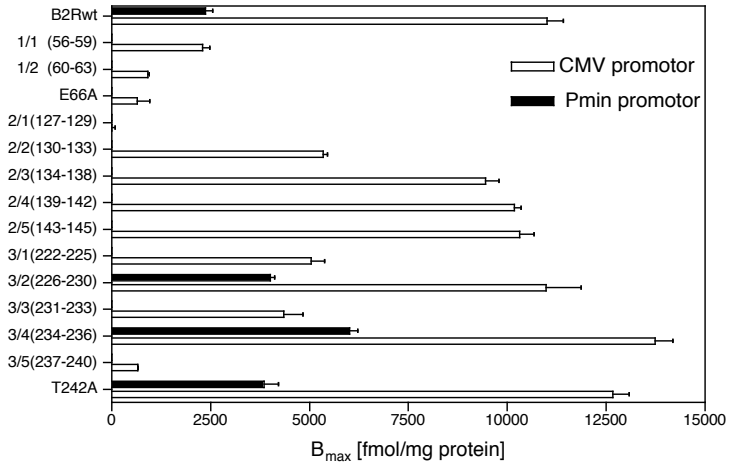

Fig. E-16: Expression levels of constructs (Faussner, Wennerberg et al).

Maximal binding of [^{3}H]BK to confluent monolayers of HEK 293 cells stably and isogenically expressing the indicated constructs was estimated with app. 30 nM [^{3}H]BK on ice as described in „Materials and Methods". The data shown are the mean ± SEM of at least 3 clones. The positions of the amino acids mutated to alanines are given in brackets. Expression of constructs under control of the CMV-promoter (open columns); constructs under control of the weaker P_{min}-promoter (closed columns).

E.2.2 Immunoblot of construct 2/1

Exchange of the highly conserved DRY-sequence located at the transition of the cytosolic extension of helix III and the N-terminus of ICL-2 for three alanines resulted in a binding deficient construct. Fig. E-17 shows the immunoblot of HA-tagged mutant 2/1 in comparison with those of B_2wt_{HIGH} and B_2wt_{LOW} (immunoblot generated by Jens Feierler). For both wild type cell lines several bands were detected between 50 and 65 kDa with densities that largely reflect their relative expression levels and two weaker bands at 42 and 39 kDa. Mutant 2/1 in contrast, displayed only strong bands at 42 and 38 kDa and two weaker ones at 36 and 33 kDa. This suggests that this receptor mutant is well expressed but might not become processed and glycosylated properly, and is therefore unable to reach the plasma membrane. In fact, a fusion protein of construct 2/1 with eGFP (enhanced green fluorescent protein) joined to the C-terminus demonstrated strong intracellular expression and did also not display any specific surface [^{3}H]BK binding activity (not shown).

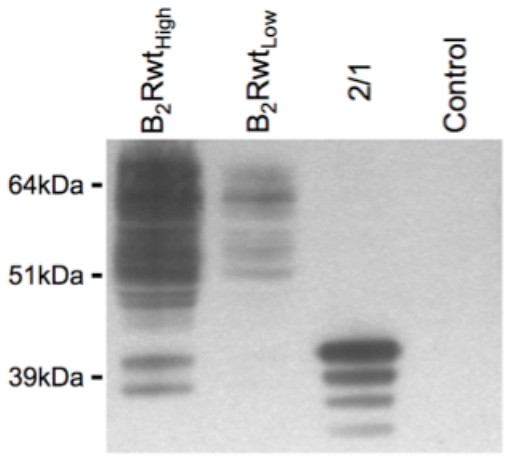

Fig. E-17: Immunoblot of B_2Rwt's and mutant 2/1 (Faussner, Wennerberg et al).

HEK 293 cells stably expressing high (B_2Rwt_{HIGH}) or low (B_2Rwt_{LOW}) amounts of HA-tagged wild type B_2R, or construct 2/1 were lysed in RIPA buffer as described in "Materials and Methods". 15 µg of protein were separated by SDS-Page and detected by western blot using a monoclonal HA-antibody. Molecular masses of standard proteins are indicated on the left side in kDa. Control, mock transfected cells. The blot shown is representative of two experiments. Immunoblot generated by Jens Feierler.

E.2.3 Some mutants are in a high affinity state at 37°C.

Receptor equilibrium binding affinities (K_d) reflect the conformation of the ligand binding site. Changes in the affinity may indicate different preferences in coupling or uncoupling of the receptor constructs to or from intracellular proteins, such as G proteins, arrestins, or receptor kinases, as these interactions might affect also the overall receptor conformation including that of the binding site.

B_2wt_{LOW} displayed at 37°C an affinity of 8.05 ± 1.10 nM that was increased by incubation on ice to 2.02 ± 0.22 nM (n=5) thus exhibiting an app. 4-fold increase in affinity (Fig. E-18, Tab. 3). This was similarly seen for B_2wt_{HIGH} with the difference that both affinities were somewhat lower (10.42 ±1.56 nM and 2.81± 0.7 nM, respectively). Mutants 1/2 and E66A had a higher affinity than B_2wt_{LOW} at 37°C (3.21 ± 0.31 nM and 3.77 ± 0.67 nM, respectively) but also showed a shift of app. 4-fold to higher affinity when incubated on ice (0.79 ± 0.11 nM and 0.94 ± 0.29 nM, respectively) thus upholding their relative higher affinity also at 4°C (Tab. 3). In contrast, mutant 2/2 in ICL-2 displayed a high affinity at 37°C but exhibited almost no shift to higher affinity on ice (2.96 ± 0.74 nM at 37°C vs. 1.8 ± 0.36 nM at 4°C) suggesting that this mutant is also at 37°C in a high affinity state. The other mutants in ICL-2 displayed affinity increases at 4°C relative to 37°C that were similar to those of the B_2Rwt's.

With exception of mutant 3/3 all constructs generated in ICL-3 displayed a binding behavior distinctly different from the B_2wt's. While the mutations located in the middle of ICL-3 (3/2, 3/4) and T242A showed affinities at 37°C that were similar to the ones of the B_2wt's they did not respond to incubation at 4°C with an increase in the affinity as strong as seen for the B_2wt's, thus displaying a shift of less than 2-fold. The constructs either at the N-terminal (3/1) or at the C-terminal (3/5) end exhibited a high affinity at 37°C as well as at 4°C (Tab. 3).

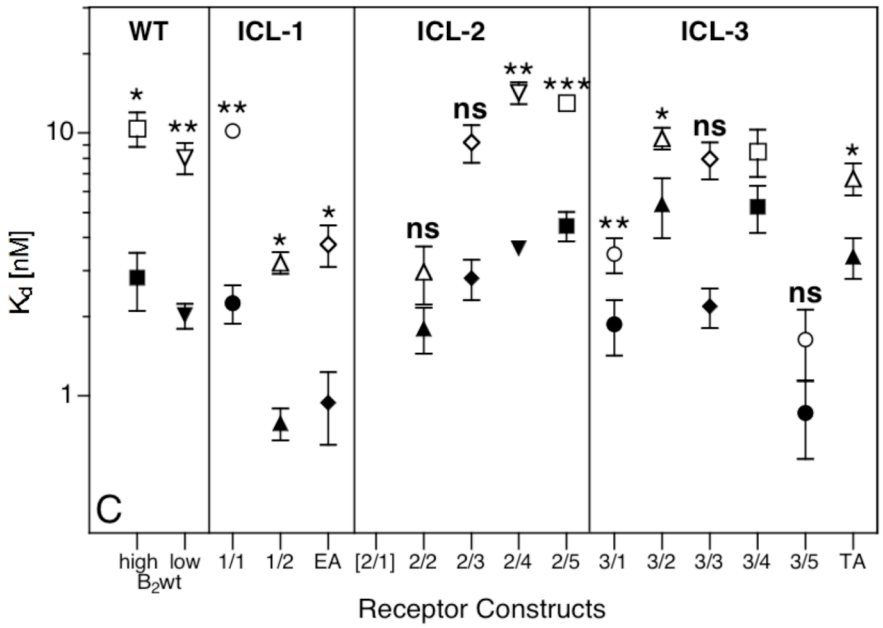

Fig. E-18: Equilibrium dissociation constants K_d at 37°C and at 4°C (Faussner, Wennerberg et al).

Binding of [^{3}H]BK (0.01 – 30 nM) to HEK 293 cells stably expressing the indicated constructs was determined at 37°C or at 4°C after inhibition of receptor sequestration by pretreatment of the cells with 100 µM PAO as described in „Material and Methods". Symbols present the K_d's as mean ± SEM of at least three experiments (also given in table 2). K_d's at 37°C (open symbols) ; K_d's at 4°C (closed symbol). Note the logarithmic scale of the y-axis. Comparison between K_d values at 37 and 4°C: $^{*}P < 0.05$; $^{**}P < 0.01$; $^{***}P < 0.001$; ns, not significant.

E.2.4 Basal activity and stimulated accumulation of inositol phosphates (IP)

Stimulation of the B_2Rwt leads to activation of phospholipase C via G protein $G_{q/11}$, resulting in the release of inositol trisphosphate. In order to determine the effect of the loop mutations on the interaction of the receptor with $G_{q/11}$, we measured the accumulation of inositolphosphates (IP) in the presence of 50 mM LiCl after 30 min with and without stimulation by BK. The fact that some of the mutants were not showed no substantial difference in their affinities at 37°C and at 4°C suggested that they may be in a permanent higher affinity state, i.e. in a semi-active conformation. If so, they might either exhibit a higher basal activity or be activated even by poor partial agonists. As mentioned before the pseudopeptides icatibant and B9430 acted as partial agonists at high receptor overexpression, but were not able to activate the B_2Rwt at all when it was expressed at lower levels. Thus, these drugs were well suited for the identification of semi-active mutants, provided that these constructs were expressed at low levels.

Activation of most constructs by 1 µM BK induced an 8 -15 fold increase over basal IP determined as the amount of IP's in cells kept on ice (E-19). In our experimental set-up there seems to be no direct linear correlation between the induced accumulation of IP's and the amount of expressed receptors as demonstrated by the example of the B_2Rwt's (see table 3) where an almost five times higher receptor level (11.0 vs. 2.4 pmol/mg protein) did not result in a significantly higher IP response (12.55 ± 1.00 nM vs. 12.11 ± 1.22 nM).

None of the loop mutations displayed an increased constitutive, i.e. e. agonist-independent, activation of the receptor, as their basal activity was not significantly higher than that observed for the B_2Rwt's.

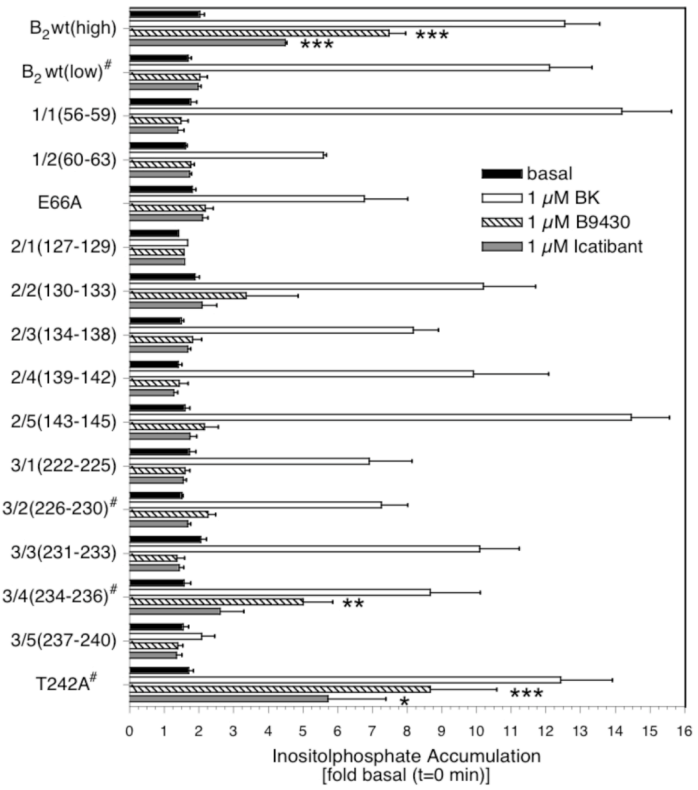

Fig. E-19: Basal and stimulated accumulation of total inositol phosphates (Faussner, Wennerberg et al).

Cells in 12-well plates were incubated overnight with 0.5 µCi [^{3}H]inositol in 0.5 ml culture medium. The monolayers were washed briefly and incubated with incubation buffer containing 50 mM LiCl ± 1 µM of the indicated peptides for 60 min on ice. IP accumulation (basal and stimulated) was started by placing the plates in a water bath at 37°C. The stimulation was stopped after 30 min and total inositol phosphates were determined as described in „Materials and Methods“. Each column represents the mean ± SEM of at least three independent experiments done in duplicates, given as fold over the IP content of identically treated control cells that had remained in the same buffer on ice. Basal (black columns), BK (open columns), B9430 (hatched columns), icatibant (grey columns). Stars indicate constructs lower expressed under the control of the P_{min}-promoter (mutant 3/2, 4.0 ± 0.2 pmol/mg protein; mutant 3/4, 6.0 ± 0.4 pmol/mg protein; mutant T242A, 3.8 ± 0.5 pmol/mg protein). Comparison between basal and stimulated IP accumulation: $^{*}P < 0.05$; $^{**}P < 0.01$; $^{***}P < 0.001$.

E.2.5 EC_{50} of IP accumulation.

There was no significant difference in the EC_{50} obtained with the two differently expressing B_2Rwt's, demonstrating that at these levels the efficiency/potency is independent of the number of receptors (Fig. E-20, Tab. 3). All mutants made in ICL-1 were almost as efficient (1/1) or even more significance (1/2, E66A) than the B_2Rwt's in stimulating IP accumulation. Of the constructs generated in ICL-2, 2/2 displayed a slightly increased (approx. 4-fold) and 2/3 and 2/4 a strongly increased EC_{50} (approx. 15-fold) when compared to the B_2Rwt's. Only mutant 2/5 exhibited a comparable EC_{50}. All cluster mutations but not point mutation T242A of ICL-3 – (due to its poor activity it was not possible to determine an EC_{50}-value for mutant 3/5) - exhibited a distinctly reduced efficiency. This reduction was more pronounced for 3/1 – 3/3 (app. 4-fold) located at the N-terminus and in the middle of the loop, and only minor (app. 2-fold) for 3/4.

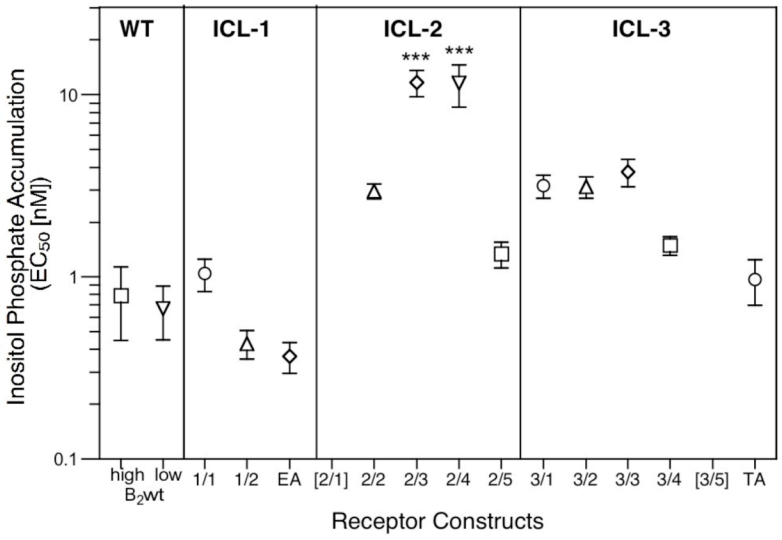

Fig. E-20: EC_{50} values of IP accumulation (Faussner, Wennerberg et al).

Cells were treated and incubated with increasing concentrations of BK (from 10^{-12} to 10^{-5} M) for 30 min at 37°C and the generation of total IP was determined as described in „Materials and Methods". The EC_{50} is given as mean ± SEM of the number of experiments indicated in table 2. Note the logarithmic scale of the *y*-axis. Comparison with EC_{50} values of both high and low B_2Rwt: $^{***}P < 0.001$.

E.2.6 Internalization

After stimulation most GPCRs including the B_2 receptor are sequestered to compartments within the cell. Recent publications indicated that the intracellular loops of GPCRs might not only be involved in the interaction with their cognate G proteins but may also serve - together with (phosphorylated) serine/threonine residues in the C-terminal tail- as contact sites for arrestins and G protein-coupled receptor kinases thus playing also a part in the internalization (Marion et al., 2006); (Huttenrauch et al., 2002). In addition, diminished/increased ability to interact with the cognate G protein(s) or an altered capability of activating them might also affect this process. We therefore also looked at the [^{3}H]BK internalization properties of the various constructs. Having demonstrated that internalization decreases when too many receptors are occupied in overexpressing cells (Faussner et al., 1999) we took care to use non-saturating concentrations of less than 2 nM [^{3}H]BK. Under these conditions, where the internalization machinery was not expected to be limiting, none of the constructs exhibited internalization that was distinctly slower than that observed for the B_2wt_{HIGH} (Fig. E-21). This suggests that the amino acid residues involved are not of pivotal significance for the internalization. It cannot, however, be excluded that the affinities for receptor kinases and arrestins have changed for the mutants as compared to the B_2wt without affecting the internalization under our conditions. Furthermore, due to its lack of surface binding activity no results could be obtained for the mutant 2/1, i.e. participation of the highly conserved DRY sequence in the internalization process cannot be excluded by our data.

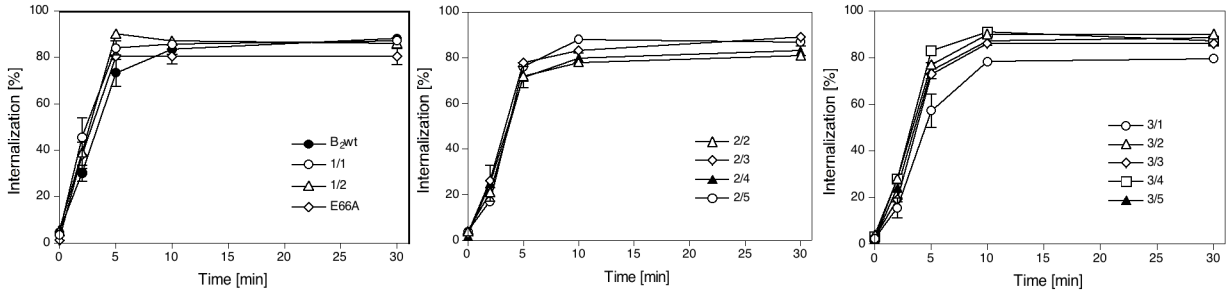

Fig. E-21: Internalization of [^{3}H]BK (Faussner, Wennerberg et al).

Cells expressing the B_2wt_{HIGH} or the indicated receptor constructs were preincubated with 2 nM [^{3}H]BK for 90 min on ice. Internalization was initiated by warming the plates to 37°C in a water bath. At the indicated time points the internalization was stopped and surface-bound and internalized [^{3}H]BK were determined by acetic acid treatment as described in „Materials and Methods“. Internalization is given as a percentage of total bound [^{3}H]BK. Data points represent the mean ± SEM of at least three experiments performed in duplicate or triplicate.

E.2.7 Summary of data for the loop mutants

Tab. 3: [^{3}H]Binding data, basal and BK-induced IP accumulation (Faussner, Wennerberg et al).

	[^{3}H]BK Binding				Inositol Phosphate Accumulation		
Receptor-construct	B_{max}[a] [pmol/mg prot.]	K_d(PAO/37°C) [nM]	K_d (PAO/4°C) [nM]	K_d-ratio 37°C/4°C	basal[b]	maximal effect[b]	EC_{50}[c] [nM]
B_2wt_{HIGH}	11.0±0.7	10.42±1.56(4)	2.81±0.7	3.7	2.02±0.13(8)	12.55±1.00	0.79±0.34(4)
B_2wt_{LOW}	2.4±0.3	8.05±1.10(5)	2.02±0.22	4.0	1.69±0.09(4)	12.11±1.22	0.67±0.22(3)
1/1(CLHK)	2.3±0.3	10.18±0.21(3)	2.25±0.37	4.5	1.76±0.17(6)	14.18±1.44	1.04±0.21(5)
1/2(SSCT)	0.9±0.1	3.21±0.31(3)	0.79±0.11	4.1	1.61±0.05(4)	5.58±0.09	0.43±0.08(6)
E66A	0.7±0.4	3.77±0.67(3)	0.94±0.29	4.0	1.81±0.11(6)	6.77±1.25	0.37±0.07(3)
2/1(DRY)	< 0.02	n.a.	n.a	n.a.	n.a.	n.a.	n.a.
2/2(LALV)	5.3±0.2	2.96±0.74(3)	1.80±0.36	1.6	1.88±0.13(5)	10.19±1.50	2.96±0.28(4)
2/3(KTMSM)	9.5±0.7	9.22±1.50(3)	2.80±0.49	3.3	1.49±0.07(3)	8.17±0.72	11.66±1.94(6)
2/4(GRMR)	10.2±0.3	14.19±1.36(3)	3.64±0.17	3.9	1.40±0.11(6)	9.90 ± 2.20	11.56±3.02(5)
2/5(GVR)	10.3±0.6	12.99±0.78(4)	4.43±0.57	2.9	1.59±0.14(8)	14.46±1.10	1.33±0.22(5)
3/1(MQVLR)	5.0±0.6	3.45±0.53(5)	1.87±0.45	1.8	1.72±0.18(5)	6.91±1.22	3.17±0.45(3)
3/2(NNEMQ)	11.0±1.3	9.54±0.90(3)	5.37±1.38	1.8	1.55±0.12(5)	7.37±0.86	3.12±0.42(5)
3/3(KFK)	4.3±0.7	7.93±1.27(3)	2.18±0.37	3.6	2.05±0.17(4)	10.09±1.14	3.78±0.64(4)
3/4(EIQ)	13.7±0.8	8.52±1.74(4)	5.24±1.07	1.6	1.87±0.33(3)	10.53±3.25	1.49±0.18(4)
3/5(TERR)	0.7±0.0	1.63±0.50(3)	0.86±0.29	1.9	1.54±0.16(5)	2.07±0.38	n.a.
T242A	12.7±0.6	6.70±0.93(3)	3.38±0.60	2.0	1.93±0.07(3)	11.37±0.72	0.97±0.27(4)

[a] estimated from at least 3 different clones in 24-wells after incubation with 200 µl 30 nM [^{3}H] BK on ice.

[b] Total IP accumulation after 30 min incubation in buffer with inhibitors and 50 mM LiCl at 37°C with (maximal effect) and without (basal) 1 µM BK, expressed as fold increase of initial total IP production (t= 0 min). The results represent the mean ± SEM of the number of experiments (given in brackets) performed in triplicates.

[c] Calculated from incubations in duplicates with 10^{-12} to 10^{-5} M BK for 30 min at 37°C in the presence of 50 mM LiCl. Results are the mean ± SEM of independent experiments (number indicated in brackets)

n.a. not applicable

E.3 R3.50 in the DRY motif and E6.30 in the TERR motif as key players for the activation and trafficking of the human bradykinin B2 receptor

The highly conserved DRY motif is located at the C-terminal end of the 3rd transmembrane helix of family A GPCRs. It is known to play a crucial role in regulating GPCR conformational states. The crystal structure of the ground state of rhodopsin indicates that the side chain of arginine 3.50 in the DRY motif forms salt bridges with the preceding aspartate side chain and with the side chain of glutamate at position 6.30 on helix 6, suggesting that disruption of these salt bridges may be a key step towards receptor activation. This interaction between R3.50 and E6.30 is also known as the "ionic lock". Positions R3.50 and E6.30 are depicted in Fig. E-22.

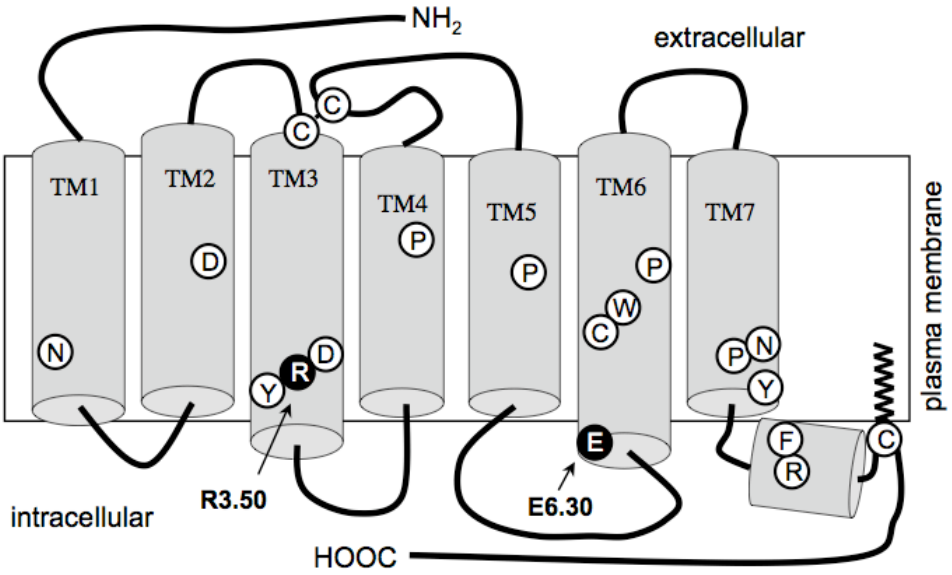

Fig. E-22: Schematic two-dimensional representation of a family A GPCR (Wennerberg et al. *submitted*).

Highly conserved residues are shown as white circles with the one letter code for the amino acid in black. The two residues involved in the formation of the "ionic lock" are depicted in black circles with white letters.

We set out to investigate the role of these two conserved amino acids in the human bradykinin B_2 receptor by mutating them to alanines (termed mutants R3.50A and E6.30A). To determine the influence of receptor densities, the two mutants were expressed under the CMV promoter and the weaker P_{min} promoter in HEK 293 cells. To determine whether both these two mutants were in semi-active conformations, their responses to the poor partial agonists, icatibant, and B9430, were examined.

E.3.1 Expression

In the cell line $R3.50A_{HIGH}$, with expression under the control of the strong CMV promoter, the yield was nearly 4 pmol receptor/mg of total membrane protein. In the cell line $R3.50A_{LOW}$, under the control of the P_{min} promoter, the level reached 1.5 pmol/mg protein (Fig. E-23). For $E6.30A_{HIGH}$ the expression was slightly lower than for $R3.50A_{HIGH}$ at 3.5 pmol/mg protein. $E238A_{LOW}$ expression reached approximately 1.3 pmol/mg protein. A saturating concentration of approximately 30 nM [^{3}H]BK was used for the experiments.

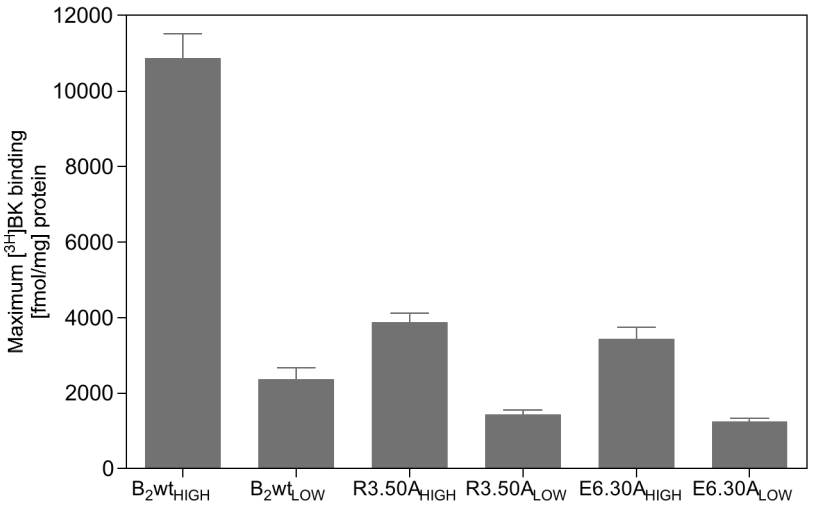

Fig. E-23: Bradykinin B_2 receptor expression levels in R3.50A and E6.30A in comparison to B_2wt (Wennerberg et al, *submitted*).

Maximal [^{3}H]BK binding B_{max} of HEK 293 cells isogenically and stably expressing high or low amounts of R3.50A and E6.30A was determined with approximately 30 nM [^{3}H]BK on ice as described in „Materials and Methods“. The data shown is the mean ± SEM of at least four binding experiments. The receptor expression in $R3.50A_{HIGH}$/$E6.30A_{HIGH}$ was under control of the CMV-promoter, whereas in $R3.50A_{LOW}$/$E6.30A_{LOW}$ expression was driven by the weaker Pmin promoter.

E.3.2 E6.30A showed no affinity shift between 37°C and 4°C.

Receptor equilibrium binding affinities (K_d) reflect the conformation of the extracellularly located ligand binding site. Coupling and uncoupling of intracellular proteins to and from the receptor also affect the conformation of the receptor, including that of the binding site (Enquist et al., 2007). Differences in the affinities of the constructs may therefore indicate a change in the receptor coupling preferences. Alternatively, they could be the consequence of a change of overall receptor conformation induced by the mutation. Representative equilibrium binding curves of B_2wt_{LOW} at 4°C (after pre-incubation at 37°C) and at 37°C are shown in Fig. E-24, A. The average K_d´s obtained from at least 4 independent experiments for B_2wt_{LOW} were 2.02 ± 0.22 nM at 4°C and 8.05 ± 1.10 nM at 37°C, and 2.81 ± 0.7 nM at 4°C and 10.42 ± 1.56 nM at 37°C for B_2wt_{HIGH} (see Tab. 4), demonstrating that the B_2R has a lower affinity at 37°C than at 4°C. Corresponding representative equilibrium binding curves at 4°C and at 37°C of $R3.50A_{LOW}$ and $E6.30A_{LOW}$ are displayed in Fig. E-24, B and Fig. E-24, C, respectively. These curves and the mean K_d's calculated from several experiments (Tab. 4) reveal that at 4°C the B_2wt and the mutant constructs have equal affinities. At 37°C, in contrast, the affinities of R3.50A and of E6.30A are significantly higher than that observed for the less well expressed B_2wt_{LOW}. Mutant $E6.30A_{LOW}$ even displayed at 37°C an affinity that was almost identical to that determined at 4°C. The fact that both mutants remain in a higher affinity state at 37°C after activation suggests, according to the extended ternary model (Samama et al., 1993), a permanent constitutive or semi-active receptor conformation.

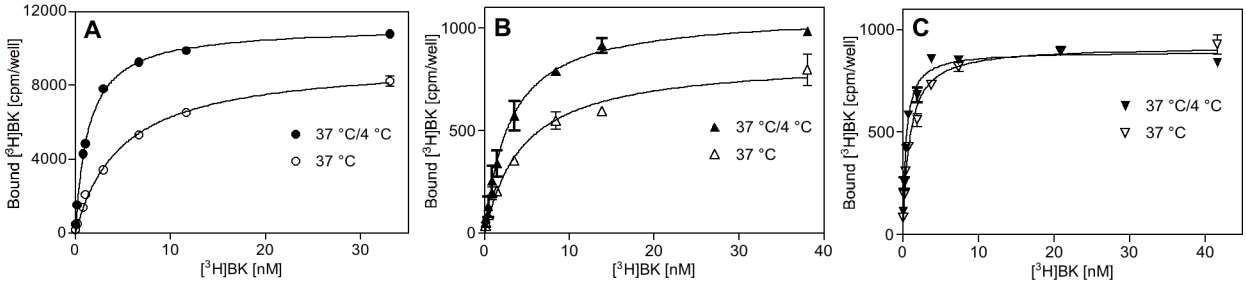

Fig. E-24: Saturation binding curves at 4°C and at 37°C (Wennerberg et al, *submitted*).

Binding of [^{3}H]BK to HEK 293 cells stably expressing the indicated constructs was determined at 4°C (after pre-incubation at 37°C) and at 37°C with inhibition of receptor sequestration by pretreatment of the cells with 100 µM PAO, as described in „Experimental". Three representative binding curves are shown: (**A**) B_2wt_{LOW}; (**B**) construct $R3.50A_{LOW}$; (**C**) construct $E6.30A_{LOW}$. The K_d values of all constructs as mean ± SEM of at least three experiments are given in Tab. 4.

E.3.3 Accumulation of inositoltrisphosphates

Next the ability of the point mutants to activate the G protein was measured. As already seen and also shown here, high and low expressed B_2Rwt cells responded to a challenge with 1 µM BK with a similar strong inositolphosphate accumulation in the presence of 50 mM LiCl (Fig. E-25). In contrast, neither the high nor the lower expressed mutant R3.50A was able to induce phosphatidylinositol hydrolysis after binding of BK, indicating that R3.50 is crucial for a productive interaction of B_2R with G protein $G_{q/11}$. Both cell lines expressing construct E6.30A responded to BK with strong accumulation of IPs, albeit the poorer expressing cell line gave a clearly weaker response.

The fact that E6.30A displayed a high affinity for BK at 37°C (Fig. E-24, C), indicated that this mutant might be in a permanent high affinity state, which usually suggests a constitutive or semi-active conformation. However, as the E6.30A construct displayed no increased basal PI hydrolysis activity (Fig. E-25, table 4) it was apparently not in a constitutively active state with regard to G protein activation.

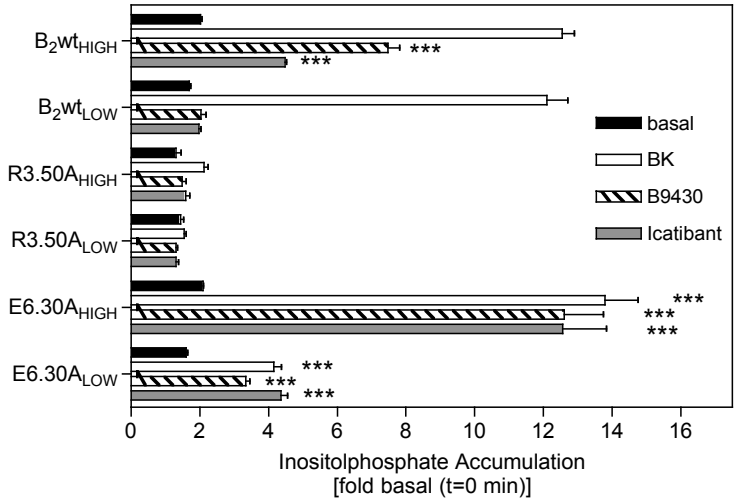

Fig. E-25: Basal and stimulated accumulation of total inositol phosphates (Wennerberg et al, *submitted*).

HEK 293 cell lines R3.50A and E6.30A together with B_2wt were incubated overnight in 12-well plates with 0.5 μCi [^{3}H]inositol in 0.5 ml medium. Stimulation was performed in the presence of 50 mM LiCl and 1 µM BK, B9430 and icatibant for 30 min at 37°C as described in „Materials and Methods“. Each value represents the mean ± SEM of at least three independent experiments done in triplicates, given as fold over the IP content of non-stimulated but other identically treated control cells that had remained on ice. Basal (black columns), BK (open columns), B9430 (hatched columns), icatibant (grey columns). $^{***}P < 0.001$.

As shown before mutant receptors with semi-active conformations can be identified by their stronger response to partial agonists than the wild type. In both cell lines expressing construct E6.30A, B9430 and icatibant behaved as full agonists inducing an IP release comparable to that obtained with BK (Fig. E-25). This strongly indicates that mutation of E6.30 to alanine induces a semi-active receptor conformation. Neither low nor high expressed mutant R3.50A gave an IP response to a challenge with the antagonists.

E.3.4 The antagonist [^{3}H]NPC17331 promotes internalization of R3.50A and E6.30A.

Due to the decisive role of R3.50 in the activation of $G_{q/11}$ it was not possible to use the poor partial agonists B9430 and icatibant as phospholipase C activation to identify a potential semi-active state of this mutant. However, the availability of a structurally related tritiated compound, [^{3}H]NPC17331, also usually considered an antagonist, allowed us to test for constitutive or semi-active receptor states by comparing the internalization properties of B_2Rwt to those of the mutants.

Both constructs R3.50A and E6.30 internalized upon application of [^{3}H]BK as efficiently as B_2Rwt, displaying approximately 80% internalization after 10 min (Fig. E-26) and thereby demonstrating that (i) these mutations do not negatively affect the internalization process under the applied conditions, and (ii) this process is obviously independent of G protein stimulation since R3.50A is G protein activation incompetent (Fig. E-25).

B_2Rwt did not internalize with [^{3}H]NPC17331 (< 5% after 10 min at 37°C). In contrast, for mutant R3.50A approximately 25% of specifically bound [^{3}H]NPC17331 was detected after 10 min in acetic acid resistant compartments (Fig. E-26). An even stronger effect was observed for E6.30A, that displayed approximately 65% internalization of bound [^{3}H]NPC17331. The results indicate semi-active or constitutively active receptor conformations for mutants E6.30A and R3.50A with regard to receptor internalization. A question arising was whether NPC17331 behaves as a partial agonist (similar to B9430 and icatibant) capable to induce ligand-mediated receptor internalization in these mutants (indication of a semi-active conformation) or whether it is a neutral antagonist that got internalized bound to constitutively internalizing receptor mutants (indication of a constitutively active conformation).

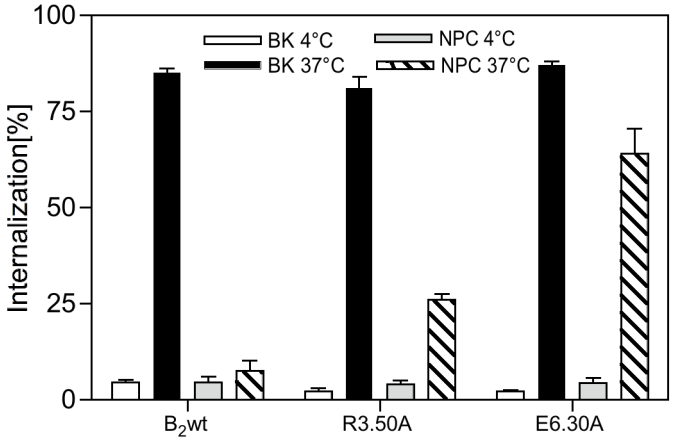

Fig. E-26: Internalization of [^{3}H]BK and [^{3}H]NPC17331 (Wennerberg et al, *submitted*).

HEK 293 cells stably expressing B_2wt_{HIGH}, $R3.50A_{HIGH}$ and $E6.30A_{HIGH}$ were preincubated with 2 nM [^{3}H]BK for 90 min on ice. Internalization was started by warming the plates up to 37°C in a water bath. After 10 min surface-bound and internalized [^{3}H]BK were determined by acetic acid treatment as described in „Materials and Methods". Internalization is given as percentage of total bound [^{3}H]BK (surface plus internalized [^{3}H]BK). Data points represent the mean ± SEM of at least three experiments performed in duplicates or triplicates. [^{3}H]BK, 4°C (open columns); [^{3}H]BK, 37°C (black columns); [^{3}H]NPC17331, 4°C (grey columns); [^{3}H]NPC17331, 37°C (hatched columns).

E.3.5 R3.50A and E6.30A are both constitutively internalized

With the biotinylation protection assay (BPA) it was possible to differentiate between ligand-dependent and -independent receptor internalization. As shown previously, B_2Rwt_{LOW} displayed strong internalization upon BK stimulation (Fig. E-26). In the absence of BK or in the presence of B9430 and icatibant no intracellular receptors were detected after 1 hour, hence B_2Rwt did not display any ligand-independent or "antagonist"-inducible internalization (Fig. E-27). Also, mutants R3.50A and E6.30 responded to BK with clear receptor internalization. But even in the absence of BK a strong signal was detected, indicating ligand-independent receptor internalization (Fig. E-27). This demonstrates that both mutants are in a constitutively active conformation where the interaction with the cellular internalization machinery is concerned. The compounds B9430 and icatibant slightly enhanced this constitutive internalization, with E6.30A reaching an internalization level similar to the one induced by BK.

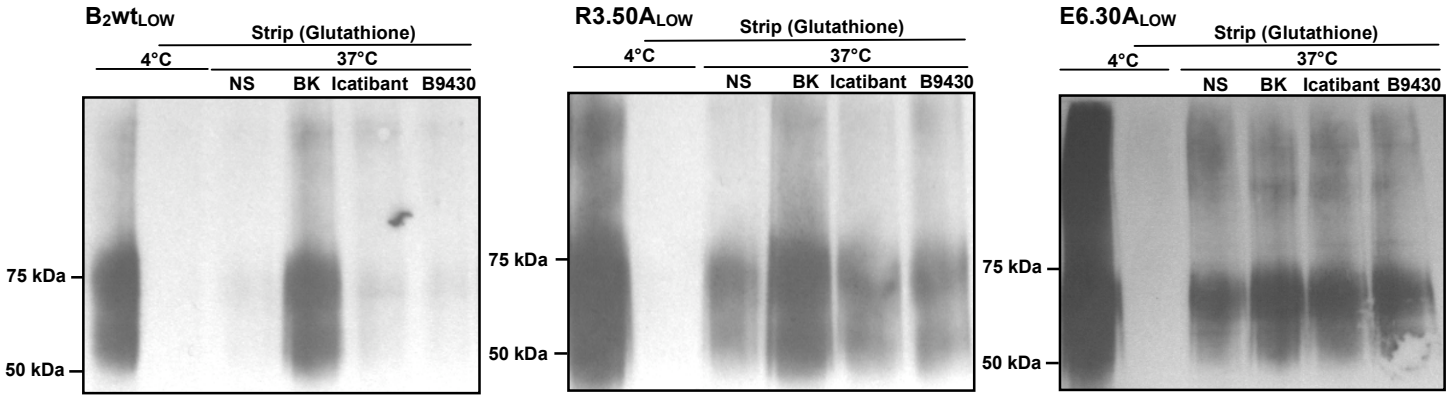

Fig. E-27: Receptor endocytosis as determined by BPA (Wennerberg et al, *submitted*).

HEK 293 cells stably expressing B_2wt_{LOW}, $R3.50A_{LOW}$ and $E6.30A_{LOW}$ having a hemagglutinin tag at the N-terminus were labeled at 4ºC with a biotin reagent containing a reducible linker. The cells were then either stripped directly or incubated in the absence (NS = nonstimulated) or presence of 10 μM BK, 5 μM B9430 or 5 μM icatibant for 1 hour at 37 ºC and then stripped. The receptors were then treated with Anti-HA agarose beads and visualized by Vectastin followed by development with ECL reagents as described for biotinylation protection assay under „Materials and Methods“. The blots shown are representative of three experiments.

E.3.6 Localization of receptor constructs with epifluorescence microscopy

For the determination of the effects of the constitutive internalization on the cellular distribution of the receptors, we visualized the localization of receptor constructs by epifluorescence microscopy using eYFP (enhanced yellow fluorescent protein) genetically fused to their C-termini. In order to avoid any receptor internalization caused by BK present in the medium, we used the tetracycline-inducible Flp-In expression system (Invitrogen) and exchanged the normal cell culture medium for serum-free OPTI-MEM before inducing receptor-eYFP expression (under P_{min} promoter control) for 16 h. B_2RwteYFP was localized exclusively at the cell membrane, and responded only to BK, but not to B9430 or icatibant, with clear translocation into intracellular vesicles (Fig. E-28). In contrast, both mutants, in particular E6.30A, displayed fluorescence at the cell membrane as well as in vesicles of various sizes throughout the cytosol in the absence of BK; most likely as a result of constitutive receptor internalization. Moreover, both constructs responded not only to BK, but also to B9340 and icatibant with additional receptor translocation into the cell, thus confirming their semi-active conformation state.

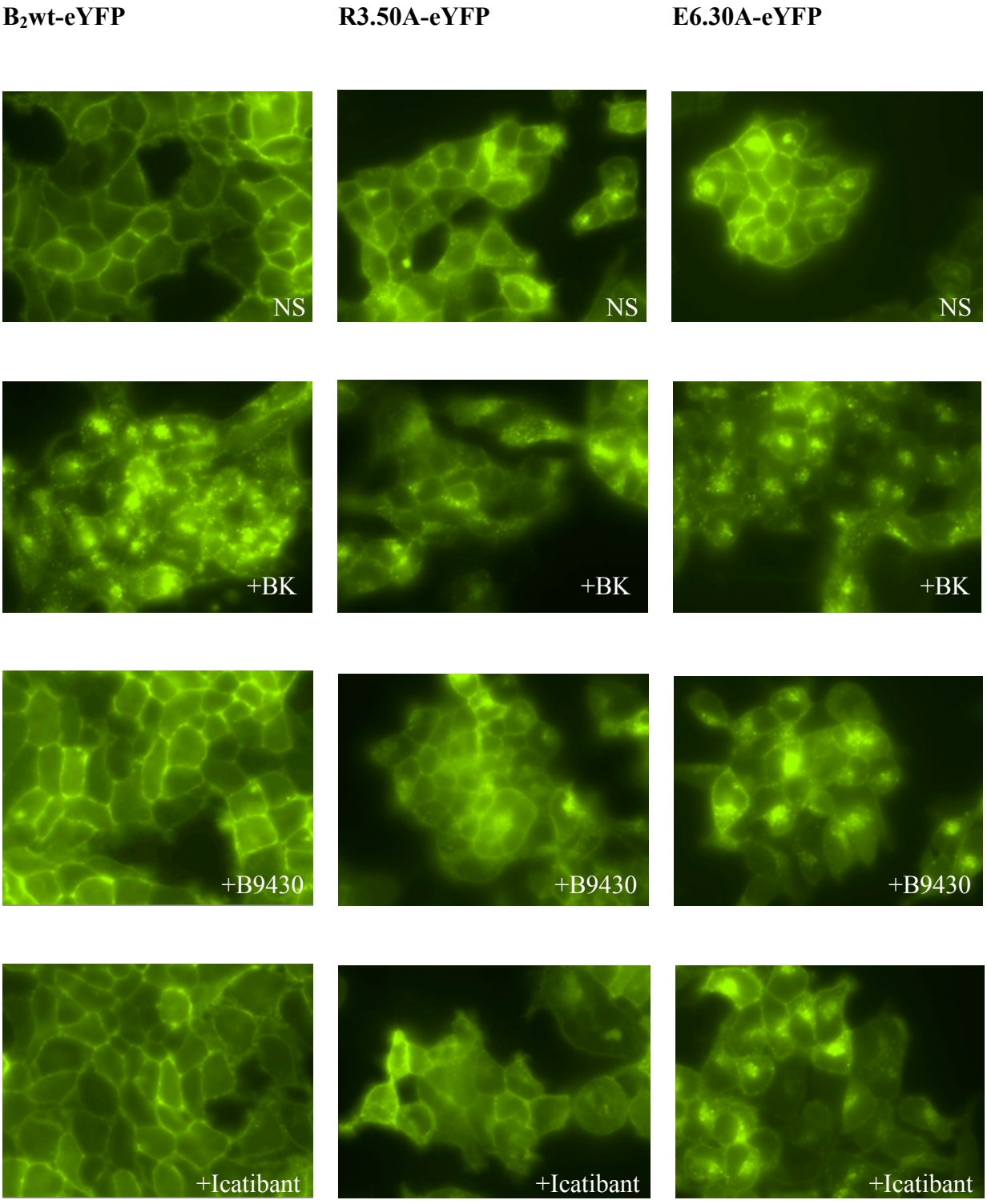

Fig. E-28: Localization of wild-type and mutant receptor-eYFP fusion proteins by epifluorescence microscopy (Wennerberg et al, *submitted*).

Live HEK 293 cells stably expressing constructs of eYFP fused to the C-terminus of B_2wt, R3.50A or E6.30A under the control of the weak P_{min} promoter were incubated in the absence or presence of 1 µM BK, B9430, or icatibant for 30 - 60 min at 37°C. Images were taken with a epifluorescent microscope focusing at a layer halfway through most of the cells.

E.3.7 Down-regulation

The effect of long-term incubation with BK, icatibant and B9430 was further investigated with a down-regulation assay (Fig. E-29). At the times indicated, all bound and free unlabeled BK was removed with an acetic acid solution and the remaining specific surface binding was determined with 2 nM [^{3}H]BK at 4°C. Once again, differences were observed concerning the same cell-line with different cell densities. In R3.50A$_{HIGH}$ both BK and B9430 induced a reduction in surface binding. The receptor number/binding capacity was reduced by 60 % after two hours with B9430 (Fig. E-29). With BK a 50% reduction was observed after two hours. Upon stimulation with icatibant much less receptor sequestration was seen, a maximum of 20 % after 8 hours. For R3.50A$_{LOW}$ the same order of binding reduction was observed after stimulation (B9430 > BK > Icatibant), but the sequestration of cell surface receptors was more rapid then with R3.50A$_{HIGH}$. Upon stimulation for half an hour with B9430 80 % of R3.50A$_{LOW}$ receptors were sequestered, while during the same time period 75 % sequestration was seen upon BK stimulation (Fig. E-30). After the immediate strong reduction of cell surface receptors a plateau was reached and no further increase in sequestration was detected. E6.30A displayed in some way a different pattern than R3.50A concerning reduction of cell surface receptors. In contrast to R3.50A$_{HIGH}$, icatibant induced receptor sequestration of E6.30A$_{HIGH}$ (Fig. E-29). After 8 hours of icatibant stimulation about 60 % sequestration was detected, which was the same level as for BK. B9430 induced approximately 90 % sequestration after 8 hours. Once again the same cell line with lower expression yielded more rapid receptor sequestration upon stimulation with all three compounds (Fig. E-30).

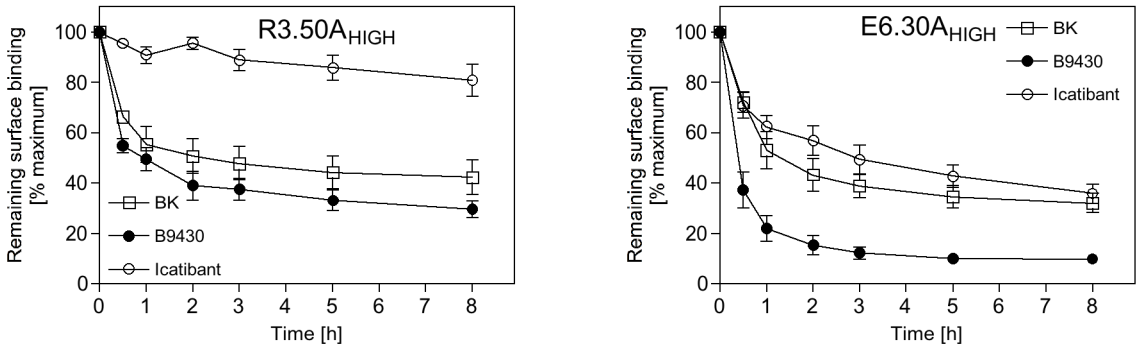

Fig. E-29: Effect of prolonged stimulation with BK, B9430 and icatibant on surface binding.

HEK 293 cells isogenically and stably expressing high amounts of R3.50A and E6.30A were incubated with 10 µM BK or 5 µM B9430 and icatibant in medium at 37°C as described in "Materials and methods". At the times indicated, all free and bound (pseudo)peptide was removed with an acetic acid/NaCl solution. Thereafter, the remaining specific surface binding was determined with 2 nM [^{3}H]BK at 4°C. Symbols represent the mean ± SEM for at least three experiments performed in duplicate.

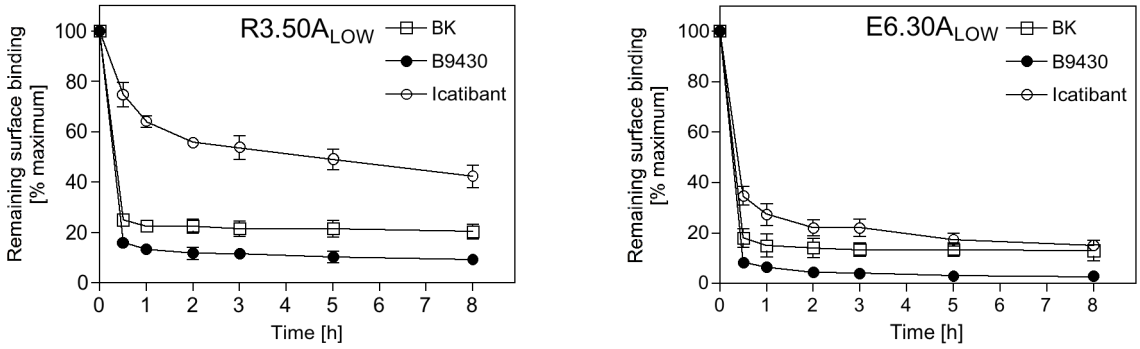

Fig. E-30: Effect of prolonged stimulation with BK, B9430 and icatibant on surface binding.

HEK 293 cells isogenically and stably expressing low amounts of R3.50A and E6.30A were incubated with 10 µM BK or 5 µM B9430 and icatibant in medium at 37°C as described in "Materials and methods". At the times indicated, all free and bound (pseudo)peptides were removed with an acetic acid/NaCl solution. Thereafter, the remaining specific surface binding was determined with 2 nM [^{3}H]BK at 4°C. Symbols represent the mean ± SEM for at least three experiments performed in duplicate.

E.3.8 R3.50A shows higher basal phosphorylation than wild type

In both HEK 293 cells and human fibroblasts, B_2wt displays distinct phosphorylation even in the absence of a stimulus (Blaukat et al., 2001); (Kalatskaya et al., 2004). Most GPCRs respond to activation of the receptor by an agonist with internalization/sequestration of the receptor to intracellular compartments. As was demonstrated (Fig. E-26) the non-signaling mutant R3.50A internalized [^{3}H]BK as rapidly as the B_2wt. This clearly demonstrates that the internalization process is largely independent of the activation of the G protein. Our phosphorylation experiments (performed by Dr. Irina Kalatskaya) revealed that R3.50A exhibits a higher basal phosphorylation compared to B_2wt (Fig. E-31). However, when challenged with BK, the phosphorylation level of R3.50A increased further.

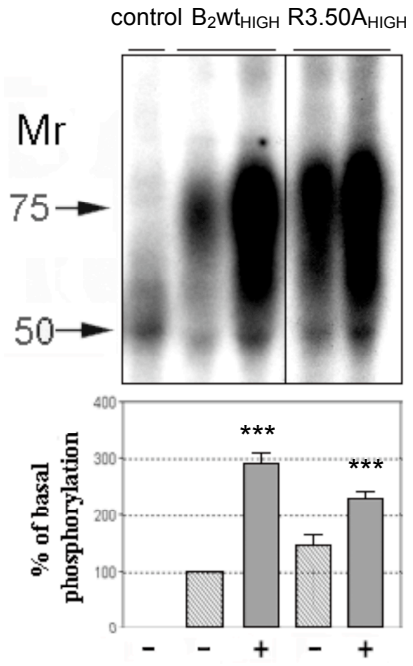

Fig. E-31: Agonist-induced phosphorylation of B_2wt and R3.50A (Wennerberg et al, *submitted*).

Upper panel, HEK 293 cells expressing B_2wt_{HIGH} or $R3.50A_{HIGH}$ were labeled for 10 h with [^{32}P]orthophosphate before stimulation with 1 μM BK for 5 min. Cells were lysed, and receptor proteins were solubilized, immunoprecipitated, and visualized by autoradiography as described in the „Materials and Methods“ section. Molecular size markers are indicated to the *left*. As a control, mock-transfected HEK 293 cells were used. *Lower panel*, protein phosphorylation, given as optical densities of the bands in the area between 50 and 85 kDa, are presented as means ± S.D. from three independent experiments; unstimulated B_2wt was set as 100%.

E.3.9 MAPK kinases ERK1/2

It was already demonstrated that BK stimulation of B_2wt induces activation of ERK1/2 phosphorylation (Fig. E-13). Here we compare the effects of the mutations R3.50A and E6.30A on the phosphorylation of ERK1/2. In contrast to the wild type receptor, mutants R3.50A and E6.30 responded to both the "antagonists" with significant ERK1/2 phosphorylation (Fig. E-32). These results confirm semi-active states for both receptor mutants and further demonstrate that ERK1/2 phosphorylation is independent of G protein activation as it was also observed for mutant R3.50A.

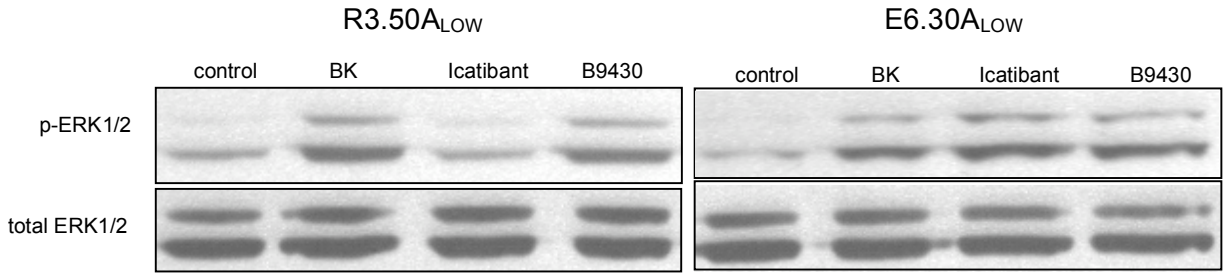

Fig. E-32: Immunoblots for phospho-ERK1/2 and total ERK1/2 (Wennerberg et al, *submitted*).

HEK293 cell lines R3.50A$_{LOW}$ and E6.30A$_{LOW}$ were maintained overnight in medium with reduced serum (0.5%). Stimulation was performed with 1 µM BK, B9430, or icatibant for 10 min at 37°C. Extraction and detection of total ERK1/2 (as loading control) and phospho-ERK1/2 was carried out as described in "Materials and Methods". One representative experiments out of at least three are shown.

E.3.10 Summary of results of R3.50A and E6.30A

Table 4: [^{3}H]Binding data and basal and BK-induced IP accumulation of all receptor constructs (Wennerberg et al, *submitted*).

	[^{3}H]BK Binding				Inositol-Phosphate Accumulation	
Receptor-construct	B_{max}[a] [fmol/mg prot.]	K_d (PAO/4°C) [nM]	K_d(PAO/37°C) [nM]	K_d-ratio 37°C/4°C	basal[b]	maximal effect[b]	EC_{50}[c] [nM]
B_2wt_{HIGH}	11.0±0.7	2.81±0.7(4)	10.42±1.56*	2.02±0.13(8)	12.55±1.00	0.79±0.34(4)
B_2wt_{LOW}	2.4±0.3	2.02±0.22(5)	8.05±1.10**	1.69±0.09(4)	12.11±1.22	0.67±0.22(3)
R3.50A$_{HIGH}$	3.87±0.64	2.09±0.17(6)	5.53±0.64***	1.30±0.26(3)	2.12±0.22	n.a
R3.50A$_{LOW}$	1.42±0.25	2.15±0.21(6)	5.15±0.30***	1.43±0.16(3)	1.55±0.10	n.a.
E6.30A$_{HIGH}$	3.44±0.61	1.10±0.19(5)	2.17±0.39 n.s.	2.09±0.02(3)	13.79±1.66	2.65±0.73(4)
E6.30A$_{LOW}$	1.28±0.18	1.19±0.25(6)	1.32±0.14 n.s.	1.60±0.09(4)	4.14±0.45	0.65±0.18(4)

[a] Estimated from at least three different clones in 24-wells after incubation with 200 µl of 30 nM [^{3}H]BK on ice.

[b] Total IP accumulation after 30 min of incubation in buffer with inhibitors and 50 mM LiCl at 37°C with (maximal effect) and without (basal) 1 µM BK, expressed as the fold increase of initial total IP production (t = 0 min). The results represent the mean ± SEM of the number of experiments (given in parentheses) performed in triplicate.

[c] Calculated from incubations in duplicate with 10^{-12}-10^{-5} M BK for 30 min at 37°C in the presence of 50 mM LiCl. Results are the mean ± SEM of independent experiments (number indicated in parentheses)

Comparison between K_d values at 37 and 4 °C: $^{*}P < 0.05$; $^{**}P < 0.01$; $^{***}P < 0.001$; n.s., not significant

n.a. not applicable

E.3.11 Influence of amino acid used for substitution of R3.50

It is known that both the acidic (Asp, position D3.49) and the basic (Arg R3.50) residues of the DRY motif are important for isomerization of receptors between the inactive and activated conformations (Flanagan, 2005). We therefore determined the accumulation of IPs when the two charged amino acids where swapped using the double mutant D3.49R3.50/R3.49D3.50 (named DR3.49/3.50RD). The double mutant DR3.49/3.50RD did not induce any IP accumulation (Fig. E-33). Furthermore, the basic arginine R3.50 was mutated to aspartic acid and to isoleucine, giving point mutants R3.50D, R3.50I, respectively. The introduction of isoleucine, as that with alanine, result in an aliphatic substitution. In contrast, with point mutation R3.50D, the basic charged amino acid was replaced with an acidic charged amino acid.

R3.50I gave approximately a 4-fold increase in IP accumulation upon BK stimulation (Fig. E-33). When the arginine was replaced with the acidic aspartic acid, no IP accumulation was observed.

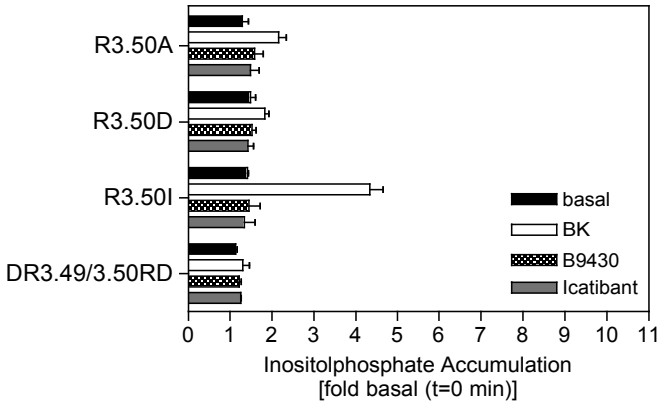

Fig. E-33: Basal and stimulated accumulation of total inositol phosphates.

HEK 293 cell lines expressing high levels of R3.50 mutants were incubated overnight in 12-well plates with 0.5 μCi [^{3}H]inositol in 0.5 ml medium. Stimulation was performed in the presence of 50 mM LiCl and 1 µM BK, B9430 and icatibant for 30 min at 37°C as described in „Materials and Methods“. Each value represents the mean ± SEM of at least three independent experiments done in triplicates, given as fold over the IP content of non-stimulated but otherwise identically treated control cells that had remained on ice.

F DISCUSSION

F.1 Functional selectivity of B9430 and icatibant concerning PLC activation receptor down-regulation, and ERK1/2 activation depends on human bradykinin B_2 receptor density and cell type

The two pseudopeptides icatibant and B9430 have a sequence that is related to that of the agonist bradykinin but they contain substitutions with artificial amino acids that renders them structurally constrained. Both are nominally used as antagonists. In the present study we demonstrate that both compounds could act as partial agonists. The agonistic/antagonistic behavior of these two compounds depends on the expression level of B_2R, the cell type and especially on the signal processes under consideration.

F.1.1 B9430 and icatibant act as poor partial agonists in HEK 293 cells expressing high amounts of recombinant B_2R

There was almost no difference in the maximal response to bradykinin between the low and the high expressing recombinant cell line concerning inositolphosphate- and calcium release. Although no difference in the maximal response to BK was detected, there was a difference in the turn off of the signal generated by the pseudopeptides icatibant and B9430. While in the lower expressing cell line the signal elicited by the pseudopeptides apparently could be kept in check by the cellular machinery, this did not function anymore with the high expressing cell line, suggesting that the inactivation machinery can be saturated. This indicated that in HEK 293 cells expressing recombinant B_2R both icatibant and B9430 are poor partial agonists, but only with very high B_2R numbers can they overcome the turn-off mechanisms and generate a signal. These results demonstrate that for the classification of a compound as an antagonist, agonist or inverse agonist the cellular context is important and – see below - also the signal transduction pathways that have been investigated.

F.1.2 B9430 induced an affinity shift in B_2wt_{LOW}

The effect of the pseudopeptides on receptor surface binding showed another scenario. Here, the lower the expression the stronger the effect of the compounds, in particular of B9430.

There was almost no reduction of binding activity after prolonged stimulation with the (pseudo)peptides in B_2wt_{HIGH}, which might indicate that the sequestration apparatus is overwhelmed by the high number of activated receptors. It has still to be determined whether this happens on the level of the phosphorylation by GRKs, the arrestins or the vesicle formation. The fact that with lower expression the "antagonists" begin to show effects regarding the receptor surface binding suggests that there are differences in the inactivation mechanisms between those concerning the release of IP_3 and calcium and those regarding receptor surface binding. The focus seems to be on protection of the cell against overstimulation, therefore the signaling is blocked efficiently in lower expressing cells, but reduction of receptor binding can be induced even by poor partial agonists.

Even though a reduction of surface binding of B_2wt_{LOW} was observed in the down-regulation assay upon incubation with B9430, no localization of intracellular receptors could be detected upon stimulation as shown using three other methods (immunoblot studies to examine for degradation of total levels of B_2R protein, receptor localization with epifluorescence microscopy and biotinylation protection assay). These results are in contrast to the sequestration induced by icatibant observed for a rabbit B_2R-GFP construct (Houle et al., 2000). This might be due to species differences although the similarity between rabbit und human B_2R is almost 80%.

One explanation for reduction of binding could be an affinity shift induced by B9430, that would not have been detected in the down regulation assay because only one concentration of [^{3}H]BK around the Kd of the B_2Rwt is used (2nM). We tested this hypothesis by generation of equilibrium binding curves with increasing concentrations of [^{3}H]BK followed by scatchard plot analysis. Indeed, long-term stimulation of B_2wt_{LOW} with B9430 resulted in a major affinity shift as compared to non-treated cells. There could be several reasons for this affinity shift upon long-term treatment with B9430. One is a slow dissociation of unlabeled ligand from the receptor or its insufficient removal after the pretreatment. This would result in competition with [^{3}H]BK and therefore in reduced binding, thus simulating an affinity shift of the B_2R. This possibility can, however, be excluded because the same effect should have then been observed also for the B_2wt_{HIGH}, which was not the case. It is, therefore, more likely that the pretreatment with B9430 affects the receptor conformation either directly, or indirectly via changing its interaction with intracellular proteins.

F.2 Alanine-screening of the intracellular loops of the B_2 receptor

The purpose of this part of the thesis was to identify which sequences of the B_2 receptor that play a major role in signal transduction and in receptor sequestration, i.e. are involved in the interaction with the G protein, the receptor kinases and the arrestins. Moreover, to obtain knowledge about which sites are involved in binding and which are involved in signaling. In order to avoid any bias by focusing only on highly conserved residues, we systematically mutated all three intracellular loops (ICLs). To reduce the number of constructs we started with the generation of 12 cluster mutations (3 - 5 amino acids) and two point mutants. In total, only one mutant (construct 2/1) out of the 14 constructs displayed no binding activity at all, several others exhibited low expression though signaling could be measured, and only one mutant (construct 3/5) displayed no signaling at all, despite detectable ligand binding.

All mutations in ICL-1 resulted in a strong reduction in expression levels without affecting either receptor signaling or sequestration. These results were in agreement with reports on the rat B_2R (Yu et al., 2005) as well as rhodopsin (Yeagle et al., 1997) indicating that ICL-1 forms a tight bend, the disturbance of which strongly affects the receptor expression level. Thus, ICL-1 is important for the maintenance of the overall receptor structure and stability, but is apparently of no functional importance otherwise.

Our results indicated that both the intracellular loops ICL-2 and ICL-3 are strongly involved in the interaction with $G_{q/11}$, but in different ways. Mutations in the ICL-2 resulted in a strong reduction in signaling potency (more than 10-fold) but not in a significantly reduced maximal response, suggesting that the sequences mutated play more a role in the coupling to $G_{q/11}$ but not in its activation. The notion of impaired coupling of the ICL-2 mutants is also supported by the fact that despite the high expression levels of mutants 2/3 – 2/5 they could not be activated by B9430 or icatibant as observed for the highly expressing B_2wt. In addition, they also displayed the lowest basal activities of all constructs, hinting at an inverse agonistic effect of these mutations with regard to the activation of $G_{q/11}$.

In contrast, the cluster mutation 3/4 and a point mutation (T242) in ICL-3 resulted in semi-active conformations, as they became clearly activated by the otherwise very poor partial agonists. Our observation that semi-active conformations do not necessarily result in increased basal activity has also been reported for bovine rhodopsin, where the mutation of tyrosine in the

highly conserved NPXXY-sequence to alanine did not result in increased basal activity, but turned a poor agonist into a potent one (Fritze et al., 2003).

Concerning the affinities of the mutants at 37°C and at 4°C only three constructs (1/1, 2/3, and 3/3) showed binding characteristics comparable to those observed for B_2Rwt. All other mutants differed significantly at either 4°C or 37 °C, demonstrating that mutations in ICLs also affect the conformation of the extracellular binding site. Whether these different K_d values are inherent properties of the mutants due to a change of the overall receptor conformation, or reflect modified interactions with cytosolic proteins stabilizing certain receptor conformations, will require further study.

Although a role of ICLs in receptor internalization has been reported for other family A GPCRs (Marion et al., 2006); (DeGraff et al., 2002) no significant differences were observed between the B_2Rwts and the loop mutants regarding their internalization of [^{3}H]BK. These results are consistent with our previous observation that the intracellular C-terminus is crucial for ligand-induced receptor internalization (Faussner et al., 1998). We cannot exclude, however, that the effects of the mutations on interactions with either receptor kinases or arrestins were not strong enough to be detected under the conditions applied. It is also possible that the region pivotal for these interactions is the DRY sequence, which due to lack of surface binding of the triple mutant, could not be examined in this regard. Results with the CXCR5 receptor do, indeed, suggest binding of arrestins to the region of the DRY sequence (Huttenrauch et al., 2002).

The sequence mutated in construct 3/5 (TERR) seems to be of high importance for expression as well as signaling. This mutant was poorly expressed and signaled poorly. This poor signaling was not necessarily due to the low expression, as demonstrated by mutants 1/2 and E66A, that exhibited similar low expression levels as 3/5 but did still signal well. Mutant 2/1 (DRY-sequence) displayed no surface binding activity at all. This is most probably due to lack of glycosylation or phosphorylation or a combination of both. Both cluster mutants that exhibited the most extreme features, constructs 2/1 and 3/5, are the ones that contain the two highly conserved amino acids to be assumed to form the “ionic lock”, R3.50 and E6.30. Therefore, two point mutants were generated by substituting each amino acid by an alanine.

F.3 R3.50 in the DRY motif and E6.30 in the TERR motif as key players for the activation and trafficking of the human bradykinin B_2 receptor

An aim of this study was to determine the structural and functional role of the conserved basic residue R3.50 at the cytosolic end of TM3 and of the acidic residue E6.30 at the end of TM6 for the B_2R. In addition, the hypothesis that they may form an ionic lock maintaining the inactive state of the receptor was tested. The latter would distinguish the B_2R from other peptide GPCRs as most of them carry a positively charged residue in position 6.30. To this purpose, both charged residues were mutated to alanine and the constructs, R3.50A and E3.50A, were stably expressed in HEK 293 cells.

F.3.1 Mutation of the arginine in the conserved DRY motif resulted in complete loss of G protein activation

The location of the DRY motif at the cytosolic surface of GPCRs led to the suggestion that it might interact directly with the G protein (Wess, 1998). As we have seen, the triple mutation of the DRY motif to alanine resulted in a construct that was binding deficient (see construct 2/1). Substitution of R3.50 alone with an alanine completely abolished the ability to induce IP accumulation or the release of arachidonic acid upon agonist stimulation, thus pointing to the crucial importance of this residue for a productive interaction with G proteins. The crystal structure of bovine rhodopsin in its G protein interacting form demonstrates that the conserved arginine directly interacts with a backbone carbonyl group of the C-terminal G protein alpha helix (Scheerer et al., 2008). Our results strongly suggest a similar role for R3.50 in the B_2R. In many GPCRs, exchange of R3.50 leads to a strong reduction in their ability to activate their cognate G proteins. The extent of this impairment, however, depends on the receptor under investigation and the amino acid used for replacement, the effect changes from total abolishment of G protein signaling as observed for the B_2R to only minor reductions. (Acharya and Karnik, 1996); (Scheer et al., 1996); (Ballesteros et al., 1998); (Wess, 1998) (Rovati et al., 2007). In part the effect may depend on the assay: for the angiotensin receptor AT_{1a}, mutation of R3.50 to alanine resulted in complete loss of G protein activation when measured as release of inositoltrisphosphate (IP_3) after 10 seconds (Ohyama et al., 2002), but did not significantly affect the signaling compared to wild-type AT_{1a} when accumulation of IP_2 and IP_3 was determined over a stimulation period of 20 min (Gaborik et al., 2003). It is therefore, difficult to compare the effects of R3.50 mutations among

different GPCRs, but the array of published data indicates that the structural/functional role of R3.50 in family A GPCRs depends strongly on its particular microenvironment in the GPCR under investigation.

R3.50A showed an increased binding affinity at 37°C compared to the B_2 wild type receptor. The observed enhanced binding affinity for agonist ligands concerning some R3.50 mutant receptors has also been reported earlier (Scheer et al., 1996); (Scheer et al., 2000); (Alewijnse et al., 2000). According to the extended ternary complex model of GPCR activation (Samama et al., 1993), mutant receptors with enhanced agonist affinity are stabilized in an activated conformation and able to bind G proteins, even though G protein signaling is disrupted.

Desensitization of many family A GPCRs is initiated by phosphorylation of serine/threonine residues located in the C-terminus via the action of GPCR kinases (GRK), mostly GRK2 and 3, resulting in recruitment of arrestins to the receptor and subsequent internalization. A proposed model for this mechanism is that GRK2 and GRK3 bind to the membrane close to the active receptor by attaching with their pleckstrin homology domains to βγ-subunits that are available only after activation of the G-protein and dissociation of the α-subunit (Willets et al., 2003). However, mutant R3.50A displaying increased basal phosphorylation (Fig. E-31) responds to BK challenge with additional phosphorylation and strong internalization, although it is G-protein-activation incompetent (Fig. E-25). A different mechanism or other GRKs or kinases may therefore be involved in its phosphorylation and internalization.

F.3.2 Mutation of E6.30 to alanine resulted in a similar phenotype as R3.50A but with quantitatively stronger effects

The present study suggests that residues R3.50 and E6.30 form an ionic lock in the B_2R as mutation of these two residues resulted in a similar receptor phenotype with regard to permanently increased receptor affinity (Fig. E-24, Tab. 4) and strong ERK1/2 phosphorylation (Fig. E-32) in response to poor partial agonists. This idea was strongly substantiated further by the fact that both mutants displayed the same constitutively activated phenotype with regard to receptor internalization, as demonstrated by, (i) the results of the biotinylation protection assay (Fig. E-27), (ii) their internalization of [^{3}H]BK and uptake of antagonist [^{3}H]NPC17331 (Fig. E-26), as well as (iii) their substantial intracellular localization in the absence of an agonist (Fig. E-28).

In addition, these data clearly demonstrate that ERK1/2 phosphorylation and ligand-induced receptor internalization can also function independently of G-protein-coupling, as both processes were observed not only for mutant E6.30A but also for G-protein activation incompetent mutant R3.50A (Fig. E-32 and Fig. E-26). Together with the fact that mutant R3.50A internalized after agonist-binding, i.e. most likely interacts with β-arrestins, this suggests that phosphorylation of ERK1/2 is β-arrestin mediated, as shown for the angiotensin II receptor AT_{1A} (Ahn et al., 2004)
Mutation of E6.30 in B_2R resulted qualitatively in a similar phenotype as mutation of R3.50 to alanine but quantitatively always imposed the stronger effects (Table 5).

Table 5. Summary of results:

	B_2Rwt	R3.50A	E6.30A
surface receptor binding	+++	+	+
high affinity at 37°C	-	++	+++
[^{3}H]BK internalization	+++	+++	+++
[^{3}H]NPC17331 uptake	-	+	++
$G_{q/11}$ activation (BK)	+++	-	+++
$G_{q/11}$ activation (B9430/icatibant)	-	-	+++
intracellular localization	-	+	++
constitutive internalization (biotinylation protection assay)	-	+	++

(-) no effect, (+) weak, (++) moderate, (+++) strong effect

This could be explained by assuming that residue E6.30 has an additional interaction partner that can partially compensate the loss of the interaction with R3.50. Arginine R3.50 is also most likely involved in interaction with other than glutamate E6.30 in helix 6. The crystal structure of dark state bovine rhodopsin (PDB 1U19) indicates that R3.50 also makes contact with threonine T6.26(251), one turn above E6.30 in helix 6 (Scheerer et al., 2008). This residue is conserved in B_2R and we have published that substitution of T6.26 by an alanine results in a semi-active mutant, as demonstrated by its higher affinity at 37°C and its antagonist-inducible IP accumulation (Faussner et al., 2009).
Depending on how mutations in the E/DRY sequence affected receptor properties, Rovati et al. proposed a classification for family A GPCRs (Rovati et al., 2007). The B_2R, however, does not fit well in either of the suggested groups: mutation R3.50A resulted in complete loss of G protein

activation, which would place it preferably in the second group, whereas the fact that R3.50A displays increased affinity for BK and responds to (ant)agonist stimulation with receptor internalization and ERK1/2 phosphorylation would rather qualify it for the first group. Further characterization of family A GPCRs not only according to the effects of mutations in the DRY sequence with regard to their G protein activation behavior but also considering effects on other signaling pathways might facilitate the classification.

In summary, the results of our study demonstrate that R3.50 at the cytosolic end of TM3 in the human B_2R plays a dual role: it is (i) pivotal for the productive interaction with G-proteins and (ii) is part of a network connecting TM3 and TM6 through a salt bridge with E6.30 and a hydrogen bond with $T242^{6.26}$ maintaining the receptor in its inactive state. Disruption of these interactions results in a semi-active, easier activatable receptor state with regard to G-protein activation and the MAPkinase pathway, and in a constitutively active state with regard to the internalization machinery. Residue E6.30 might have an additional interaction partner as its mutation resulted in higher constitutive activity than mutation of R3.50. As an acidic residue in position 6.30 is only poorly conserved among the peptide receptors of family A GPCRs and often is replaced by a positively charged arginine or lysine, different mechanisms for maintaining their inactive state in the absence of an agonist must exist.

F.3.3 Three-dimensional model of the bradykinin B_2 receptor

A three-dimensional model of the bradykinin B_2 receptor based on the crystal structure of inactive bovine rhodopsin as seen from the cytosol was generated by homology modeling (Fig. F-2). It indicates that sequences where mutations result in semi-active/constitutively active conformations are all part of a network and are clearly separated from those related to potency reduction. The latter ones, sequences mutated in constructs 2/4 and 2/5, apparently contribute to the binding but not to the activation of G protein $G_{q/11}$ by the receptor. Thus, this model provides a link between our screening study of the intracellular loops and the more detailed study of R3.50 (R128) and E6.30 (E238). Finally, this model suggests K142 as an additional interaction partner for E6.30 (E238), that might help to compensate to some degree a loss of R3.50, which would explain the fact that mutant R3.50A displayed weaker semi- and constitutive activity than mutant E6.30A.

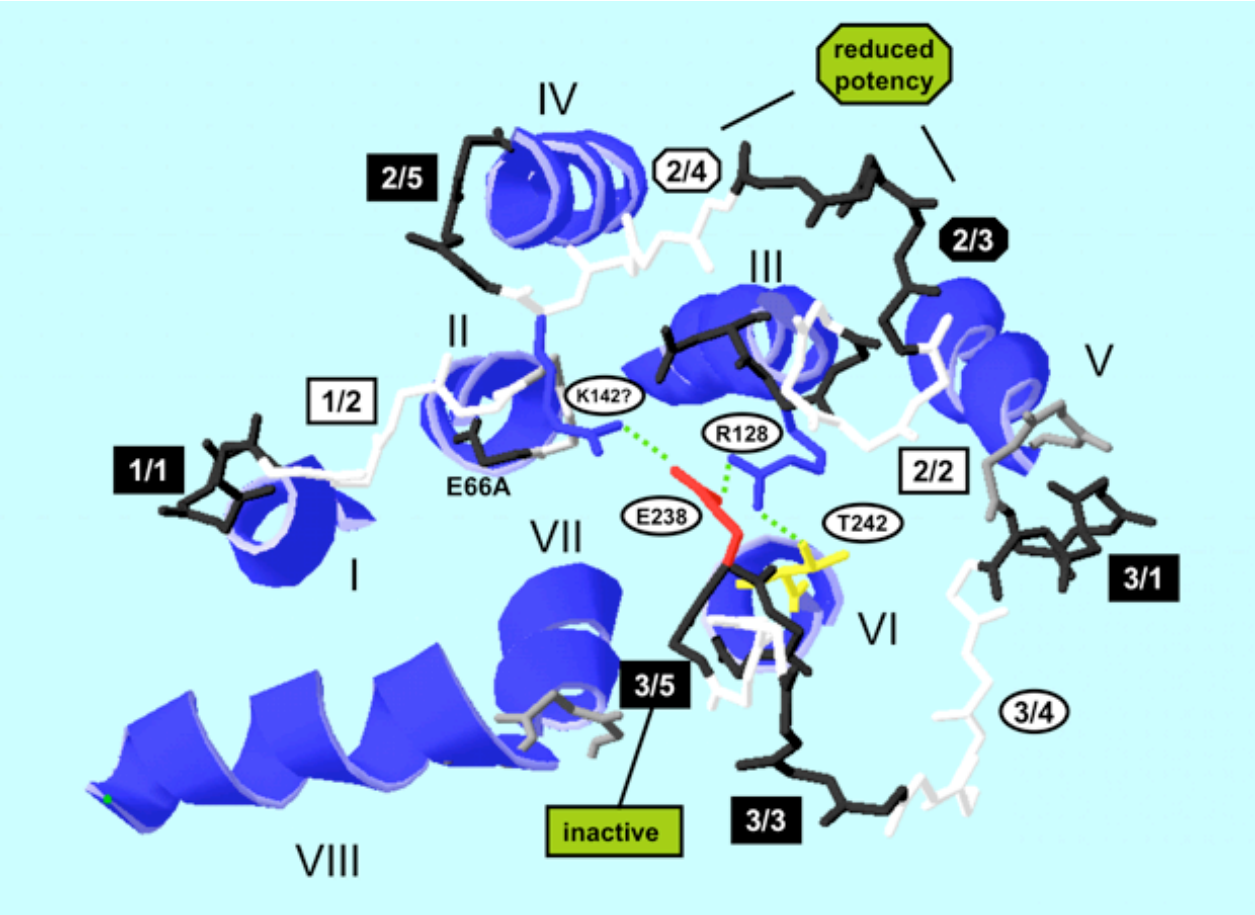

Fig. F-1: Position of mutations and their effects in a three-dimensional model of the bradykinin B_2 receptor based on the crystal structure of inactive bovine rhodopsin as seen from the cytosol.

Position of mutants and annotation of their effects in a computational model of B_2R as seen from the cytosol. The structure was generated with SWISS-model (Arnold et al.) based on the crystal structure of bovine rhodopsin in its inactive form (PDB 1U19A [Okada et al.]). Dark blue, cytosolic ends of the seven transmembrane helices I – VII and cytosolic helix VIII; point and cluster mutants are depicted in black and white as in Fig. E-15 (only alpha-carbon chain shown, no side chains, with the exception of R3.50 [R128] in blue, E6.30 [E238] in red, and T6.26[T242] in yellow, and K142 in blue; grey, amino acids not mutated outside of the helices; green squares, effect of indicated mutations on receptor properties. Mutant names depicted in black oval indicate semi-/constitutively active conformations.

G SUMMARY

The aim of the presented thesis was to study the regulation of the human bradykinin B_2 receptor (B_2R) with regard to signal transduction pathways, receptor desensitization, and receptor internalization.

In the first part the influence of human bradykinin B_2 receptor densities and cell types on receptor internalization and signal transduction was investigated. The properties of the B_2R stably expressed at two considerably different expression levels by using two different promoters in HEK 293 cells, and the endogenously expressed B_2R in human fibroblasts were analyzed. It was demonstrated that two B_2R antagonists, icatibant and B9430 that differ from BK through the insertion of unnatural amino acids, under certain conditions become partial agonists. This partial agonism was only obtained in HEK 293 cells expressing high amounts of recombinant B_2R. In contrast, in lower (HEK 293) or endogenously (foreskin fibroblasts) expressing cells, no partial agonism of these two compounds was observed. However, in low expressing HEK293 cells as well as in the fibroblasts long-term challenge with B9430, but not icatibant, strongly reduced receptor surface binding, comparable to the effect seen for the endogenous agonist BK. Further studies revealed that in contrast to BK, which reduced surface binding through induction of receptor internalization, B9430 reduced binding apparently via a change in the affinity of the B2R on the cell surface without promoting its internalization.

In the second part of this thesis the role of the intracellular loops of the human bradykinin B_2 receptor was explored in detail. G proteins, receptor kinases and adaptor proteins of the internalization machinery most likely interact with the cytosolic parts of the receptor. In order to more closely define the receptor sequences that are involved in these interactions, we systematically mutated all three intracellular loops either as point mutants or in groups of 3-5 amino acids to alanines (obtaining 14 mutants). All constructs were stably and isogenically expressed in HEK 293 cells. Our results show that changes in the intracellular loop 1 (ICL-1) strongly affect receptor surface expression but not receptor signaling or receptor internalization. Even more important for receptor maintenance are the DRY-sequence at the N-terminus of intracellular loop 2 (ICL-2) and the TERR-sequence at the C-terminus of intracellular loop 3 (ICL-3), as cluster mutations here completely abolish or strongly reduce surface receptor

expression, respectively. Both ICL-2 and ICL-3 are involved in the interaction with G protein $G_{q/11}$ but in different ways. Sequences in ICL-2 contribute apparently more to the coupling, regions in ICL-3 preferentially to the activation of $G_{q/11}$.

As a consequence of the results of the second part, a closer look was taken at the role of single amino acids in the DRY- and the TERR sequence. For bovine rhodopsin it has been shown that the arginine in the DRY motif (R3.50 according to the Ballesteros/Weinstein numbering) (Ballesteros et al., 1998) and a glutamate at the cytosolic end of transmembrane domain 6 (Ballesteros/Weinstein position 6.30) corresponding to the glutamate in the TERR sequence of the B_2R, form an intramolecular interaction keeping rhodopsins in its inactive state. This interaction in bovine rhodopsin is also known as the "ionic lock" and is assumed to be disrupted as part of receptor activation. The B_2R is one of the very few peptide GPCRs where both R3.50 and a glutamic acid in position 6.30 can be found. Therefore, in the third part of the thesis the structural and functional role of the conserved basic residue R3.50 and the acidic residue E6.30 in the human B_2R were investigated. In addition, the hypothesis was tested that they may form an "ionic lock" participating in maintaining the inactive state of the B_2R. This goal was pursued by generation of two receptor point mutants, termed R3.50A and E6.30A, and their extensive biochemical and functional characterization.

The results of this study demonstrate that R3.50 plays a dual role: it is (i) pivotal for the productive interaction with G-proteins and (ii) is most likely part of a network where it connects TM3 and TM6 through a salt bridge with E6.30 and a hydrogen bond with T6.26 maintaining the receptor in its inactive state. The second point is indicated by the fact, that - with exception the of G-protein activation - both mutants R3.50A and E6.30 displayed an almost identical pattern of constitutive and semi-active activity, as expected when both residues interact with each other.

Residue E6.30 might have an additional interaction partner as its mutation resulted in stronger active conformations than mutation of R3.50. As an acidic residue in position 6.30 is not well conserved among the peptide receptor of family A GPCRs and often is replaced by a positively charged arginine or lysine, different regulation mechanisms must exist in this GPCR subfamily.

GPCRs are an ideal therapeutic target as they are on the one hand well accessible on the cell surface on the other hand act very specifically by binding their endogenous ligands with high selectivity and display cell specific expression patterns. Deeper insight into structure, differences

and similarities of their regulation should allow a more rational, structure-based development of drugs and thus make better use of their full therapeutic potential.

H REFERENCES

AbdAlla, S., Godovac-Zimmermann, J., Braun, A., Roscher, A.A., Muller-Esterl, W., and Quitterer, U. (1996). Structure of the bradykinin B2 receptors' amino terminus. Biochemistry *35*, 7514-7519.

Acharya, S., and Karnik, S.S. (1996). Modulation of GDP release from transducin by the conserved Glu134-Arg135 sequence in rhodopsin. J Biol Chem *271*, 25406-25411.

Ahn, S., Wei, H., Garrison, T.R., and Lefkowitz, R.J. (2004). Reciprocal regulation of angiotensin receptor-activated extracellular signal-regulated kinases by beta-arrestins 1 and 2. J Biol Chem *279*, 7807-7811.

Alewijnse, A.E., Timmerman, H., Jacobs, E.H., Smit, M.J., Roovers, E., Cotecchia, S., and Leurs, R. (2000). The effect of mutations in the DRY motif on the constitutive activity and structural instability of the histamine H(2) receptor. Mol Pharmacol *57*, 890-898.

Andrade S.O. & Rocha e Silva M. (1949) Purification of bradykinin ion-exchange chromatography. Biochem J. 64, 701-705

Angelova, K., Fanelli, F., and Puett, D. (2002). A model for constitutive lutropin receptor activation based on molecular simulation and engineered mutations in transmembrane helices 6 and 7. J Biol Chem *277*, 32202-32213.

Austin, C.E., Faussner, A., Robinson, H.E., Chakravarty, S., Kyle, D.J., Bathon, J.M., and Proud, D. (1997). Stable expression of the human kinin B1 receptor in Chinese hamster ovary cells. Characterization of ligand binding and effector pathways. J Biol Chem *272*, 11420-11425.

Ballesteros, J., Kitanovic, S., Guarnieri, F., Davies, P., Fromme, B.J., Konvicka, K., Chi, L., Millar, R.P., Davidson, J.S., Weinstein, H.*, et al.* (1998). Functional microdomains in G-protein-coupled receptors. The conserved arginine-cage motif in the gonadotropin-releasing hormone receptor. J Biol Chem *273*, 10445-10453.

Ballesteros, J.A., Jensen, A.D., Liapakis, G., Rasmussen, S.G., Shi, L., Gether, U., and Javitch, J.A. (2001). Activation of the beta 2-adrenergic receptor involves disruption of an ionic lock between the cytoplasmic ends of transmembrane segments 3 and 6. J Biol Chem *276*, 29171-29177.

Birnboim, H.C., and Doly, J. (1979). A rapid alkaline extraction procedure for screening recombinant plasmid DNA. Nucleic Acids Res *7*, 1513-1523.

Blaukat, A., Alla, S.A., Lohse, M.J., and Muller-Esterl, W. (1996). Ligand-induced phosphorylation/dephosphorylation of the endogenous bradykinin B2 receptor from human fibroblasts. J Biol Chem *271*, 32366-32374.

Blaukat, A., Barac, A., Cross, M.J., Offermanns, S., and Dikic, I. (2000). G protein-coupled receptor-mediated mitogen-activated protein kinase activation through cooperation of Galpha(q) and Galpha(i) signals. Mol Cell Biol *20*, 6837-6848.

Blaukat, A., and Muller-Esterl, W. (1997). Inhibition of B2 receptor internalization delays its dephosphorylation. Immunopharmacology *36*, 115-119.

Blaukat, A., Pizard, A., Breit, A., Wernstedt, C., Alhenc-Gelas, F., Muller-Esterl, W., and Dikic, I. (2001). Determination of bradykinin B2 receptor in vivo phosphorylation sites and their role in receptor function. J Biol Chem *276*, 40431-40440.

Boissonnas, R.A., Guttmann, S., Jaquenoud, P.A., Konzett, H., and Stuermer, E. (1960). Synthesis and biological activity of peptides related to bradykinin. Experientia *16*, 326.

Bokoch, G.M., Katada, T., Northup, J.K., Ui, M., and Gilman, A.G. (1984). Purification and properties of the inhibitory guanine nucleotide-binding regulatory component of adenylate cyclase. J Biol Chem *259*, 3560-3567.

Burch, R.M., and Axelrod, J. (1987). Dissociation of bradykinin-induced prostaglandin formation from phosphatidylinositol turnover in Swiss 3T3 fibroblasts: evidence for G protein regulation of phospholipase A2. Proc Natl Acad Sci U S A *84*, 6374-6378.

Campbell, D.J., Kladis, A., Briscoe, T.A., and Zhuo, J. (1999). Type 2 bradykinin-receptor antagonism does not modify kinin or angiotensin peptide levels. Hypertension *33*, 1233-1236.

Campbell, D.J., Kladis, A., and Duncan, A.M. (1993). Bradykinin peptides in kidney, blood, and other tissues of the rat. Hypertension *21*, 155-165.

Cayla, C., Merino, V.F., Cabrini, D.A., Silva, J.A., Jr., Pesquero, J.B., and Bader, M. (2002). Structure of the mammalian kinin receptor gene locus. Int Immunopharmacol *2*, 1721-1727.

Chan, D., Gera, L., Helfrich, B., Helm, K., Stewart, J., Whalley, E., and Bunn, P. (1996). Novel bradykinin antagonist dimers for the treatment of human lung cancers. Immunopharmacology *33*, 201-204.

Chan, D.C., Gera, L., Stewart, J.M., Helfrich, B., Zhao, T.L., Feng, W.Y., Chan, K.K., Covey, J.M., and Bunn, P.A., Jr. (2002). Bradykinin antagonist dimer, CU201, inhibits the growth of human lung cancer cell lines in vitro and in vivo and produces synergistic growth inhibition in combination with other antitumor agents. Clin Cancer Res *8*, 1280-1287.

Cherezov, V., Rosenbaum, D.M., Hanson, M.A., Rasmussen, S.G., Thian, F.S., Kobilka, T.S., Choi, H.J., Kuhn, P., Weis, W.I., Kobilka, B.K.*, et al.* (2007). High-resolution crystal structure of an engineered human beta2-adrenergic G protein-coupled receptor. Science *318*, 1258-1265.

Cohen, G.B., Yang, T., Robinson, P.R., and Oprian, D.D. (1993). Constitutive activation of opsin: influence of charge at position 134 and size at position 296. Biochemistry *32*, 6111-6115.

Cotecchia, S., Bjorklof, K., Rossier, O., Stanasila, L., Greasley, P., and Fanelli, F. (2002). The alpha1b-adrenergic receptor subtype: molecular properties and physiological implications. J Recept Signal Transduct Res *22*, 1-16.

DeGraff, J.L., Gurevich, V.V., and Benovic, J.L. (2002). The third intracellular loop of alpha 2-adrenergic receptors determines subtype specificity of arrestin interaction. J Biol Chem *277*, 43247-43252.

DeWire, S.M., Ahn, S., Lefkowitz, R.J., and Shenoy, S.K. (2007). Beta-arrestins and cell signaling. Annu Rev Physiol *69*, 483-510.

Duncan, A.M., Kladis, A., Jennings, G.L., Dart, A.M., Esler, M., and Campbell, D.J. (2000). Kinins in humans. Am J Physiol Regul Integr Comp Physiol *278*, R897-904.

Dziadulewicz, E.K., Ritchie, T.J., Hallett, A., Snell, C.R., Ko, S.Y., Wrigglesworth, R., Hughes, G.A., Dunstan, A.R., Bloomfield, G.C., Drake, G.S.*, et al.* (2000). 1-(2-Nitrophenyl)thiosemicarbazides: a novel class of potent, orally active non-peptide antagonist for the bradykinin B(2) receptor. J Med Chem *43*, 769-771.

Enquist, J., Skroder, C., Whistler, J.L., and Leeb-Lundberg, L.M. (2007). Kinins promote B2 receptor endocytosis and delay constitutive B1 receptor endocytosis. Mol Pharmacol *71*, 494-507.

Faussner, A., Bathon, J.M., and Proud, D. (1999). Comparison of the responses of B1 and B2 kinin receptors to agonist stimulation. Immunopharmacology *45*, 13-20.

Faussner, A., Proud, D., Towns, M., and Bathon, J.M. (1998). Influence of the cytosolic carboxyl termini of human B1 and B2 kinin receptors on receptor sequestration, ligand internalization, and signal transduction. J Biol Chem *273*, 2617-2623.

Faussner, A., Wennerberg, G., Schussler, S., Feierler, J., Seidl, C., Jochum, M., and Proud, D. (2009). Alanine screening of the intracellular loops of the human bradykinin B(2) receptor - effects on receptor maintenance, G protein activation and internalization. Febs J. *276*: 3491-3503

Fierens, F.L., Vanderheyden, P.M., De Backer, J.P., and Vauquelin, G. (1999). Insurmountable angiotensin AT1 receptor antagonists: the role of tight antagonist binding. Eur J Pharmacol *372*, 199-206.

Flanagan, C.A. (2005). A GPCR that is not "DRY". Mol Pharmacol *68*, 1-3.

Frey E.K. (1926) Zusammenhange zwischen Herzarbeit und Nierentätigkeit. Arch. Klin. Chir. 142, 663-669.

Frey E.K. & Kraut H. (1926) Über einen von der Niere ausgeschiedenen, die Herztaetigkeit anregenden Stoff. Hoppe-Seyler´s Z. Physiol. Chemie 157, 32-61

Fritze, O., Filipek, S., Kuksa, V., Palczewski, K., Hofmann, K.P., and Ernst, O.P. (2003). Role of the conserved NPxxY(x)5,6F motif in the rhodopsin ground state and during activation. Proc Natl Acad Sci U S A *100*, 2290-2295.

Gaborik, Z., Jagadeesh, G., Zhang, M., Spat, A., Catt, K.J., and Hunyady, L. (2003). The role of a conserved region of the second intracellular loop in AT1 angiotensin receptor activation and signaling. Endocrinology *144*, 2220-2228.

Gera, L., and Stewart, J.M. (1996). A new class of bradykinin antagonists containing indanylglycine. Immunopharmacology *33*, 174-177.

Gradman, A.H. (2002). AT(1)-receptor blockers: differences that matter. J Hum Hypertens *16 Suppl 3*, S9-S16.

Greasley, P.J., Fanelli, F., Rossier, O., Abuin, L., and Cotecchia, S. (2002). Mutagenesis and modelling of the alpha(1b)-adrenergic receptor highlight the role of the helix 3/helix 6 interface in receptor activation. Mol Pharmacol *61*, 1025-1032.

Greasley, P.J., Fanelli, F., Scheer, A., Abuin, L., Nenniger-Tosato, M., DeBenedetti, P.G., and Cotecchia, S. (2001). Mutational and computational analysis of the alpha(1b)-adrenergic receptor. Involvement of basic and hydrophobic residues in receptor activation and G protein coupling. J Biol Chem *276*, 46485-46494.

Griesbacher, T., and Legat, F.J. (1997). Effects of FR173657, a non-peptide B2 antagonist, on kinin-induced hypotension, visceral and peripheral oedema formation and bronchoconstriction. Br J Pharmacol *120*, 933-939.

Hess, J.F., Borkowski, J.A., Young, G.S., Strader, C.D., and Ransom, R.W. (1992). Cloning and pharmacological characterization of a human bradykinin (BK-2) receptor. Biochem Biophys Res Commun *184*, 260-268.

Hibino, T., Takemura, T., and Sato, K. (1994). Human eccrine sweat contains tissue kallikrein and kininase II. J Invest Dermatol *102*, 214-220.

Hopkins, A.L., and Groom, C.R. (2002). The druggable genome. Nat Rev Drug Discov *1*, 727-730.

Houle, S., Larrivee, J.F., Bachvarova, M., Bouthillier, J., Bachvarov, D.R., and Marceau, F. (2000). Antagonist-induced intracellular sequestration of rabbit bradykinin B(2) receptor. Hypertension *35*, 1319-1325.

Huttenrauch, F., Nitzki, A., Lin, F.T., Honing, S., and Oppermann, M. (2002). Beta-arrestin binding to CC chemokine receptor 5 requires multiple C-terminal receptor phosphorylation sites and involves a conserved Asp-Arg-Tyr sequence motif. J Biol Chem *277*, 30769-30777.

Kalatskaya, I., Schussler, S., Blaukat, A., Muller-Esterl, W., Jochum, M., Proud, D., and Faussner, A. (2004). Mutation of tyrosine in the conserved NPXXY sequence leads to constitutive phosphorylation and internalization, but not signaling, of the human B2 bradykinin receptor. J Biol Chem *279*, 31268-31276.

Katada, T., Bokoch, G.M., Smigel, M.D., Ui, M., and Gilman, A.G. (1984). The inhibitory guanine nucleotide-binding regulatory component of adenylate cyclase. Subunit dissociation and

the inhibition of adenylate cyclase in S49 lymphoma cyc- and wild type membranes. J Biol Chem *259*, 3586-3595.

Katada, T., and Ui, M. (1979). Islet-activating protein. Enhanced insulin secretion and cyclic AMP accumulation in pancreatic islets due to activation of native calcium ionophores. J Biol Chem *254*, 469-479.

Kraut H., Frey E.K., & Werle E. (1930) Der Nachweis eines Kreislaufhormons in der Pankreasdruse. Hoppe-Seyler's Z. Physiol. Chemie *187*, 97-106

Laemmli, U.K. (1970). Cleavage of structural proteins during the assembly of the head of bacteriophage T4. Nature *227*, 680-685.

Lagerstrom, M.C., and Schioth, H.B. (2008). Structural diversity of G protein-coupled receptors and significance for drug discovery. Nat Rev Drug Discov *7*, 339-357.

Lamb, M.E., Zhang, C., Shea, T., Kyle, D.J., and Leeb-Lundberg, L.M. (2002). Human B1 and B2 bradykinin receptors and their agonists target caveolae-related lipid rafts to different degrees in HEK293 cells. Biochemistry *41*, 14340-14347.

Lee, C.H., Park, D., Wu, D., Rhee, S.G., and Simon, M.I. (1992). Members of the Gq alpha subunit gene family activate phospholipase C beta isozymes. J Biol Chem *267*, 16044-16047.

Lembeck, F., Griesbacher, T., Eckhardt, M., Henke, S., Breipohl, G., and Knolle, J. (1991). New, long-acting, potent bradykinin antagonists. Br J Pharmacol *102*, 297-304.

Liebmann, C. (2001). Bradykinin signalling to MAP kinase: cell-specific connections versus principle mitogenic pathways. Biol Chem *382*, 49-55.

Madeddu, P., Emanueli, C., Bonaria Salis, M., Franca Milia, A., Stacca, T., Carta, L., Pinna, A., Deiana, M., and Gaspa, L. (2001). Role of calcitonin gene-related peptide and kinins in post-ischemic intestinal reperfusion. Peptides *22*, 915-922.

Madeddu, P., Varoni, M.V., Palomba, D., Emanueli, C., Demontis, M.P., Glorioso, N., Dessi-Fulgheri, P., Sarzani, R., and Anania, V. (1997). Cardiovascular phenotype of a mouse strain with disruption of bradykinin B2-receptor gene. Circulation *96*, 3570-3578.

Marion, S., Oakley, R.H., Kim, K.M., Caron, M.G., and Barak, L.S. (2006). A beta-arrestin binding determinant common to the second intracellular loops of rhodopsin family G protein-coupled receptors. J Biol Chem *281*, 2932-2938.

Meneton, P., Bloch-Faure, M., Hagege, A.A., Ruetten, H., Huang, W., Bergaya, S., Ceiler, D., Gehring, D., Martins, I., Salmon, G*., et al.* (2001). Cardiovascular abnormalities with normal blood pressure in tissue kallikrein-deficient mice. Proc Natl Acad Sci U S A *98*, 2634-2639.

Menke, J.G., Borkowski, J.A., Bierilo, K.K., MacNeil, T., Derrick, A.W., Schneck, K.A., Ransom, R.W., Strader, C.D., Linemeyer, D.L., and Hess, J.F. (1994). Expression cloning of a human B1 bradykinin receptor. J Biol Chem *269*, 21583-21586.

Morissette, G., Houle, S., Gera, L., Stewart, J.M., and Marceau, F. (2007). Antagonist, partial agonist and antiproliferative actions of B-9870 (CU201) as a function of the expression and density of the bradykinin B1 and B2 receptors. Br J Pharmacol *150*, 369-379.

Nishizuka, Y. (1992). Intracellular signaling by hydrolysis of phospholipids and activation of protein kinase C. Science *258*, 607-614.

Northup, J.K., Sternweis, P.C., Smigel, M.D., Schleifer, L.S., Ross, E.M., and Gilman, A.G. (1980). Purification of the regulatory component of adenylate cyclase. Proc Natl Acad Sci U S A *77*, 6516-6520.

Ohyama, K., Yamano, Y., Sano, T., Nakagomi, Y., Wada, M., and Inagami, T. (2002). Role of the conserved DRY motif on G protein activation of rat angiotensin II receptor type 1A. Biochem Biophys Res Commun *292*, 362-367.

Palczewski, K., Kumasaka, T., Hori, T., Behnke, C.A., Motoshima, H., Fox, B.A., Le Trong, I., Teller, D.C., Okada, T., Stenkamp, R.E.*, et al.* (2000). Crystal structure of rhodopsin: A G protein-coupled receptor. Science *289*, 739-745.

Panek, R.L., Lu, G.H., Overhiser, R.W., Major, T.C., Hodges, J.C., and Taylor, D.G. (1995). Functional studies but not receptor binding can distinguish surmountable from insurmountable AT1 antagonism. J Pharmacol Exp Ther *273*, 753-761.

Park, J.H., Scheerer, P., Hofmann, K.P., Choe, H.W., and Ernst, O.P. (2008). Crystal structure of the ligand-free G-protein-coupled receptor opsin. Nature *454*, 183-187.

Patel, S., Robb-Gaspers, L.D., Stellato, K.A., Shon, M., and Thomas, A.P. (1999). Coordination of calcium signalling by endothelial-derived nitric oxide in the intact liver. Nat Cell Biol *1*, 467-471.

Perez, D.M., and Karnik, S.S. (2005). Multiple signaling states of G-protein-coupled receptors. Pharmacol Rev *57*, 147-161.

Pizard, A., Blaukat, A., Muller-Esterl, W., Alhenc-Gelas, F., and Rajerison, R.M. (1999). Bradykinin-induced internalization of the human B2 receptor requires phosphorylation of three serine and two threonine residues at its carboxyl tail. J Biol Chem *274*, 12738-12747.

Pruneau, D., Paquet, J.L., Luccarini, J.M., Defrene, E., Fouchet, C., Franck, R.M., Loillier, B., Robert, C., Belichard, P., Duclos, H.*, et al.* (1999). Pharmacological profile of LF 16-0687, a new potent non-peptide bradykinin B2 receptor antagonist. Immunopharmacology *43*, 187-194.

Rasmussen, S.G., Choi, H.J., Rosenbaum, D.M., Kobilka, T.S., Thian, F.S., Edwards, P.C., Burghammer, M., Ratnala, V.R., Sanishvili, R., Fischetti, R.F.*, et al.* (2007). Crystal structure of the human beta2 adrenergic G-protein-coupled receptor. Nature *450*, 383-387.

Roberts, R.A., and Gullick, W.J. (1990). Bradykinin receptors undergo ligand-induced desensitization. Biochemistry *29*, 1975-1979.

Rodbell, M., Krans, H.M., Pohl, S.L., and Birnbaumer, L. (1971). The glucagon-sensitive adenyl cyclase system in plasma membranes of rat liver. IV. Effects of guanylnucleotides on binding of 125I-glucagon. J Biol Chem *246*, 1872-1876.

Roscher, A.A., Manganiello, V.C., Jelsema, C.L., and Moss, J. (1983). Receptors for bradykinin in intact cultured human fibroblasts. Identification and characterization by direct binding study. J Clin Invest *72*, 626-635.

Rovati, G.E., Capra, V., and Neubig, R.R. (2007). The highly conserved DRY motif of class A G protein-coupled receptors: beyond the ground state. Mol Pharmacol *71*, 959-964.

Sabourin, T., Bastien, L., Bachvarov, D.R., and Marceau, F. (2002). Agonist-induced translocation of the kinin B(1) receptor to caveolae-related rafts. Mol Pharmacol *61*, 546-553.

Samama, P., Cotecchia, S., Costa, T., and Lefkowitz, R.J. (1993). A mutation-induced activated state of the beta 2-adrenergic receptor. Extending the ternary complex model. J Biol Chem *268*, 4625-4636.

Sambrook, J., and Gething, M.J. (1989). Protein structure. Chaperones, paperones. Nature *342*, 224-225.

Scheer, A., Costa, T., Fanelli, F., De Benedetti, P.G., Mhaouty-Kodja, S., Abuin, L., Nenniger-Tosato, M., and Cotecchia, S. (2000). Mutational analysis of the highly conserved arginine within the Glu/Asp-Arg-Tyr motif of the alpha(1b)-adrenergic receptor: effects on receptor isomerization and activation. Mol Pharmacol *57*, 219-231.

Scheer, A., Fanelli, F., Costa, T., De Benedetti, P.G., and Cotecchia, S. (1996). Constitutively active mutants of the alpha 1B-adrenergic receptor: role of highly conserved polar amino acids in receptor activation. Embo J *15*, 3566-3578.

Scheer, A., Fanelli, F., Costa, T., De Benedetti, P.G., and Cotecchia, S. (1997). The activation process of the alpha1B-adrenergic receptor: potential role of protonation and hydrophobicity of a highly conserved aspartate. Proc Natl Acad Sci U S A *94*, 808-813.

Scheerer, P., Park, J.H., Hildebrand, P.W., Kim, Y.J., Krauss, N., Choe, H.W., Hofmann, K.P., and Ernst, O.P. (2008). Crystal structure of opsin in its G-protein-interacting conformation. Nature *455*, 497-502.

Schremmer-Danninger, E., Hermann, A., Fink, E., Fritz, H., and Roscher, A.A. (1999). Identification and occurrence of mRNAs for components of the kallikrein-kinin system in human skin and in skin diseases. Immunopharmacology *43*, 287-291.

Shapiro, D.A., Kristiansen, K., Weiner, D.M., Kroeze, W.K., and Roth, B.L. (2002). Evidence for a model of agonist-induced activation of 5-hydroxytryptamine 2A serotonin receptors that involves the disruption of a strong ionic interaction between helices 3 and 6. J Biol Chem *277*, 11441-11449.

Sternweis, P.C., Northup, J.K., Smigel, M.D., and Gilman, A.G. (1981). The regulatory component of adenylate cyclase. Purification and properties. J Biol Chem *256*, 11517-11526.

Stewart, J.M. (2004). Bradykinin antagonists: discovery and development. Peptides *25*, 527-532.

Stewart, J.M., Gera, L., Hanson, W., Zuzack, J.S., Burkard, M., McCullough, R., and Whalley, E.T. (1996). A new generation of bradykinin antagonists. Immunopharmacology *33*, 51-60.

Taylor, S.J., Chae, H.Z., Rhee, S.G., and Exton, J.H. (1991). Activation of the beta 1 isozyme of phospholipase C by alpha subunits of the Gq class of G proteins. Nature *350*, 516-518.

Teller, D.C., Okada, T., Behnke, C.A., Palczewski, K., and Stenkamp, R.E. (2001). Advances in determination of a high-resolution three-dimensional structure of rhodopsin, a model of G-protein-coupled receptors (GPCRs). Biochemistry *40*, 7761-7772.

Tippmer, S., Quitterer, U., Kolm, V., Faussner, A., Roscher, A., Mosthaf, L., Muller-Esterl, W., and Haring, H. (1994). Bradykinin induces translocation of the protein kinase C isoforms alpha, epsilon, and zeta. Eur J Biochem *225*, 297-304.

Urban, J.D., Clarke, W.P., von Zastrow, M., Nichols, D.E., Kobilka, B., Weinstein, H., Javitch, J.A., Roth, B.L., Christopoulos, A., Sexton, P.M.*, et al.* (2007). Functional selectivity and classical concepts of quantitative pharmacology. J Pharmacol Exp Ther *320*, 1-13.

van Biesen, T., Luttrell, L.M., Hawes, B.E., and Lefkowitz, R.J. (1996). Mitogenic signaling via G protein-coupled receptors. Endocr Rev *17*, 698-714.

Vanderheyden, P.M., Fierens, F.L., and Vauquelin, G. (2000). Angiotensin II type 1 receptor antagonists. Why do some of them produce insurmountable inhibition? Biochem Pharmacol *60*, 1557-1563.

Vauquelin, G., and Van Liefde, I. (2005). G protein-coupled receptors: a count of 1001 conformations. Fundam Clin Pharmacol *19*, 45-56.

Warne, T., Serrano-Vega, M.J., Baker, J.G., Moukhametzianov, R., Edwards, P.C., Henderson, R., Leslie, A.G., Tate, C.G., and Schertler, G.F. (2008). Structure of a beta(1)-adrenergic G-protein-coupled receptor. Nature. *454*, 486-491

Werle E., Gotz W., & Kepler A. (1937) Über die Wirkung des Kallikreins auf den isolieren Darm und über eine neue darmkontrahierende Substanz. Biochem. Z. *289*, 217-233.

Werle E. & Grund M. (1939) Zur Kenntnis der darmkontrahierende Uterus erregenden und blutdrucksenkenden Substanz DK. Biochem. Z. *301*, 429-436

Wess, J. (1998). Molecular basis of receptor/G-protein-coupling selectivity. Pharmacol Ther *80*, 231-264.

Willets, J.M., Challiss, R.A., and Nahorski, S.R. (2003). Non-visual GRKs: are we seeing the whole picture? Trends Pharmacol Sci *24*, 626-633.

Yeagle, P.L., Alderfer, J.L., and Albert, A.D. (1997). Three-dimensional structure of the cytoplasmic face of the G protein receptor rhodopsin. Biochemistry *36*, 9649-9654.

Yu, J., Polgar, P., Lubinsky, D., Gupta, M., Wang, L., Mierke, D., and Taylor, L. (2005). Coulombic and hydrophobic interactions in the first intracellular loop are vital for bradykinin B2 receptor ligand binding and consequent signal transduction. Biochemistry *44*, 5295-5306.

Zhang, M., Mizrachi, D., Fanelli, F., and Segaloff, D.L. (2005). The formation of a salt bridge between helices 3 and 6 is responsible for the constitutive activity and lack of hormone responsiveness of the naturally occurring L457R mutation of the human lutropin receptor. J Biol Chem *280*, 26169-26176.

I ACKNOWLEDGEMENT

My first acknowledgement goes to my supervisor Dr. Alexander Faussner. Thank you for taking a chemist to your lab. Thank you for always being supportive during my work. Thank you for bringing new ideas, providing criticism and advice, for scientific discussions, but also more daily life discussions (football for instance).

Prof. Dr. Marianne Jochum gave me the opportunity to do my PhD thesis in the institute. For this I am more than grateful. For me it could not have been a better place. I want to thank Prof. Jochum for her financial and scientific support.

In my first year I was working on surface plasmon resonance. For this time I am very grateful to Prof. Dr. Werner Machleidt and to Irmgard Machleidt. Without you this work would not have been possible.

I want to thank Dr. Peter Neth for being in charge of the seminar for the graduate students. This I found very important and the interactions during these seminars have given me a lot.

I also express my thanks to Prof. Dr. Christian Sommerhoff, Prof. Dr. Edwin Fink, Dr. Christian Ries, and Dr. Dorit Nägler. I think you are doing a great job in charge of your own research groups.

I want to thank Prof. Dr. Hanz Fritz for his establishment of the Winter School and to come there every year and making the atmosphere very nice for everyone.

Further I would like to acknowledge Anne-Marie Oettl. I think you are doing a great job with the student course and I am happy I could give some contribution to that.

Coming to our lab group. Since I started I have been working with Steffen Schüssler and Cornelia Seidl. I want to acknowledge both of you for your excellent technical assistance. Furthermore for your support during my thesis. For great technical assistance I am also grateful to Heidrun Grondinger. Thank you Dr. Irina Kalatskaya for introducing me to the “PhD world” and showing

me the different assays in our lab. It was pleasure to have Markus Wirth in our group. You put in a great amount of work in the lab even though you had your medical studies at the same time. It was also a pleasure to have another medical student, Benjamin Welte, in our group. Thomas Pitsch made my beginning a lot easier by helping out with different methods.

With Jens Feierler starting his PhD in 2007 things kind of change. Only to the positive. For me I felt more inspiration. Suddenly I was not the only one with the thesis. We also established a friendship, which I am sure we will keep.

I am very happy to have Jasmin Leschner as my successor in our working group. I wish you good luck with your PhD.

Talking about friendship and people you respect I want to acknowledge Dr. Virginia Egea, Dr. Marisa Karow, Tanja Popp and Dr. Victoryia Sidarovich. You made these years special for me. Thank you.

Furthermore I wish to acknowledge my family back in Stockholm. Even though the distance you have been very supportive. With the background of my parents as pharmacists I felt a true interest on my topic. I want to acknowledge my two brothers for coming frequently to Munich to visit me.

I thank Stephen Marino for critical reading of the thesis.

Last but not least I acknowledge Pinar. We made it through Kansas, Stockholm, Italy and Munich. And we made it together. Now I am really excited for you receiving your PhD in Computer Science.

J CURRICULUM VITAE

PERSONAL DATA

Name: Göran Olof Wennerberg

Date of birth: 4. October 1977

Place of birth: Stockholm, Sweden

Citizenship: Swedish

GRADUATE STUDIES

PhD Thesis, Department of Clinical Chemistry and Clinical Biochemistry, Ludwig Maximilians University, Munich, 2005-2009

UNIVERSITY EDUCATION

Master of Science with a major in Chemistry, University of Stockholm 2004

Concentration: Organic Chemistry

Thesis: Methyl 2,2´-di-*O*-methyl-β-maltoside

Bachelor of Science in Chemical Engineering, University of Mälardalen, 2002

Concentration: Chemical Engineering

Thesis: The use of *N*-alkyl oligopyrroles and mixed oligoheteroaryls as building blocks for molecular wires

EDUCATION

Courses in Mathematics, Physics, Chemistry and Biology, High school, Stockholm, 1998-1999

Social science program, High school, Stockholm, 1993-1996

Compulsory school, Stockholm, 1984-1993

EXPERIENCE

Teaching assistant in laboratory, 2005-2009, Ludwig Maximilians University, Munich

Teaching assistant in laboratory, 2002-2003, Kansas State University

PUBLICATIONS

Faussner A., **Wennerberg G.,** Schüssler S., Feierler J., Seidl C., Jochum M., Proud D.
Alanine screening of the intracellular loops of the human bradykinin B_2 receptor – effects on receptor maintenance, G protein activation and internalization
The FEBS Journal. 2009; 276: 3491-3503

Wennerberg G., Kalatskaya I., Schüssler S., Feierler J., Welte B., Jochum M., Faussner A.
Role of the highly conserved arginine R128(3.50) and glutamate E238(6.30) in signaling and maintenance of the human bradykinin B2 receptor
(manuscript submitted to Biochemical Journal)

Wennerberg G., Schüssler S., Seidl C., Stewart J.M., Gera L., Grondinger H., Jochum M., Faussner A.
Functional selectivity of B9430 and icatibant concerning PLC activation, receptor down-regulation and ERK1/2 activation depends on human bradykinin B2 receptor density and cell type
(manuscript in preparation)

PRESENTATIONS

Invitation to a Seminar by Prof. Hartmut Michel (interview for a post-doc position)
April 2009, MPI for Biophysics, Frankfurt, Germany
Wennerberg G: Human bradykinin B_2 receptor: structure-function relationship

24th Winterschool "Proteases and their inhibitors"
March 2007, Tiers, Italy
Wennerberg G., Faussner A. Function analysis of bradykinin B2 receptor domains using surface plasmon resonance

25th Winterschool "Proteases and their inhibitors"
March 2008, Tiers, Italy

Wennerberg G., Faussner A. Functional selectivity of B9430 and icatibant concerning PLC activation, receptor down-regulation, and ERK1/2 activation depends on human bradykinin B2 receptor density and cell type

26th Winterschool "Proteases and their inhibitors"
March 2009, Tiers, Italy
Wennerberg G., Faussner A. Role of the highly conserved arginine in the DRY motif and the glutamate in the TERR motif concerning activation and trafficking of the human bradykinin B_2 receptor

POSTERS

2nd International Conference on "Exploring the Future of Vascular and Inflammatory Mediators"; May 2007, Berlin, Germany
Wennerberg G., Faussner A., Schuessler S., Kalatskaya I., Seidl C., Jochum M., Proud D. Alanine-screening of the loops of the human bradykinin B2 receptor reveals different functions for second and third intracellular loop in G protein interaction

Gordon Research Conference on "Molecular Gating and Ligand Recognition"
March 2008, Ventura (CA), USA
Wennerberg G., Faussner A., Schuessler S., Kalatskaya I., Seidl C., Jochum M., Proud D. Alanine-screening of the loops of the human bradykinin B2 receptor reveals different functions for second and third intracellular loop in G protein interaction

Keystone Symposium "G Protein-Coupled Receptors: New Insights in Functional Regulation and Clinical Application"
May 2008, Killarney, Ireland
Wennerberg G., Schuessler S., Seidl C., Stewart J.M., Gera L., Grondinger H., Jochum M., Faussner A. Functional selectivity of B9430 and icatibant concerning PLC activation, receptor down-regulation, and ERK1/2 activation depends on human bradykinin B2 receptor density and cell type